Spring 5-15-2017

Developing an In Vitro Assay for Detection and Characterization of Functional Connectivity within Transplantation Candidate Embryonic Stem Cell-Derived V2a Interneuron Networks

Jeffrey Robert Gamble
Washington University in St. Louis

WASHINGTON UNIVERSITY IN ST. LOUIS

School of Engineering and Applied Sciences

Department of Biomedical Engineering

Dissertation Examination Committee:
Dennis Barbour, Chair
James Huettner
Daniel Moran
Shelly Sakiyama-Elbert
Paul Stein

Developing an *In Vitro* Assay for Detection and Characterization of Functional Connectivity within Transplantation Candidate Embryonic Stem Cell-Derived V2a Interneuron Networks

by
Jeffrey Gamble

A dissertation presented to
The Graduate School
of Washington University in
partial fulfillment of the
requirements for the degree
of Doctor of Philosophy

May 2017
St. Louis, Missouri

Table of Contents

List of Figures

List of Tables

Acknowledgements

None of this work would have been possible without the support of dozens of individuals, near and far, over the last six years. First and foremost, I would like to thank my committee for supporting this work from just the nugget of an idea to a full-fledged research project. Dr. Barbour, Dr. Stein, Dr. Huettner, Dr. Moran, and Dr. Sakiyama-Elbert, your expertise was the foundation upon which this work was built. Dr. Huettner and Dr. Stein, thank you for taking countless hours of your time to meet with me individually and get me up to speed on the ventral interneuron literature and cell culture electrophysiology, both of which have become essential aspects of this project. To my PI, Dennis Barbour, thank you for having faith in my abilities no matter the circumstance. I first came to him as a junior in college, looking for a summer position close to home. Dr Barbour was willing to meet with me personally on short notice and offer me a paid position for the summer even though we had only had a brief interaction. From that point on, he has consistently believed in my capacity to achieve the task at hand, giving me complete autonomy on multiple projects throughout my time at Washington University, whether they succeeded or failed. It was within this environment that I grew into an independent thinker and nurtured my love for science and the search for truth. Dr. Barbour's mentorship will have a lasting effect on my life as both a professional and a scholar.

My lab-mates in the Barbour group have also played a crucial role over the last six years. We've had many people come through the lab during that time, and every last one of them became part of our family. Our lab tech, Kim, and our two post-docs, Noah and Ammar, taught me so much about the daily practices of conducting scientific research. They truly were fundamental influences on the scientist I am today. David, Wensheng, and Ruiye: you have all become brothers and sisters in my eyes, and your daily support and comradery made our lab a

place that I looked forward to being every day. Our periodic two hour lunch conversations about anything from US or Chinese politics to whether or not Amazon is the precursor to SkyNet always had a way of taking my mind off of the marathon that is an engineering PhD. I would also like to give a special thanks to my collaborators, the Sakiyama-Elbert lab for taking me in as one of their own at the beginning of my third year. Dr Sakiyama-Elbert treated me like one of her own students and has been nothing but supportive throughout the entire process. Her students and laboratory manager never hesitated to assist me whenever I was struggling with cell culture-related endeavors and made coming in on the weekends a fun experience. One student in particular, Nisha Iyer, went above and beyond. In the nearly four years in which we collaborated, she and I became intellectual partners in attacking our overlapping projects. The lifelong friendship we developed while working together is something that I will always cherish. I wish her the very best on her endeavor to become a wonderful, accomplished PI.

I would also like to thank Washington University for providing an environment that breeds successful research. Both Washington University as a whole and more specifically the Department of Biomedical Engineering have created an extremely collaborative environment that made the work documented in this thesis possible. I would like to thank my first collaborators, the Maurer lab, for the opportunity they gave me the first two years of my program. Although the project never quite got off the ground, they taught me about what it takes to be a thoughtful collaborator and integrate into someone else's space. Thank you to the staff and professors within the Cognitive, Computational, and Systems Neuroscience pathway. Not only was my thinking heavily influenced by the framework laid down in that two-year curricular pathway, but the financial support CCSN provided for two years helped make this work possible. In particular, I'd like to thank Dr. Herzog, who while helping me run CCSN's outreach program,

became a mentor with an enormous impact on me (Go Duke!!). His lab's work eventually became the foundation of the analysis methods used within this thesis, and his generosity with the use of his lab's multi-electrode array rigs generated the preliminary data that allowed me to write two successful grants. With that in mind, I would like to also thank the Hope Center and the University of Missouri system for providing the funding enabling the work documented here.

Within my department, I'd like to thank the staff for the supportive role they play for all of us researchers. Glenn, Karen, Kate, and Amanda: I have come to you all frantically on probably too many occasions, and you never hesitated to take time out of your busy schedules to assist me on any matter. We've also had two department chairs during my tenure here, Dr. Yin and Dr. George. They both have tirelessly nurtured this department into the center of excellence that it is today. And to my classmates, you all have been amazing over the past six years. Your collective excellence and drive constantly keep me motivated and accountable. We had a lot of adventures, and I look forward to where your careers and lives take you. Juan, Shiv, Boyle, Mrinal, and too many others to name: your energy and carefree nature outside of the lab could make up for any rough week. You all will accomplish wonderful things in this life. Rob, your friendship means a lot to me, and I will also be indebted to you for the opportunities you and Dr. Moran gave me outside of the lab that directly influenced how I think about this project. I need to also thank Juan in particular for helping me trouble-shoot my multi-electrode array set-up when I struggled for months to record noise-free data. The data contained in this document was made possible because of your willingness to help a brother in need.

I would be remissed if I did not mention the impact that my family and friends outside of the university community had on my time here. To my dear friends, Paul and Maddy, your consistent friendship is a constant reminder that time and distance do not define our lives. David

and Merritt, our family dinners are always a wonderful break from the everyday responsibilities that come with adulthood. I look up to you both and am excited to see the family you're building together (a special thanks to David for solving my page numbering problem in this document!). I also finished high school in the St Louis area, so there are a handful of people that I have known for a decade that I have consistently leaned upon during my tenure in this program. TJ and Jimmy in particular, who I have known since we ran track together senior year of high school, have been an amazing support network during the ups and downs a PhD program brings. They have truly become brothers to me, and the constant laughter has and always will be a bright spot in the daily grind. We are going to build amazing things here in St Louis. To my college friends (Gechi, Lucas, Beth, Jamal, Brandon, Martin, James, and Ryan), your black excellence holds me to the highest of standards. We continue to uplift each other, year after year, and I cannot wait to see the fruits of our collective labor and sacrifices moving forward.

It is extremely difficult to put into words the impact my parents and brother, Chris, have had on me over the years. My father's 30-year career as an officer in the military was a family endeavor. Moving from state to state every 2-4 years was difficult as a child, but I would not trade that experience for anything. It forged us into a strong, close family unit and my parents bred a household full of both laughter and academic rigor. Chris, I am extremely proud of the man you have become and look forward to the amazing accomplishments ahead of you in the mental health field. Last but definitely not least, I need to thank my girlfriend, Kayla, for the love and support she has given me over the last four years. Kayla, when I met you, your energy and kindness were just the medicine I needed to have the courage to jump-start this collaborative research endeavor with nothing but a vague idea. I have had the absolute pleasure of seeing you come into your own professionally and dominate criminal law in St Louis County. I am ecstatic

to see the beginnings of the life we are building here in St Louis together and know that there are many more fun adventures ahead of us. None of this is possible without you.

Jeffrey Gamble

Washington University in St Louis

May 2017

ABSTRACT OF THE DISSERTATION

Developing an *In Vitro* Assay for Detection and Characterization of Functional Connectivity within Transplantation Candidate Embryonic Stem Cell-Derived V2a Interneuron Networks

By Jeffrey Gamble

Doctor of Philosophy in Biomedical Engineering

Washington University in St. Louis, 2017

Professor Dennis L. Barbour, Chair

Facilitating plasticity after spinal cord injury tends to be the focus of most modern interventions for this condition. In particular, stem cell therapies attempt to both modulate and mimic some of the native plasticity after injury through multiple mechanisms. One such mechanism, the creation of new exogenous relay circuits bridging the injury, has been explored extensively, revealing serious impediments to its optimization and adoption for clinical settings. Our collaborator, the Sakiyama-Elbert group, has spent years addressing the first limitation, the variability of cellular graft composition, by perfecting protocols to generate embryonic stem cell (ESC)-derived populations of neurons with pre-determined genetic identity. Recently, they developed a protocol to develop highly-enriched populations of Chx10-expressing V2a interneurons (INs), a ventral interneuron population that has garnered recent interest due to its role in central pattern generating function and favorable phenotypic properties. This predominantly glutamatergic and long, ipsilaterally projecting population appears to be a prime candidate for transplantation therapies for SCI, especially for the creation of relay circuits that can potentially circumnavigate injuries. The research documented in this thesis attempts to begin

to address the second limitation of stem cell transplantation therapy, our minimal understanding of intra-graft network connectivity after transplantation. Due to the limitations of current techniques for evaluating the connectivity of populations like ESC-derived V2a INs, the relationship between functional recovery and the functional properties of the novel circuits formed within the graft still eludes researchers. This thesis focuses on the development of an assay capable of rapidly detecting connectivity within ESC-derived candidate populations. By extending previous work in the stem cell field, we combine *in vitro* multi-electrode arrays (MEAs) with an extensively studied metric of functional connectivity, cross-correlation, to detect and characterize individual functional connections between ESC-derived neurons. We first validated this assay by culturing ESC-derived populations differentiated for increased expression of Chx10 on MEAs. We found that both dissociated and aggregated cultures formed functional busting networks with significant functional connectivity detected with the use of Between-Sample Analysis of Connectivity, a methodology originally developed for *in vitro* circadian networks. Aggregated networks, however, had much more consistent electrode coverage and individual neuron detection that dissociated networks. After this validation study, we characterized the functional connectivity within highly-enriched populations of ESC-V2a INs, comparing their connectivity to populations of ESC-MN/glia and mixed populations of ESC-V2a/MN/glia. We found that ESC-MN/glia aggregates formed active networks with a variety of activity and functional connectivity that was dependent on the transmission of glutamate. ESC-V2a INs could only survive out to the 4-week time point if they were grown in media conditioned with glial factors, but these cultures still lacked spontaneous extracellular activity. Mixed ESC-V2a/MN/glia populations formed the most active networks and had thousands of detectable connections which were also dependent on glutamate transmission. Application of

glycine antagonist modulated network activity but the underlying cause is fairly inconclusive due to possible secondary effects. High growth factor concentrations in the growth media actually decreased network activity and detectable functional connections in the mixed populations. All of these findings in this proof of concept study collectively suggest that a mixture of ESC-V2a INs and ESC-MN/glia may be the most viable candidate for transplantation and sets the stage for future investigations into the manipulability of their connectivity with electrical stimulation, as well as scaled versions of this assay performed in combination with animal studies.

Chapter 1: Introduction

1.1. Spinal Cord Injury

Spinal cord injury (SCI) causes disruptions in the native function of the spinal cord that result in complex biophysical outcomes depending on the location, severity, and type of insult to the cord. Developing and optimizing therapies for this condition requires a fundamental understanding of the cascade of events following the initial disruption and their individual effects on the anatomy and function of this neural system. Spinal cords have also been shown across various animal models and in humans to spontaneously recovery some level of function depending on the type of plasticity occurring after the injury. Any therapy must be developed in the context of these complex, interrelated processes in order to maximize efficacy. This section will walk through an overview of the pathology of SCI as well as the regeneration and plasticity that occur after the injury. This review will set the foundation for more in-depth discussions of therapeutic strategies later in this thesis.

1.1.1. Pathology

SCI is a physically debilitating condition that currently affects approximately 276,000 people in the US with 12,500 new cases annually (NCSISC, 2014). This form of neurotrauma becomes a severe physical, emotional, psychological, and financial burden for the patients and their respective families. The highest frequency of SCI occurs in males between the ages of 15 and 25, and is estimated to have a lifetime cost of over $3 million for their medical care and lifestyle changes (McDonald and Sadowsky, 2002; Priebe et al., 2007). In order of frequency, the majority of SCIs are the result of motor vehicle accidents, work-place injuries, falls, violent

crimes, and sports injuries (Rowland et al., 2008). SCI is caused by a physical trauma to the spinal cord, typically resulting in partial or complete deficits in motor and/or sensory function below the site of injury depending on the category, severity, and location of the trauma along the cord. A convenient categorization system, developed by Bunge and colleagues, uses four classes of injury based on outward appearance and histology: 1) contusion or cavity 2) laceration 3) solid cord injury and 4) massive compression (Bunge et al., 1993). SCI as a whole is characterized by a series of biological events that are typically divided into two broad phases, primary and secondary, the second of which is subdivided into sub-phases according to time from the primary injury.

The primary injury refers to the initial mechanical insult to the cord and results in a collection of immediate phenomena depending on the category of injury. Lacerations of the spinal cord can lead to severing of passing axons (Bunge et al., 1993; Nashmi and Fehlings, 2001; Totoiu et al., 2004). Vascular disruption during this phase can also cause hemorrhaging that plays a role in the detriments occurring during the secondary phase of injury (Rawe et al., 1977; Tator and Koyanagi, 1997). It is important to note that the majority of the pathology of SCI is not the result of the primary injury and actually follows from the confluence of events within the secondary injury (Norenberg et al., 2004; Rowland et al., 2008).

The secondary injury includes a cascade of immune and vascular responses that lead to cell death of initially undamaged neural tissue proximal to the site of the mechanical injury and create an environment minimally permissive to neuro-regeneration. The early acute phase (1-48 hours) includes hemorrhaging that can occur from rupture of capillaries or coagulation of blood within the vasculature, but these typically happen on a small scale (Tator and Koyanagi, 1997). A complex inflammatory response including a cascade and interaction of chemical mediators and

free radicals generates an environment rampant with NMDA-mediated excitotoxicity, free-radical toxicity, necrosis, and disperse apoptosis (Fleming et al., 2006; Park et al., 2004; Xiong et al., 2007). Breakdown of the blood-brain barrier can lead to plasma leaking into neuronal spaces, leading to an increase in pressure-induced damage (Griffiths and Miller, 1974; Noble and Wrathall, 1989). Cellular changes, such as demyelination and Wallerian degeneration also occur during this period (Salgado-Ceballos et al., 1998; Waxman, 1989).

In the subacute phase (48 hours to 2 weeks), microglia are activated, having both positive and negative impacts on the site of injury by releasing harmful molecules into the environment as well as beneficial cytokines (Banati et al., 1993; Rabchevsky et al., 1998). Microglia are also converted into macrophages which facilitate the removal of cell debris through the phagocytic process (Donnelly and Popovich, 2008; Norenberg et al., 2004). During this time period, reactive astrocytes play a critical role in restoring a normal extracellular environment but also begin to grow large cytoplasmic processes that eventually play a role at later time points (Eddleston and Mucke, 1993; Herrmann et al., 2008; Norton et al., 1992). In the intermediate and late phase of secondary injury (1 month to years), the reactive astrocytes intertwine themselves and harden into what is known as the glial scar around this region, containing the spread of the immune cascade and necrosis and in many cases creating a cystic cavity (Berry et al., 1983; Hill et al., 2001).

1.1.2. Native Regeneration and Plasticity

Although the SCI environment has been shown to be very resistant to recovery of lost synaptic connectivity, native regeneration and plasticity do variably occur post-injury, depending on the animal model. Much of our understanding of plasticity changes after SCI have come in

the context of rehabilitative training, highlighting its importance in reorganization for recovery. Below the site of injury, there appears to be a preservation of the motor circuits, and these networks are capable of activation with appropriate afferent input, especially after motor training (Dietz, 2006; Lovely et al., 1986). This has been supported by observations that preservations of as little as 10% of descending spinal cord fibers after SCI can still support some locomotor recovery (Basso, 2000; Metz et al., 2000). The need for load-bearing for effective training emphasizes the importance of proprioceptive feedback in the activity of these spared central pattern generating circuits (Dietz, 2008; Harkema et al., 1997; Pearson and Collins, 1993). Motor neurons have been shown to upregulate neuromodulatory receptors to drive up neuronal excitability post-injury (Giroux et al., 1999; Murray et al., 2010). Negative plastic changes also occur in circuits below the lesion, such as the loss of descending corticospinal and brainstem input leading to maladaptive changes in spinal reflex circuits potentially mediated by a shift towards inhibitory transmission within these reflex pathways (Dietz and Sinkjaer, 2007; Tillakaratne et al., 2002).

Long-distance axonal sprouting across the site of injury, despite the glial scar and non-permissive environment, can generate some recovery as shown in amphibians, fish, and newborn mammals, but is minimal in humans (Kalil and Reh, 1979; Michel and Reier, 1979; Wood and Cohen, 1979). However, fibers adjacent to the injury can sprout and re-innervate local spinal targets that may have lost related descending drive. Both rodent and primate models have shown extensive sprouting of descending corticospinal, reticulospinal, and rubrospinal projections that proved relevant for functional recovery (Belhaj-Saif and Cheney, 2000; Rosenzweig et al., 2010; Takeoka et al., 2014; Zaaimi et al., 2012). All of these sprouting mechanisms attempt to take

advantage of the plasticity that occurs within the interneuron circuits adjacent to incomplete injuries, described below.

Propriospinal circuits spared by the injury have also demonstrated the capacity to rewire around the site of injury, potentially aiding motor and sensory recovery in mice and rats by increasing neuronal communication along the damaged cord through novel endogenous relays. Bareyre and colleagues demonstrated that corticospinal sprouting and synapsing onto spared propriospinal interneurons created functional bridges around the hemi-section of the cord. Use-dependent pruning of the new corticospoinal synapses left only long-projecting interneurons as members of the novel pathway (Bareyre et al., 2004). Staggered hemi-sections of the rodent spinal cord also showed the development of novel relays around the injury mediated by sprouting onto spared interneuron circuits that structurally rewired around the injury (Courtine et al., 2008). Treadmill training that engaged corticospinal pathways compared to automated treadmill training was able to engage propriospinal circuits spared by a staggered hemi-section to partially regain rodent hindlimb function (van den Brand et al., 2012). Reticulospinal tracts have also been shown to increase sprouting and excitatory synapse formation onto specific propriospinal circuits that crossed a single hemisection injury in rodents (Filli et al., 2014).

Not only does plasticity occur at the level of the spinal cord, but also takes place in higher cortical and subcortical sensorimotor systems. Cortical reorganization has been observed across multiple forms of chronic neurological injury (Donoghue et al., 1990; Sanes et al., 1990; Wu and Kaas, 1999). In all cases, cortical maps controlling periphery unaffected by the injury begin to displace affected maps. The same hold true in cases of SCI: neuroimaging has been used in humans to detect changes in the organization of sensorimotor cortical maps in response to deinnervation following SCI (Bruehlmeier et al., 1998; Levy et al., 1990; Lotze et al., 2006).

Subcortical motor centers, such as the red nucleus, have also been shown to reorganize as a compensatory mechanism for spinal cord lesions (Lawrence and Kuypers, 1968). Taken together, all native forms of regeneration and reorganization after SCI need to be considered when designing potential therapeutics. Most therapies for SCI typically aim to further facilitate or, even at times, mimic these inherent recovery processes in order to regain spinal cord synaptic connectivity across the injury. A deep understanding of the native behavior of the both the injured and uninjured cord will provide an avenue to maximize the chances of intervention success.

1.2. Propriospinal Interneurons

Neurons contained within spinal cord circuits are compelling targets for SCI interventions because of the previously described rewiring after the injury. In the uninjured cord, these neurons participate in central pattern generating (CPG) circuits. The function of these networks is predicated on precise connectivity and genetically-defined neuronal phenotypic diversity, both of which are achieved in development. One participating ventral interneuron population, V2a interneurons, appears to be a particularly viable target for SCI therapeutic strategies due to its favorable phenotypic properties. This section describes CPG function and how this arises from specific interconnectivity between ventral populations including V2a INs. Reasoning for focusing on these populations for transplantation therapies are discussed in detail prior to elaborating on the phenotype and role of V2a INs in CPGs and spontaneous recovery. Matching ventral population phenotype to the appropriate therapeutic strategy is an essential step in therapy design and optimization.

1.2.1. CPG Function

In the native spinal cord of vertebrates, CPGs are responsible for generating rhythmic movements, as well as the precise patterns of activation of muscle groups for both intentional and reflexive motions. Extensive knowledge of the CPG networks that control swimming and movement has been acquired in invertebrates and non-mammalian vertebrates. In particular, lobster, lamprey, and Xenopus tadpoles have provided scientists with direct insights into CPG connectivity and composition and their relation to motor output in those systems (Grillner, 2003; Harris-Warrick et al., 1992; McLean et al., 2000; Roberts et al., 1998). Relative to that wealth of knowledge, less is known about control of movement in mammals, which becomes inherently more complex as movements require coordination of increasing numbers of muscle groups for complex motions (Clarac et al., 2004; Kiehn and Butt, 2003; McCrea, 1998). In general, CPGs receive descending command inputs from motor control centers in cortex and brainstem, descending input from neuromodulatory neurons, and sensory feedback from the periphery, all of which interact in co-localized fashion to modulate the output of CPGs (Christie et al., 1995; Elson et al., 1992; Grillner and Wallen, 2002; Grillner et al., 2008; Skiebe, 2001).

Typically, CPG circuits are discussed in the context of three categories: 1) rhythm generation 2) extensor/flexion 3) left/right coordination (Kiehn, 2006). The rhythmogenic capacity of the spinal cord appears to be distributed from strongest to weakest capacity along the rostral-caudal axis of the cord, where rostral CPGs are more excitable than those located more caudally (Christie and Whelan, 2005; Hao et al., 2014; Mortin and Stein, 1989). This distribution may be governed by a decreasing density of neuromodulator receptors on CPG neurons as you move caudally down the cord (Kiehn, 2006; Schmidt and Jordan, 2000) and mediated by descending excitatory propriospinal axons belonging to neurons that potentially couple adjacent

rostro-caudal CPG modules (Grillner et al., 1981; Grillner, 2003; Stein, 2005), some of which may potentially contain neurons that change module or ensemble membership depending on the intended locomotor output (Hooper and Moulins, 1989; Meyrand et al., 1991; Weimann and Marder, 1994). Inquiries into CPG function are usually focused on the ventral region of the cord because movement-related neurons are generally located ventrally in the transverse plane of the spinal cord in laminae VII, VIII, and X, as identified by activity-labeling studies (Dai et al., 2005; Kjaerulff et al., 1994).

A unique property of CPGs is their ability to generate rhythms and precise patterns of activity in the absence of cortical input and sensory feedback. Many have extensively characterized the ability of spinalized, a chronic transection of the spinal cord, cats to generate walking motion on treadmills due to sensory reflexive circuits in CPGs (Barbeau and Rossignol, 1987; Delcomyn, 1980; Forssberg et al., 1975). In early invertebrate preparations, Wilson and colleagues were able to completely remove afferents in locusts, an extremely difficult procedure, to show the isolated rhythmogenic capabilities of CPGs (Wilson and Wyman, 1965; Wilson, 1966). A large proportion of our current knowledge about CPG function has been derived from assays where spinal cord is removed and placed in a bath solution for patch clamp or suction electrode recordings of CPG activity, also known as “fictive locomotion.” In these preparations, cocktails of neuromodulatory substances such as NMDA and serotonin are applied to induce rhythms in order to allow for electrophysiological characterizations of rhythm properties of specific CPG circuit neurons relative to motor outputs such as burst duration, phase, and intensity (Brodin et al., 1985; Cazalets et al., 1992; Charrier and Cabelguen, 2013; Mentel et al., 2008; O'Donovan, 1989). Evidence suggests that three fundamental circuit models may be underlying rhythm generation: 1) excitatory oscillatory pacemaker neurons coupled to tonic CPG

neurons 2) reciprocally connected tonic inhibitory neurons or 3) some combination of the two (Brocard et al., 2010; Feldman et al., 2013; Kiehn, 2016; Marder and Bucher, 2001). The importance of intrinsic membrane properties of excitatory neurons and their interplay with network properties has been especially highlighted when pertaining to mammalian CPG function (Harris-Warrick, 2002; Kiehn et al., 2000). Recent data also suggests that there may exist two separate modules within a single CPG circuit that control locomotion: 1) a rhythm generating module and 2) a pattern generating module (McCrea and Rybak, 2007; Rybak et al., 2006; Rybak et al., 2006). Much of this theory has been supported by work investigating "deletions" or moments where the rhythmic output of a CPG temporarily drops-out where it should be temporally and then comes back to its normal pattern (Grillner and Zangger, 1979; Stein and Daniels-McQueen, 2002; Zhong et al., 2012).

1.2.2. CPG Genetic Specificity

In the past two decades, developmental biology has made great strides in elucidating the molecular signaling and genetic transcriptional regulation accounting for the diversification of spinal circuit neurons that may contribute to native pattern generation and rhythmicity in the spinal cord. The time-course and combination of activations of specific transcription factors and guidance molecules has been characterized to identify neuronal population position within the spinal cord as well as the phenotypes and connectivity patterns of specific subpopulations that partake in CPG circuitry. Eleven molecularly and genetically defined progenitor domains defined early in development along the dorso-ventral axis by gradients of sonic hedgehog (shh) and retinoic acid (RA) give rise to the 6 cardinal classes of dorsally located interneurons and 5 cardinal classes of ventrally located neurons (Goulding, 2009; Jessell, 2000; Kiehn, 2011).

The five ventrally located ones (MN, V0-V3), each consisting of multiple phenotypically unique subclasses identified by their expression of various transcription factors, develop and interconnect to form motor-related spinal circuits (Alvarez et al., 2005; Arber, 2012; Crone et al., 2008; Lanuza et al., 2004; Panayi et al., 2010; Satou et al., 2012; Zhang et al., 2008).

The distribution of genetically-defined populations and the relative time course of neurogenesis appear to be correlated with the specificity of CPG circuit connectivity in the spinal cord. Zebra fish motor neurons and interneurons have been shown to segregate circuit recruitment during fast and slow swimming along the dorso-ventral axis which also happens to coincide with the timing of the neurogenesis of these circuits (McLean et al., 2007; McLean and Fetcho, 2009). Mice lumbar spinal cord has also been shown to segregate synaptic connections to flexor and extensor muscles by the birthdate and position of interneuron populations (Tripodi et al., 2011). Although most evidence for this correlation exists in invertebrate spinal cord preparations, these vertebrate studies suggest that further investigations into CPG connectivity and neurogenesis may reveal intertwined properties.

The interaction of this highly specific connectivity and the cellular properties of the individual subclasses gives rise to class-specific functions. Using genetic-knockout studies, scientists have been able to elucidate the effects of suppressing these class-specific roles. V0 interneurons can be subdivided into excitatory and inhibitory commissural neurons involved in left-right alternation (Griener et al., 2015; Moran-Rivard et al., 2001; Pierani et al., 2001; Satou et al., 2012; Talpalar et al., 2013; Zagoraiou et al., 2009). The inhibitory V1 population contains Ia interneurons and Renshaw cells and have been shown to participate in flexor-extensor coordination along with the speed of locomotor cycles (Alvarez et al., 2005; Benito-Gonzalez and Alvarez, 2012; Britz et al., 2015; Gosgnach et al., 2006; Moran-Rivard et al., 2001; Pierani

et al., 2001; Renshaw, 1946; Zhang et al., 2014). V2 interneurons, which include the predominantly glutamatergic ipsilaterally projecting V2a interneurons, as well as the inhibitory V2b and V2c populations, are involved in a broad range of CPG circuit roles including skilled reaching, left-right alternation, burst robustness, and flexor-extensor coordination (Al-Mosawie et al., 2007; Ampatzis et al., 2014; Crone et al., 2008; Crone et al., 2009; Dougherty and Kiehn, 2010, 2010; Dougherty et al., 2013; Panayi et al., 2010; Zhong et al., 2011). V3 interneurons, the least characterized of the ventral interneuron populations, are excitatory and predominantly commissural and are involved in modulating locomotor symmetry and burst robustness (Borowska et al., 2013; Zhang et al., 2008).

1.2.3. Propriospinal Neurons as Transplantation Candidates

Collectively, the CPG literature suggests that specific CPG functions are not conducted by single classes of propriospinal neurons. No particular locomotor output property was ever entirely ablated by the silencing or knockout of a specific interneuron subtype. In reality, circuit functions may be redundantly modulated by multiple genetically-defined populations, further highlighting the complexity of CPG circuits driven by precise cell identity and connectivity. In an earlier section, we discussed how propriospinal neurons can mediate recovery from SCI through propriospinal circuit reorganization (Bareyre et al., 2004; Courtine et al., 2008). This spontaneous plasticity appears to be heavily driven by phenotypic identity (i.e. long vs. short projecting interneurons). Previous transplantation attempts have also highlighted the importance of population identity. White and colleagues transplanted either dorsal or ventral pieces of fetal spinal cord tissue into a cervical hemisection, with greater recovery being elicited in the animals

that received ventral tissue, thus suggesting neuronal identity may play a critical role in these therapies moving forward (White et al., 2010).

As discussed in the "CPG Genetic Specificity" section of this thesis, the precise connectivity that drives the complexity of locomotor control occurs during development due to a highly specific time course of genetic activation and guidance molecule upregulation. This suggests that, as of now, it is extremely unlikely with current technologies that transplanted propriospinal neurons will be able to incorporate themselves into the spared spinal circuits in order to create new exogenous central pattern generating circuits at the site of the injury. This would require a level of specificity that most likely does not exist in the post-SCI environment of an adult. More likely is an upregulation of guidance molecules that help descending axons to reconnect with spared CPG centers caudal to the site of injury. For the purpose of bridging the connectivity lost in SCI (this will be discussed in further detail in the stem cell therapy portion of the thesis introduction), an interneuron population would serve as an ideal candidate for transplantation if it 1) natively lied in the ventral portion of the cord 2) made long ipsilateral projections 3) was excitatory and 4) had the capacity to make connections with CPG interneurons as well as motor neurons. This thesis primarily focuses on characterizing the exogenous network properties of one such propriospinal cell type, V2a interneurons, in order to help elucidate its therapeutic potential for SCI.

1.2.4. V2a Interneurons and Role in Uninjured and Injured Spinal Cord

One particular subtype that has recently garnered interest in its relevance to recovery due to its native properties and role in CPGs is the V2a interneuron (IN). V2a INs are a specific subclass of spinal cord propriospinal neurons derived from the Lhx3 progenitor domain,

identified by the transcription factor Chx10. In development V2a INs differentiate away from the V2b subpopulation of INs, identified by transcription factor expression of Gata2 and Gata3, a process governed by notch signaling (Ericson et al., 1997; Karunaratne et al., 2002; Peng et al., 2007; Smith et al., 2002; Zhou et al., 2000). Although it was previously thought that Lhx3 alone drove V2a IN differentiation, recent evidence suggests that Chx10 is the primary transcription factor necessary to secure the V2a fate through non-V2a gene repression (Clovis et al., 2016). Approximately 80% of V2a INs are excitatory neurons expressing Vglut2 while a small subset (<5%) appear to be inhibitory glycinergic neurons (Al-Mosawie et al., 2007; Lundfald et al., 2007).

V2a INs are a morphologically heterogeneous population distributed in lamina VII, VIII, and X from the central canal to the outer edge of the gray matter (Al-Mosawie et al., 2007; Crone et al., 2008; Dougherty and Kiehn, 2010; Kiehn and Kjaerulff, 1998). They also have solely ipsilaterally projecting axons (Lundfald et al., 2007) with projection patterns that vary depending on their location along the rostro-caudal axis of the spinal cord and the particular animal model of focus. In mammals, $Chx10^{+}$ INs make a small subset of projections to motor neurons, but predominantly project to CPG interneurons such as V0s (Al-Mosawie et al., 2007; Crone et al., 2008; Dougherty et al., 2013). In mice specifically, V2a INs located at the cervical level bridge communication between supraspinal centers in the lateral reticular nucleus and CPG spinal cord regions (Azim et al., 2014). In zebrafish, however, a majority of V2a INs are last-order neurons that make direct monosynaptic connections with motor neurons (Ampatzis et al., 2014; Eklof-Ljunggren et al., 2012; Kimura et al., 2006; Kimura et al., 2008; Kimura et al., 2013). They also form gap junctions with motor neurons which allow them to modulate CPG recruitment (Song et al., 2016).

The role and behavior of $Chx10^+$ spinal neurons has been extensively characterized in mammalian CPG circuits. Silencing or genetic knockout of V2a INs in mice results in speed-dependent gait, locomotor burst variability, and an overall disruption in left-right coordination (Crone et al., 2008; Crone et al., 2009; Dougherty et al., 2013). Recently, genetic silencing of V2a INs in mice showed that this subclass is involved in a feedback circuit that controls skilled reaching (Song et al., 2016). Patch experiments performed both in spinal cord slices and whole cord preparations have identified a variety of intrinsic membrane properties, firing behavior, and synaptic connectivity patterns. Zhong and colleagues revealed that V2a INs are recruited into locomotor patterns dependent on the frequency of the induced locomotion (Zhong et al., 2011). Firing properties of V2a neurons have also been characterized in patch clamp experiments where the neurons exhibited baseline activity when synaptically isolated. These experiments demonstrate that V2a INs can be categorized into three different classes based on their firing in response to stimulation: tonic, delay, and phasic, and that they receive rhythmic excitatory input (Dougherty and Kiehn, 2010; Zhong et al., 2010). Although the interconnectivity of V2a interneurons has been examined in multiple studies, the results are fairly inconclusive. Only electrical synapses were discovered in transverse spinal cord slices (Zhong et al., 2010), while dorsal horn removed preparations (longitudinal cut) demonstrated excitatory synaptic connections between $Chx10^+/Shox2^+$ neurons (Dougherty et al., 2013). V2a interneurons have also been reported to respond to a variety of both excitatory and inhibitory receptor agonists *in situ* and *in vitro* (Dietz et al., 2012; Miles et al., 2004).

A few recent studies have focused on the role of V2a IN in propriospinal networks post-SCI. After spinal cord transection, transgenically-labeled Chx10 mice exhibited 100 to 1000-fold upregulations of serotonin receptors on identified V2a INs independent of membrane excitability

(Husch et al., 2012). This could potentially be a compensatory behavior to account for a lack of descending neuromodulation post-injury. In a rat hemi-section model of SCI, a bolus of docosahexaenoic acid (DHA), a neuroprotective agent, was injected into the spinal cord, increasing sprouting of corticospinal tracts which was correlated with functional recovery. These axons were shown to make direct synaptic contacts on propriospinal INs, including V2a INs (Liu et al., 2015). This does not suggest that V2a's alone mediate recovery, but that they are likely participatory in the recovery process. Taking into consideration the phenotype, projection patterns, and role of V2a INs in the native recovery process, this interneuron class appears to be a potential candidate for SCI therapies, in particular stem cell therapy. In the following thesis section, we will discuss broadly the SCI interventions that have been investigated thus far and focus-in on stem cell transplantation therapies and their current benefits, caveats, and limitations.

1.3. Stem Cell Therapy

The goals of most SCI treatments are to increase neuroprotection, minimize the adverse effects caused by the secondary injury, promote/enhance regeneration that leads to restored connectivity across the site of injury, or directly control surviving sensorimotor pathways. Although increased sexual function, bladder control, and limb function are the highest rated desires of patients suffering from a spinal cord injury (Anderson, 2004), this section will focus primarily on those pertaining to restoring limb function, briefly covering molecular therapies, electrical stimulation, and physical rehabilitation, prior to exploring cell therapy, in particular a detailed examination of the goals, shortcomings, and needs of therapies using neural stem cells. In reality, some combination of these therapies will prove most promising depending on the location, type, and severity of the SCI, but for the scope of this thesis, we'll limit ourselves to

optimizing stem cell therapy with the specific use of V2a INs due to their previously described advantages.

1.3.1. SCI Therapy Overview

Molecular therapy has been widely explored both in animal studies and clinical trials as a means to promote recovery from SCI. Neuroprotective molecular therapies aim to protect spared host cells from the damaging environment of the secondary injury and rely on molecules such as steroids and antibodies (Gris et al., 2004; Hall and Springer, 2004). Axonal sprouting has been encouraged with the delivery of cyclic cAMP and modulation of GTPases (Dergham et al., 2002; Lu et al., 2004; Qiu et al., 2002), while inhibitors of growth-inhibiting molecules such as Nogo-A can also support increased sprouting of axons (Bregman et al., 1995; Schnell and Schwab, 1993; Thallmair et al., 1998). Administration of growth factors, such as BDNF, GDNF, and NT-3, can serve both duties, increasing neurite outgrowth and sprouting while also encouraging cell survival during secondary injury due to their interactions with neuronal cell receptors (Houweling et al., 1998; Jakeman et al., 1998; Schnell et al., 1994).

Electrical stimulation has been used as a means to induce plasticity in motor systems after SCI through chronic stimulation at various levels of the motor system. Axon outgrowth and progenitor proliferation have both been achieved with this paradigm (Carmel et al., 2010; Carmel et al., 2013; Li et al., 2010). On the other hand, functional electrical stimulation (FES) uses implantable, percutaneous, or surface electrodes to stimulate and activate neural pathways associated with a specific function. FES has been used to elicit upper limb movement, lower limb movement, and respiration, and bladder contraction (Bamford and Mushahwar, 2011; Brindley et al., 1982; DiMarco et al., 2006; Ragnarsson, 2008). Recently, exciting results were

achieved in a study where transected monkeys were fitted with a brain-machine interface that included implanted intracortical electrodes and an epidural stimulator located below the SCI (Capogrosso et al., 2016). Motor signals recorded from cortex were used to active the spatially selective epidural stimulator in motor-related patterns, reducing gait deficits. This is an extremely promising outcome for therapies potentially capable of minimizing paralysis.

Rehabilitative physical training has traditionally been used as a means to promote recovery with incomplete SCIs. Circuits spared below the site of injury are capable of coordinated movement during body-weight supported treadmill training, which becomes important for the long-term preservation of these systems (Edgerton et al., 2006; Engesser-Cesar et al., 2005) As also discussed earlier, spared fibers have the potential to either strengthen surviving connections or sprout after SCI in order to improve connectivity along use-dependent pathways in the spinal cord (Bareyre et al., 2004; Belhaj-Saif and Cheney, 2000; Courtine et al., 2008; Filli et al., 2014; Rosenzweig et al., 2010; Takeoka et al., 2014; van den Brand et al., 2012; Zaaimi et al., 2012). This type of therapy appears to be most effective when used in combination with other therapeutic modalities (Hutchinson et al., 2004; Ichiyama et al., 2005; Moon et al., 2006).

1.3.2. Stem Cell Therapy as Repair Strategy

Cell therapies have become especially promising as a potential treatment strategy for SCI and can provide neuroprotective qualities, replace cells lost in the primary and secondary injury, and support and encourage axon spouting and synaptic formation (Ruff et al., 2012; Thuret et al., 2006). For example, peripheral nerve grafts, particularly in combination with molecular therapies, promote growth of supraspinal axons through the grafts (Lee et al., 2002; Lee et al.,

2004). Schwann cells, which have been widely used in transplantation studies, have the capacity to physically support regrowing axons and possibly myelinate them, creating a more growth permissive environment, especially when applied in combination with molecular therapies (Fouad et al., 2005; Lavdas et al., 2010). Olfactory ensheathing cells derived from the olfactory mucosa have proliferative, glial-like properties and have been shown to have mixed results in terms of axon sprouting and regeneration (Lima et al., 2006; Lima et al., 2010). Differential responses of macrophages in the periphery nervous system, which appear to be beneficial, have led to the transplantation of activated microphages that have been pre-incubated in skin or peripheral nervous system tissue (Bomstein et al., 2003; Rapalino et al., 1998).

In particular, stem cell therapy offers the potential of achieving many of the goals of SCI repair simultaneously. The self-renewing and pluripotent capacity of stem cells makes them prime candidates for replacing damaged cells, restoring neural circuitry, repairing damaged axons, releasing trophic factors, and overall creating favorable environment for plasticity post-SCI (Mothe and Tator, 2012; Mothe et al., 2013). Neural stem cells are restricted to a neural fate, differentiating into glia, oligodendrocytes, or neurons, while neural progenitors are further restricted towards particular genetically defined neuronal or glial fates. Neural stem cells and progenitors can be acquired from multiple sources including the adult and fetal brain and spinal cord, embryonic sources, or induced from mature somatic cells (Chiasson et al., 1999; Gritti et al., 1996; Kulbatski et al., 2007; Palmer et al., 1997; Takahashi and Yamanaka, 2006; Weiss et al., 1996). Protocols have been developed to differentiate these variable source cells into particular neural or glial precursors (Brustle et al., 1999; Cao et al., 2005; Carpenter et al., 2001; Lepore and Fischer, 2005; Wada et al., 2009; Zhang et al., 1998) prior to transplantation into the spinal cavity of typically mouse or rat models of SCI for a plethora of therapeutic targets

(Abematsu et al., 2010; Bonner et al., 2011; Davies et al., 2006; Fujimoto et al., 2012; Hains et al., 2002; Hooshmand et al., 2009; Ikegami et al., 2005; Nori et al., 2011; Ogawa et al., 2002; Teng et al., 2002).

Rationale for this intervention has varied through the decades, but there has recently been a push to graft embryonic cells because they have the capacity to differentiate into neurons and glia and incorporate themselves into the endogenous circuitry, forming new spinal circuits both within the grafted population and between the grafted cells and host cells that can potentially bridge neuronal communication along the injured cord (Abematsu et al., 2010; Bonner et al., 2011; Fujimoto et al., 2012; Hou et al., 2013; Lu et al., 2012; Sharp et al., 2014). This behavior is analogous to the spontaneous recovery discussed earlier, where sprouting axons synapse onto rewiring spared interneurons to create new pathways around the injury (Bareyre et al., 2004; Courtine et al., 2008). Early fetal graft work demonstrated the ability of grafted stem and progenitor-derived neurons to interact with host networks (Houle and Reier, 1989; Jakeman and Reier, 1991). Abematsu and colleagues demonstrated with electron microscopy that transplanted neural stem cells form synapses with native axons descending into the graft as well as native cell bodies located caudal to the graft. Ablation of grafted circuits with diphtheria toxin returned the mice's recovered ability to generate volitional movement to the post-injury baseline, suggesting that these novel networks play a critical role in the recovery of pre-injury movement (Abematsu et al., 2010). Other studies closely examined the formation of grafted relay circuits and their ability to receive synapses from descending axons and extend axons that synapse onto host neurons and their relationship to functional recovery (Bonner et al., 2011; Lu et al., 2012; Sharp et al., 2014).

1.3.3. Pitfalls and Optimization of Stem Cell-Derived Relays

Although the improvements elicited by this particular type of intervention are encouraging, they have been variable in animal models of SCI (Bonner and Steward, 2015; Lu et al., 2012; Sharp et al., 2014). Three overarching problems have been impediments to the increased success of this therapeutic regime: 1) low grafted cell survival 2) the heterogeneity of the populations being grafted and 3) a lack of understanding of the novel circuits created post-transplantation. The secondary injury environment, particularly within the cytotoxic lesion cavity, greatly inhibits stem cell-derived neuron and glia survival (Mothe and Tator, 2012, 2013). Variable compositions of ESC-derived spinal cell subtypes can lead to variability in graft efficacy depending on the phenotype and properties of the pre- and postsynaptic neurons (Bonner and Steward, 2015; Mothe and Tator, 2013). The presence of undifferentiated stem cells can also lead to tumor formation, further confounding improvement (Johnson et al., 2010). Substantial sprouting of transplanted neurons across the lesion, coupled with the formation of novel synapses between graft and native neurons, does not guarantee consistent functional recovery, suggesting the importance of understanding network level graft interactions with the host tissue (Bonner and Steward, 2015; Lu et al., 2012; Sharp et al., 2014).

The generally low survival rate of grafted cells (~10%) appears to be greatly improved when transplantation occurs during the subacute time period of the injury before the secondary injury cascade begins (Okada et al., 2005; Tarasenko et al., 2007) and with the administration of immunosuppressants and growth factors (Guo et al., 2012; Johnson et al., 2010; Karimi-Abdolrezaee et al., 2006), but further work needs to be done to optimize these adjustments. In order to address the heterogeneity issue, a spectrum of *in vitro* protocols has been developed to consistently differentiate neural stem cells into well-characterized populations enriched for

predetermined neural subtypes, as well as purify these populations through antibiotic selection to leave the spinal cord neuronal subpopulation of choice (Brown et al., 2014; Iyer et al., 2016; McCreedy et al., 2012; McCreedy et al., 2014; Xu et al., 2015; Xu and Sakiyama-Elbert, 2015). Neurons within these cultures, identified by their expression of particular transcription factors, have been shown in many cases to share both geno- and phenotypes with well-studied propriospinal neural and glial subtypes, which can potentially lead to some level of predictability in the behavior of the graft at the cellular level (Iyer et al., 2016; Kim et al., 2011; McCreedy et al., 2014; Xu et al., 2015). In particular, highly-enriched populations embryonic stem cell-derived (ESC) V2a INs were generated and shown to have properties comparable to those found endogenously (Iyer et al., 2016). Extensive strategies for neural differentiation and purification in transplantation therapies have been heavily informed by knowledge accumulated in the field of developmental biology, which will continue to drive more precise interventions for better transplantation outcomes (Iyer et al., 2017).

Contrarily, very little progress has been made investigating the properties of grafted neural networks necessary to promote a therapeutically relevant increase in connectivity for the recovery of motor and sensory function. The task of relaying neural signals across the injured spinal cord with minimal distortion requires a particular functional connectivity structure within the graft that has yet to be ascertained with traditional methodologies due to both the intrinsic complexity of the native spinal cord and post-injury environment, as well as suboptimal use of currently available technologies. Descending axons have a spectrum of well-defined sources, targets, and functions and will synapse onto grafted neurons that interconnect and have heterogeneous phenotypes, forming non-specific networks that are required to process and propagate information (Bonner and Steward, 2015). Typical measures of the network efficacy of

stem cell-derived grafts in animal models of SCI *in vivo* involves the use of behavioral and electrophysiological assessments of gross signal conduction across the lesion which fail to examine differences in cellular graft attributes (Abematsu et al., 2010; Bonner et al., 2011; Fujimoto et al., 2012; Lu et al., 2012; Sharp et al., 2014). For more cellular assessments of electrophysiological graft properties, whole cell patch-clamp between pairs of neurons has been used both *in vitro* and *in vivo* to assess neuron-neuron synaptic connectivity, but requires time-intensive recordings from neuron pairs sequentially, painting an incomplete picture of the network as a whole (Bain et al., 1995; Buhnemann et al., 2006; Finley et al., 1996; Iyer et al., 2016; Jungling et al., 2003; Strubing et al., 1995; Xu et al., 2015). Multi-electrode arrays have been inserted into fetal stem cell grafts *in vivo*, but out of the ten grafts examined, only twenty-three neurons were discernable for auto-correlation analysis (Lee et al., 2014). Molecular and histological *in vitro* assays can quantify graft axon outgrowth and synapse formation between the graft and host tissue, and perform neurotransmitter and receptor characterizations of the stem cell-derived networks grown in isolation (Abematsu et al., 2010; Bain et al., 1995; Bonner et al., 2011; Finley et al., 1996; Fujimoto et al., 2012; Iyer et al., 2016; Strubing et al., 1995; Xu et al., 2015). Thus far, these modalities have collectively not been able to effectively elucidate the connectivity within graft circuits and its relationship to successful recovery, an inquiry essential to pushing stem cell transplantation therapies forward as effective strategies for consistent, sustainable recovery.

1.4. Functional Connectivity

As previously discussed, optimizing stem cell-derived grafts for SCI requires an understanding of neural network connectivity at the circuit level. In order to do so, the

appropriate measures of connectivity need to be selected with considerations of their respective interpretations along with their utility in SCI therapeutics. In this section, we will explore the concept of functional connectivity, one that was originally derived at the neuronal circuit level but has since also been applied at the level of neural systems. After discussing its origins and relationship to other forms of connectivity, one common measure of functional connectivity used in quantifying correlations between the activities of neuronal pairs, the cross-correlation function, will be examined in detail. Although this measure has complications in the interpretations that can be made from the resulting function, the application of functional connectivity in diagnostics and therapeutics in brain imaging may provide an avenue for framing our thinking moving forward with investigations of functional connectivity in stem cell-derived graft networks using measures like cross-correlation.

1.4.1. Structure and Function in Neuronal Circuits

Neural networks consist of individual functional neuronal units that connect to one another with long axonal processes that end in synaptic connections. Each neuronal unit is capable of generating action potentials that propagate along these projections to then activate connected neurons. This network of interconnectivity gives rise to functional interactions and neural dynamics that underpin the integration and transfer of information through neural networks (Alonso et al., 1996; Bair et al., 2001; Bargmann and Marder, 2013; deCharms and Merzenich, 1996; Gerstein et al., 1989; Sporns et al., 2000; Sporns et al., 2004; Sporns, 2011). To begin to investigate the relationship between connectivity and function, we must first define the categories of connectivity and interplay between them. Structural, or anatomical, connectivity refers to the physical connection that links two neurons to each other such as an axon from one

neuron projecting and synapsing onto the dendrite of another. Physical structure provides a constraint to other forms of connectivity, and at the level of neuronal circuits, focuses on the patterns of synaptic connectivity, both chemical and electrical, within the circuit (Alexander and Crutcher, 1990; Murre and Sturdy, 1995). Functional connectivity simply refers to the temporal relatedness between two sets of neural activities (Friston et al., 1993; Friston, 1994; Friston, 2011). In the context of neural circuits, this implies a measure of relatedness between the spiking activities of two neurons, with no assumption about the underlying circuit giving rise to the measured relatedness. Effective connectivity, however, does require a causal model of the process underlying a measured temporal interaction, and depending on the measure, can be inferred from functional connectivity (Aertsen et al., 1991; Aertsen et al., 1989; Friston et al., 1993; Friston, 1994; Friston, 2011; Gerstein and Perkel, 1972; Moore et al., 1966; Perkel et al., 1967). The three concepts have a particular interplay that arises from the constraints structural connectivity places on functional and effective connectivity and the ability of functional interactions to drive structural changes. This reciprocity allows a focus on one to address some aspects of the others. For the remainder of this section, we will discuss functional connectivity and its importance in understanding structure-function relationships in neural networks.

1.4.2. Differentiating Functional and Effective Connectivity

"Functional connectivity" is a terminology that can carry a lot of baggage depending on which domain it's being used within. In recent years, the explosion of publications in the whole-brain imagining field pertaining to resting state and task-based correlations of regional activity has led to a strong association between the term and this particular field. A Google Scholar search of "resting state" and "functional connectivity" results in over 100,000 publications being

returned, 65,000 of which were published after the year 2000. In reality, the concept of functional connectivity was originally explored in neuronal-level electrophysiological investigations of correlations between neuronal single/multi-unit activities measured on different electrodes to identify neuronal assemblies (Gerstein and Perkel, 1972; Moore et al., 1966; Perkel et al., 1967). A useful definition for "functional connectivity" that broadly allows for its history in investigations both in electrophysiology at the neuron-level as well as those at the level of the whole-brain is: "temporal dependency between spatially remote neurophysiological events" (Aertsen et al., 1989; Friston et al., 1993).

More specifically, functional connectivity refers to a correlation between two time series without any underlying model of what is causing the correlations (Aertsen et al., 1991; Aertsen et al., 1989; Friston et al., 1993; Friston, 1994; Friston, 2011; Gerstein and Perkel, 1972; Moore et al., 1966; Perkel et al., 1967). It should be noted that this definition specifically highlights an important difference between functional connectivity and what has come to be known as effective connectivity. As will be discussed later in this chapter, any interpretations of the specific circuit element that determines the measured functional connectivity, such as cross-correlation, require assumptions that fall beyond the scope of functional connectivity and within the bounds of effective connectivity. Although these two concepts at times get intertwined or misconstrued, effective connectivity refers to the direct effect one event has on another. It models what specific relationship or structure underlies the measured functional connectivity (Aertsen et al., 1989; Friston, 1994). In electrophysiology, effective connectivity can refer to the simplest possible circuit diagram that can reproduce the measured correlations between neurons, recognizing that there is no unique solution for the circuit (Aertsen et al., 1991; Aertsen et al., 1989). This delineation becomes increasingly important when making determinations as to

whether connectivity is being talked about in the context of diagnostics or how connectivity relates to neural dynamics, investigating whether a measure occurs repeatedly within a particular group or determining what is causing that repeated measure for that particular group. This will be discussed in more detail in a later section in this chapter in the context of resting state fMRI and its potential influence on investigating stem-cell derived neurons for SCI therapeutics.

Pragmatically speaking, measuring functional structure allows scientists to investigate the relationship between network structure and overall function in a way they cannot with traditional physical structure. In 1983, Gerstein and colleagues posed a utilitarian question: Are their metrics that can potentially circumvent having to measure the entire wiring diagram such that we can define states of the overall networks as well as changes in these states (Gerstein et al., 1983)? In other words, are there neural network outputs that are readily measurable that would allow us avoid the tedious task of attempting to determine all-inclusive structural connectivity, something that has only been accomplished in a small subset of invertebrates (White et al., 1986). In the context of neural circuits, extracellular signals of simultaneously recorded neurons combined with decades of statistical advances have provided a window into the structure of neuronal assemblies and how this relates to the population dynamics (Alonso et al., 1996; Gerstein and Perkel, 1972; Moore et al., 1966; Perkel et al., 1967).

Neuronal activity can be generated in two ways. First, some neurons in networks tend to have relatively high spontaneous rates of activity, even in the absence of a task. This spontaneous activity may be related to the transfer of information at rest or possibly preparing the network for optimal performance or reaction time when a task occurs by keeping the network in an ongoing active state (Fox et al., 2006; Fox and Raichle, 2007; Tsodyks et al., 1999). Neural activity can also be driven by the presence of a stimulus which can fall into multiple categories

including a behavioral task, pharmacological application, or electrical stimulation. Traditional studies of neural circuit connectivity were stimulus based in order to determine the minimum circuit diagrams underlying the measured neural dynamics (Gerstein and Perkel, 1969, 1972), while many modern inquiries focus on the role of functional interactions between neurons on stimulus processing (Averbeck et al., 2006; Pillow et al., 2008; Schneidman et al., 2006). It should be noted that spontaneous and evoked activities do not necessarily reveal equivalent connectivity patterns, at both the levels of neuronal assemblies and neural systems (Goel and Buonomano, 2013; Hampson et al., 2004; Jiang et al., 2004; Kohn and Smith, 2005; Lowe et al., 2000; Morgan and Price, 2004). This again highlights the need to make extensive considerations of what interpretations can be taken away from acquired results when using any type of functional connectivity measure.

1.4.3. Cross-correlation Function in Neuronal Connectivity

The cross-correlation function or histogram has been one of the more ubiquitously used metrics of one-to-one temporal relationships between the activities of neuron pairs. Fundamentally, this metric averages many occurrences of spikes of two neurons relative to one another to compute the probability of firing of a "target" neuron relative to a "reference" neuron (Aertsen et al., 1989). Taken without any interpretation of the meaning the histogram's shape, the cross-correlation function specifically represents the *functional* connectivity between a pair of neurons. Assumptions about the *effective* connectivity, or underlying causal relationships between neurons, are actually a difficult endeavor that requires particular assumptions to be made (Alonso and Martinez, 1998; Melssen and Epping, 1987; Moore et al., 1970; Palm et al., 1988; Trong and Rieke, 2008). The firing rates of the neurons must be assumed to be stationary,

or constant rate over the timescale of investigation. If stationarity assumptions cannot be met, there are complex corrections that can be made to the spike trains depending on the timescale of the non-stationarity (Aertsen et al., 1989; Gerstein and Perkel, 1969; Perkel et al., 1967).

Typically, interpretations of the cross-correlation histogram are talked about in two generic categories: direct synaptic connections or receiving direct input from the same neuron. Direct synaptic connections have been heavily investigated in different systems of the brain with the use of cross-correlation to make assertions about the relationship between connectivity and neuronal coding (Bartho et al., 2004; Csicsvari et al., 1998; Fujisawa et al., 2008; Snider et al., 1998). Quantitative considerations of the ability to elicit synaptic connections from cross-correlograms have been published (Ashby and Zilm, 1982; Fetz and Gustafsson, 1983; Herrmann and Gerstner, 2002; Knox, 1974; Veredas et al., 2005). Common input has also been inferred from this metric (Binder and Powers, 2001; Constantinidis et al., 2001; Sears and Stagg, 1976; Turker and Powers, 2001, 2002), but only a small set of studies have quantitatively investigated confounding factors on interpretations (Kirkwood and Sears, 1978). Other properties, such as the synaptic properties of the neurons considered and the network properties, can affect the shape of the histogram (Aertsen et al., 1989; Constantinidis et al., 2001; Poliakov et al., 1996). Recently, the effects of background network inputs into the two neurons considered can have profound effects on the histogram shape and raises questions of previous interpretations of underlying effective circuits (Herrmann and Gerstner, 2001; Ostojic et al., 2009). All of this work collectively demonstrates that correlated variations in spiking at different time scales have been observed and need to be taken into deep consideration because they can completely alter the interpretation of the data for the purpose of effective connectivity.

1.4.4. Functional Connectivity as a Diagnostic Tool

Advances in the use of functional connectivity in other fields can greatly inform how to overcome the previously described shortcomings in interpreting cross-correlation histograms, especially in the context of optimizing therapeutic ESC-derived neuronal networks for SCI. In particular, functional magnetic resonance imaging (fMRI) has been used for decades to image whole brain dynamics during task-based conditions for humans and other primates (Logothetis, 2003; Raichle and Mintun, 2006). Originally, changes in BOLD signaling in the presence of a task were only considered, while the vast majority of the recorded data, thought to be noise, was thrown away. Recently, studies have demonstrated that the low-frequency spontaneous "noise" can be used to calculate reliable correlations between brain areas at rest, constructing whole-brain functional connectivity maps that correspond nicely to known neural systems relationships (Fox and Raichle, 2007). When investigated in disease states, especially Alzheimer's disease, research has shown that resting state functional connectivity is capable of capturing repeatable group differences between healthy and diseases populations, opening the door for this method's use as a diagnostic tool in clinical settings (Greicius et al., 2004; Li et al., 2002; Supekar et al., 2008). This brings us back to the question posed by Gerstein back in 1983, whether or not we can detect state changes in neural networks without having to measure the entire wiring diagram (Gerstein et al., 1983). Advances in fMRI analyses suggest that the answer may be "yes."

Little is known about what type of anatomical connectivity underlies the fMRI-measured functional connectivity maps. Some studies have shown white matter tracts to be directly correlated to resting state functional connectivity, but there is not a 1:1 correspondence (Honey et al., 2009). Even though the genesis of the measured signal and correlations are poorly understood, this measure still has utility as a diagnostic tool due to the repeatable capture of

group differences when data manipulation are held reasonably constant (Fox and Greicius, 2010). It is plausible that the same logic can be applied to the use of metrics like the cross-correlation function in detecting group differences in populations of ESC-derived neuronal networks. As presented earlier, protocols for purified populations of genetically-defined ESC-derived neurons have been developed (Iyer et al., 2016; Iyer et al., 2017; McCreedy et al., 2012; McCreedy et al., 2014; McCreedy et al., 2014; Xu et al., 2015). By enriching ESC-derived populations in such a way, the within-population variability of the phenotypic properties of the neurons and how they interconnect may be greatly reduced. Simple measures of functional connectivity between neuron pairs, such as the cross-correlation function, may then be used to assess functional network correlations in such a way that captures population differences without having to make the exhaustive considerations necessary to deduce the underlying circuit diagrams. Interconnectivity will likely drive a population's efficacy as a grafted relay (Bonner and Steward, 2015), suggesting that elucidating network differences between efficacious ESC-derived populations and those with little effect, depending on the context of the SCI, is essential to optimizing these therapies.

1.5. *In Vitro* Multi-Electrode Arrays

Due to their parallel channels of extracellular recording, planar multielectrode arrays (MEAs) are particularly well-suited to analyze the propagation of activity across dissociated populations of cultured stem cell-derived neurons and provide high-throughput measurements of the connectivity between individual pairs of neurons. These measurements may potentially set the foundation for reliably quantifying the group differences necessary for diagnostic potential described in the previous section. First, this section will explore the history of MEAs in the

context of how their development led to today's use-cases. We will then explore the most common modern measurements in neural dynamics from cultured networks prior to discussing MEA's more recent applications in the field of neural network connectivity. Lastly, we will summarize how MEAs have been applied in the field of stem cell-derived neuronal cultures and describe the importance of extending their utilization to address the shortcomings related to our understanding of ESC-derived network integration into host tissue after SCI interventions.

1.5.1. *In Vitro* Studies with Multi-Electrode Arrays

MEAs were originally constructed as planar arrays consisting of photolithographed gold/nickel conductors on glass for the purpose of recording from cardiac myocytes (Thomas et al., 1972). Gross and colleagues then extended this work to record action potentials from spontaneously active individual neurons from snail ganglia (Gross et al., 1977; Gross, 1979). This trailblazing work was then followed by a slew of studies performed on mammalian neural tissue predominantly excised from murine spinal cords prior to the modernization of the technology with the addition of transparent indium oxide electrodes to greatly increase basic science research applications of the methodology (Droge et al., 1986; Gross et al., 1982; Gross et al., 1985; Pine, 1980). Advances in cell-adhesion promoting processes for long-term culture led to a further increase in the utilization of MEAs as an *in vitro* method of inquiry into neural dynamics. Poly-lysine, poly-ornithane, and laminin, especially in combination with plasma etching or flaming, have all been established as substances capable of masking the initially hydrophobic surface and creating a growth-permissive environment for less variable outcomes (Hunter et al., 1991; McKeehan and Ham, 1976). Improvements and cost reductions in

photolithographic techniques for imbedding semi-conductors into glass surfaces then led to commercially available MEA systems in the 1990s (Obien et al., 2014).

With the use of MEAs, activity has been recorded from both brain and heart tissue slice preparations, as well as dissociated neural and heart tissue, taken from a multitude of animal and human tissue sources (Frey et al., 2009; Hafizovic et al., 2007; Imfeld et al., 2008; Menzler and Zeck, 2011; Stutzki et al., 2014). In particular, dissociated *in vitro* neural networks are pseudo-random self-organizing networks that, over long periods of time, can generate patterns of activity unique to the tissue from which they came (Bettencourt et al., 2007). Although cultures can survive for up to 12 months with proper maintenance, most neuronal experiments tend to be performed within the 4 to 8 week period of growth *in vitro* (Potter and DeMarse, 2001). By 3 to 4 weeks, cultures tend to have reached phenotypic stability, after which there is a high probability of observing the aforementioned unique properties (Wagenaar et al., 2006). Various types of extracellular activity can be recorded from low-impedance cultures including single-unit and multi-unit spiking, network bursts, and low field potentials (LFP) (Buzsaki et al., 2012).

The long-term stability of neural network structure within cultures, as well as the stable extracellular recordings, have made MEAs suitable for many electrophysiological applications that require both spatial and temporal information. Pharmacological and toxicological screening are both fields that currently utilize animal models as the primary means to determine novel compound efficacy and toxicity. MEAs have become a high-throughput means to reduce the use of animals and rapidly determine the effects of both known and unknown compounds on neural network function and cell viability (Johnstone et al., 2010). MEA-neuronal cultures have also been proposed as a means to develop biosensors, but neuronal culture maintenance and repeatability remain impediments to their adoption (Pancrazio et al., 1999). MEAs have been

most widely used in the study of neural network dynamics and structure *in vitro*. Bursting measures are typically the most accessible metrics of network dynamics. Many methods have been developed to detect and characterize the stereotyped population bursting within cultures of neurons (Bakkum et al., 2013; Raichman and Ben-Jacob, 2008; Wagenaar et al., 2005). Because of the reduced complexity of the these networks and the readily computed population outputs, MEAs have been used to investigate fundamental neural network properties such as learning, plasticity, and population activity patterns (Demarse et al., 2001; Eytan et al., 2003; Jimbo et al., 1999; Maeda et al., 1995; Segev et al., 2001; van Pelt et al., 2004). More complex measures have also been used to describe and track dynamics across conditions in MEA cultures (Bakkum et al., 2008; Chao et al., 2007).

1.5.2. MEAs and Network Functional Connectivity

MEAs also allow for investigations into function connectivity within neuronal cultures using any of the methods previously described in the "Neural Connectivity" section of this thesis introduction. MEA studies of functional connectivity can be thought of in two categories: 1) those that measure functional connectivity to investigate individual neuron-neuron connections and 2) those that measure functional connectivity in order to construct network topologies or structures. Most commonly used metric for MEAs is the cross-correlation function and has been used to characterize neural network development, plasticity, and structure (Chao et al., 2007; Cutts and Eglen, 2014; Freeman et al., 2013; Garofalo et al., 2009; Maccione et al., 2012; Pastore et al., 2016; Poli et al., 2015). Other metrics, such as entropy or information theory-based measures, have also been applied to *in vitro* neuronal spike trains to quantify correlations between neuron activities (Garofalo et al., 2009).

In terms of analyzing individual connections and their properties, 60-channel MEAs were recently used to map thousands of pairwise functional connections between spike-sorted neurons in dissociated cultures of mouse suprachiasmatic nuclei (Freeman et al., 2013). Cross-correlation combined with a newly developed methodology to threshold significant connections allowed for tracking changes in connection magnitude and polarity (excitatory vs. inhibitory) over time, and determining the neurotransmitter underlying the connectivity. High-density MEA (~1000 electrodes) provide a means to begin coupling the measured functional connectivity to visual inspections of cultures using microscopy and staining. Maccione and colleauges coupled high-density MEAs with low-density hippocampal cultures to map both functional and effectivity connectivity and investigate the relationship between connection delays and path length (Maccione et al., 2012).

Once the functional connections between individual neurons have been defined, topological maps can be constructed to facilitate comparisons of network structure across conditions or groups. Graph theory has become a popular framework for quantifying characteristic of network topology in MEA cultures (Poli et al., 2015). It has been used to observe changes in network topology during development (Downes et al., 2012; Schroeter et al., 2015) and structure-function relationships in engineered networks (Boehler et al., 2012; Marconi et al., 2012). It must be noted that under-sampling of the networks with the widely used low-density arrays must be taken into account when considering possible variability in the measured functional network topologies (Maccione et al., 2010).

1.5.3. MEAs and Stem Cell-Derived Networks

Utilizing these tools to perform *in vitro* electrophysiological analyses on transplantation candidate stem-cell derived neuronal populations offers a unique opportunity to characterize the types of neuronal connectivity present within induced populations. Only in recent years have MEAs been established as a modality for functionally analyzing the network properties of such populations. Ban and colleagues originally opened the door for characterizations of ES-derived neuronal networks. Not only did they demonstrate the capacity for ES-derived GABAergic cultures to form functional networks when cultured on MEAs, but also showed that the connectivity, as measured by correlation between electrodes, resembled that of dissociated hippocampal neural cultures (Ban et al., 2007). This work became the basis for a handful of studies over the past decade that have explored the functional properties of ES-derived neural networks *in vitro*. Over an 8 week time period, it was shown that a variety of spontaneous activity, spiking as well as synchronized and unsynchronized bursting, develops in ES-derived populations and change their relative prevalence over that extended period of time (Illes et al., 2007). Multiple groups have shown that this spatial activity can be modulated both in human and mouse stem cell-derived populations by the application of neurotransmitters and channel antagonists, suggesting the expression of synaptic ionic channels native to endogenous neuronal populations (Heikkila et al., 2009; Illes et al., 2007; Lappalainen et al., 2010).

In terms of studies that explicitly explored network connectivity, beyond the original Ban work, the effects of neural aggregation on long-term ES-derived culture viability were explored, demonstrating that aggregation leads to stronger spontaneous synchronicity between bursting across electrodes (Illes et al., 2009). GABAergic-dominated networks derived from murine ESCs were shown to contain intrinsically activity pacemaker neurons when disconnected from the network by blocking fast synaptic connections. These neurons, when reconnected, had calcium

transients highly correlated with the network bursting (Illes et al., 2014). Structural connectivity has also been characterized in ES-derived networks with transsynaptic tracers, demonstrating that 70 day old cultures exhibit scale free physical connectivity (Kirwan et al., 2015).

Although this work collectively has contributed to our knowledge-base of fundamental characteristics of ES-derived networks *in vitro*, they each have caveats associated with them when extending the work forward towards determinations of neuron-neuron connectivity in the context of SCI repair. In all of the studies, the mature networks displayed some form of bursting, which is expected in MEA cultures, but this bursting behavior has little relevance to whether or not a particular ES-derived population will have therapeutic benefit after transplantation. As discussed in the "Propriospinal Neurons as Transplantation Candidates" section of this thesis introduction, functional CPG circuits require a precise pattern of genetically-specific connectivity that is unlikely to be achieved with currently developed stem cell technologies. The timing of bursting in MEA cultures has too much variability to be of any benefit to restoring central pattern generation at the site of injury. With this in mind, characterizations of the bursting or activity levels within ES-derived MEA cultures will not have much relevance to therapeutics.

Ideally, characterizing how individual neurons functionally interconnect will provide the most relevant information pertaining to this goal. The first ESC-derived MEA study, in fact, attempts to assess this type of connectivity, but the analysis in this study also has shortcomings in this regard (Ban et al., 2007). Two caveats to the study were 1) their connectivity analysis was primarily focused on non-sorted multiunit spikes between electrodes and 2) the cross-correlation measure used in the study utilized broad time bins (>100ms), both of which would result in connectivity less representative of synaptic interactions. Using multiunit (no spike-sorting) activity can potentially hide neuronal level interactions, especially when multiple pairs

are interacting on the same time scale or latency. Broad time bins in any connectivity measure become representative of noise correlations in the network as opposed to synaptic interactions (Doiron et al., 2016). Measures that allow for the emphasis of differences between specific connections within an ESC-derived network or between two networks from different ESC-derived populations are essential to furthering stem cell therapies for SCI. This thesis focuses on the combined use of MEAs and such metrics in order to facilitate therapeutically relevant investigations of functional network connectivity within transplantation candidate populations.

1.6. Concluding Remarks

Spinal cord injury is a complex condition with intricacies that need to be taken into account when designing and optimizing potential therapies. The difficult SCI environment, variable plasticity post-injury, and interruptions to complex and self-contained CPG circuits, can complicate any seemingly viable intervention. In particular, this thesis focuses on the optimization of stem cell therapy, which has been shown to be promising but still has serious limitations that need to be overcome before clinical translation truly becomes an option. Two limitations are dealt with in this text: graft composition variability and minimal understanding of intra-graft network connectivity. Our collaborator, the Sakiyama-Elbert group, has spent years perfecting protocols to generate ESC-derived populations of neurons with pre-determined genetic identity. Recently, they developed a protocol to develop highly-enriched populations of Chx10-expressing V2a INs, a ventral interneuron population that has garnered recent interest due to its role in CPG function and phenotypic properties. This predominantly glutamatergic and long, ipsilaterally projecting population appears to be a prime candidate for transplantation

therapies for SCI, especially for the creation of relay circuits that can potentially circumnavigate incomplete injuries.

Due to the limitations of current techniques for evaluating the potential of such populations, this thesis focuses on the development of an assay capable of rapidly detecting connectivity within ESC-derived candidate populations. By extending previous work in the stem cell field, we combine *in vitro* multi-electrode array with an extensively studied metric of functional connectivity, cross-correlation, to attempt to detect and characterize individual connections between ESC-derived neurons. The proof of concept studies presented here will explore the validation of such an assay in less-defined ESC-derived populations prior to its application to well-defined ESC-derived candidate populations of V2a INs. Assessing their functional connectivity is imperative to optimizing their therapeutic potential in studies moving forward.

Chapter 2: *In Vitro* Assay for the Detection of Network Connectivity in Embryonic Stem Cell-Derived Cultures

2.1. Abstract

Stem cell transplantation holds great promise as a repair strategy following spinal cord injury (SCI). Embryonic stem cell (ESC) transplantation therapies have elicited encouraging though limited improvement in motor and sensory function with the use of heterogeneous mixtures of spinal cord neural progenitors and ESCs. Recently, transgenic lines of ESCs have been developed to allow for pre-determined purification of transplantation candidate populations, but the functional network connectivity of these populations and its relationship to recovery is difficult to examine with current technological limitations. In this study, we combine an ESC differentiation protocol, multi-electrode arrays (MEAs), and previously developed neuronal connectivity detection techniques to develop an *in vitro* high-throughput assay of network connectivity in ESC-derived populations of neurons. Neural aggregation results in more consistent electrode coverage in culture than neural dissociation. Both culture types exhibited synchronized bursting behaviors at days 16 and 17 in MEA culture, and thousands of statistically significance functional connections were detected in both culture types with the use of cross-correlation histograms and Between-Sample Analysis of Connectivity (BSAC). These results demonstrate the ability to supplement assessments of the therapeutic potential of ESC-derived transplantation candidate populations by characterizing their network properties *in vitro* prior to or simultaneously with *in vivo* studies.

2.2. Introduction

In recent decades stem cell therapy has become promising as a potential treatment strategy for spinal cord injury (SCI). Typically, heterogeneous mixtures of embryonic stem cells (ESCs), neural-restricted progenitors, or glial-restricted progenitors are loaded into gels or scaffolds that are then either injected or surgically inserted into the spinal cavity (Brustle et al., 1999; Duncan et al., 1981; McCreedy et al., 2014; Mothe et al., 2013; Nori et al., 2011; Tetzlaff et al., 2011). One rationale for this intervention is that the grafted cells have the capacity to differentiate into neurons or glia and incorporate themselves into the endogenous circuitry spared by the injury, forming new spinal circuits within the grafted population and between the grafted cells and host cells. These circuits can then serve as neuronal relays for communication along the injured cord (Abematsu et al., 2010; Bonner et al., 2011; Fujimoto et al., 2012; Hou et al., 2013; Lu et al., 2012; Sharp et al., 2014).

Although the functional motor improvements elicited by this particular therapy are encouraging, they have been variable in animal models of SCI (Bonner and Steward, 2015; Lu et al., 2012; Sharp et al., 2014). Two major problems appear to be at the root of this therapeutic strategy's limitations: 1) the heterogeneity of the populations being grafted and 2) a lack of understanding of the novel circuits created post-transplantation. Variable compositions of ESC-derived spinal cell subtypes and undifferentiated stem cells can lead to variability in graft efficacy as well as tumorigenesis (Bonner and Steward, 2015; Johnson et al., 2010). To address the former, a spectrum of *in vitro* protocols has been developed to consistently differentiate ESCs into well-characterized populations enriched for predetermined neural subtypes, as well as to purify the spinal cord neuronal subpopulation of choice through genetic-engineering

(Anderson et al., 2007; Brown et al., 2014; Iyer et al., 2016; Li et al., 1998; McCreedy et al., 2012; McCreedy et al., 2014; Xu et al., 2015; Xu and Sakiyama-Elbert, 2015).

Different subclasses of transplanted neurons will have different phenotypes relevant to the functional connectivity required to relay information across the site of injury (e.g., dendritic branching, membrane properties, neurotransmitters, axon length, etc.). The task of relaying neural signals across the injured spinal cord with minimal distortion therefore becomes a task requiring in-depth inquiries into the neuron-neuron connectivity between ESC-derived transplantation candidate neurons (Bonner and Steward, 2015). The intrinsic complexity of the post-SCI environment, as well as severe limitations of traditional *in vivo* technologies, currently present challenges to studying intra-graft connectivity properties post-transplantation (Bonner et al., 2011; Lee et al., 2014). *In vitro* assessments, such as dual whole cell patch-clamp and molecular histology are inherently limited by the time required to collect sufficient data to assess the spatiotemporal functional connectivity relationships within whole ESC-derived networks (Iyer et al., 2016). Collectively, these modalities have not been able to effectively elucidate the functional connectivity within graft circuits and its relationship to successful recovery—an accomplishment essential to push stem cell transplantation therapies forward as effective strategies for consistent, sustainable recovery and to prevent negative side effects, such as spasticity, allodynia, and pain.

In vitro electrophysiology methodologies from other fields, in conjunction with cell induction and cell culture methods developed within the SCI field, present a compelling alternate platform not only to investigate how different stem cell-derived subpopulations interconnect within the overall neuronal population, but also in conjunction with *in vivo* methods to determine which graft connectivity properties promote an increase in gross spinal cord functional

connectivity post-injury. Due to their parallel channels of extracellular recording, planar multi-electrode arrays (MEAs) have been shown to be particularly well-suited to analyze the connectivity within populations of cultured ESC-derived neurons (Ban et al., 2007; Heikkila et al., 2009; Illes et al., 2007; Illes et al., 2014). Ban and colleagues opened the door for more in-depth inquiries into the spatial and temporal properties ES-derived neuronal interactions by demonstrating with the use of MEAs the capacity for ES-derived neurons to form functional networks (Ban et al., 2007). This seminal work inspired further characterizations of the maturation of ESC-derived network activities and modifications of their properties through the application of neurotransmitters and channel antagonists (Heikkila et al., 2009; Illes et al., 2007).

In the current study we extend the previously discussed findings by combining planar MEAs and a computational methodology recently shown to be capable of mapping thousands of pairwise functional connections between spike-sorted neurons in neuronal cultures (Freeman et al., 2013). Cross correlation, the measure of connectivity here, has historically been used to detect a spectrum of connectivity, from neuron-neuron monosynaptic connections to polysynaptic synchrony (Aertsen et al., 1989; Freeman et al., 2013; Fujisawa et al., 2008; Moore et al., 1966). By consistently detecting connectivity within ESC-derived spinal cord neuronal populations from a well-established protocol in a high-throughput manner, we present an assay that is essential to the advancement and optimization of ESC-derived graft relays for SCI repair.

2.3. Methods

2.3.1. ESC Culture

Cultures enriched for moderate expression Chx10-expressing V2a interneurons (V2a INs) were induced as previously described (Brown et al., 2014). Mouse RW4 ESCs were derived

from Sv129 mice and maintained in T-25 flasks in complete media, consisting of Dulbelcco's Modified Eagle Medium (DMEM; Life Technologies #11965-092) containing 10% newborn calf serum (Life Technologies #26140-079), and 1× Embryomax Nucleosides (Millipore #ES-008-D). Every two days, ESCs were passaged at a 1:5 ratio with fresh complete media supplemented with 100 μM β-mercaptoethanol (βME; Life Technologies #21985-023) and 1000 U/mL leukemia inhibitory factor (LIF; Millipore #ESG1106).

2.3.2. Chx10 Induction ($2^-/4^+$)

At the beginning of the induction, 10^6 ESCs were suspended in 10 mL of DFK5 media, which consists of a DMEM/F12 base supplemented with βME, 1:200 100× Embryomax Nucleosides, 50 μM nonessential amino acids (Life Technologies #11140-050), 100× insulin transferrin-selenium (Life Technologies #41400-045) and 5% knockout replacement serum (Life Technologies #10828-028) on an agar-coated 100 mm petri dish for two days in order to form embryoid bodies (EBs) (2^-). Media was then aspirated from the EBs and changed to DFK5 media containing 10 nM retinoic acid (RA; Sigma #R2625) and 1 μM purmorphamine (EMD Millipore #540223) for 2 days (2^+) prior to the media being aspirated and changed to DFK5 with 10 nM RA, 1 μM purmorphamine, and 5 μM of a gamma secretase inhibitor N-[N-(3,5-difluorophenacetyl-L-alanyl)]-(S)-phenylglycine t-butyl ester (DAPT; Sigma-Aldrich #D5942) for the last two days (4^+).

2.3.3. Dissociation and Aggregation

After the 6-day induction protocol, EBs were either dissociated or underwent a neural aggregation protocol prior to plating for MEA cultures. For dissociation-alone cultures, EBs

were collected, suspended in 0.25% Tryspin-EDTA (Life Technologies #25200-056) for 10 minutes, and mechanically separated by repeated pipetting. For neural aggregation cultures, EBs were initially dissociated as previously described, but were then plated on poly-L-ornithine (Sigma-Aldrich #P4957) and laminin-coated T75 flasks at a density of 5×10^5 cells/cm^2 in DFK5 supplemented with B-27 (Life Technologies #17504-044), glutaMAX (Life Technologies #35050-061), 5 ng/mL glial-derived neurotrophic factor (GDNF; Peprotech #450-10), 5 ng/mL brain-derived neurotrophic factor (BDNF; Peprotech #450-02) and 5 ng/mL neurotrophin-3 (NT-3; Peprotech #450-03). After 24 hours, the flask cultures were washed twice with DMEM/F12 and then lifted from flasks using Accutase (Sigma, #A6964) for 30 min at room temperature. A total of 5×10^5 cells were seeded into each well of a 400 μm Aggrewell plate (StemCell Technologies, #27845) in a modified DFKNB media consisting of DFK5 and Neurobasal media (NB; Life Technologies #21103-049) supplemented with B-27, glutaMAX, 5 ng/mL GDNF, 5 ng/mL BDNF, and 5 ng/mL NT-3 for 2 days of aggregate formation. Half the media was replaced daily. Aggregates were lifted by trituration and allowed to settle in micro-centrifuge tubes prior to plating as appropriate.

2.3.4. MEA Cell Culture

Either dissociated cells or aggregated cells were plated on individual 8×8 electrode grid S1-type MEAs with 200 μm electrode spacing and 10 μm electrode diameter (Warner Instruments #890102) that had been coated with poly-L-ornithine/laminin. Dissociated cells were plated uniformly at a cell density of 5×10^5 cells per MEA, while neural aggregates were plated at the center of each MEA at a cell density of 1.5×10^5. Both types were cultured in DFKNB with B-27, glutaMAX, 5 ng/mL GDNF, 5 ng/mL BDNF, and 5 ng/mL NT-3. Full media changes of the

supplemented DFKNB media were performed every two days up to day 6 in culture. After 6 days, the media was replaced with NB containing the same supplements for the duration of culture, with a full change of media performed every two days. Images of MEA cell cultures were captured using an Olympus IX70 inverted microscope with an attached MICROfire camera.

2.3.5. MEA Recording

The recorded signals were amplified with a Multichannel Systems MEA2100 60-channel signal amplifier (ALA Scientific Instruments, Inc). The Multichannel Systems software gain was set to 1200× with a sampling rate of 20 ksamples/s. Channels with high-amplitude noise were turned off in order to avoid the spread of noise to other channels. All experiments were conducted at 37^{o} C with the use of a MultiChannelSytems temperature-controller (ALA Scientific Instruments, Inc). Recordings were performed using the MultiChannel Systems data acquisition software, MC Rack, during which all 60 channels were filtered in parallel with a 4th order digital Butterworth band-pass filter from 300 Hz to 5000 Hz. Neural activity of all non-noisy channels was recorded for one hour, which ensured enough spiking activity to construct meaningful cross-correlograms. For each one-hour recording, only neuronal spikes passing a 5 standard deviation negative voltage deflection threshold, along with the time stamp of the threshold crossing, were extracted and saved to disk. Each spike waveform consisted of 1 ms of samples pre-threshold crossing and 2 ms of samples post-threshold crossing.

2.3.6. Offline Spike-Sorting

Extracted spike waveforms were spike sorted offline by the MC Rack software then imported into MATLAB (Mathworks, Inc). The spike time associated with each waveform

initially corresponded to the time at which the negative deflections of action potentials crossed the negative thresholds. Once imported into MATLAB, the sample rate was used to shift the spike times to correspond to the minimum point in the negative deflection of the spike waveforms in order for the waveforms to be evenly aligned during feature extraction. Waveforms were also trimmed to include only 0.5 ms before the minimum value of the negative deflection and 1.5 ms after the minimum value of the negative deflection. For feature extraction, principal components analysis (PCA) was performed on a feature matrix created by stacking the vectors corresponding to each waveform on a single channel. K-means clustering was then used to assign indexes to each cluster, identifying anywhere from one to five individual neurons for each channel.

2.3.7. Spike-Timing Cross-Correlation Histogram (CCH)

A spike-timing cross-correlation histogram (CCH), a measure of the relatedness of the timing of action potentials between two isolated neurons, was used as the measure of functional connectivity in this study (Freeman et al., 2013; Fujisawa et al., 2008). For the first spike-time in neuron A's spike train, a 2005 ms window was centered around the spike-time such that the location in time at which the spiked occurred became 0 on the spike delay axis. The window was then divided into 5 ms bins by centering a bin at time 0 on the delay axis and shifting the 5 ms bin in 1 ms increments in both the positive and negative directions. With this current spike from train A as a frame of reference at delay 0, the number of spikes in train B that fell into each spike delay bin were counted, leaving a histogram of the spike delay counts for a single spike in train A. These operations were then repeated for each spike in train A. The spike-timing CCH for

neuron A compared to neuron B was then generated by summing all of the single spike histograms for neuron A and low-pass filtering the final result with a 5-point boxcar filter.

Comparison of connections relied on the calculation of z-scores and strengths (Freeman et al., 2013). Z-scores are indicators of whether a neuron modulated the firing rate of a target neuron and was calculated as follows:

$$Z = \left|\frac{Y-\mu}{\mu_{sd}}\right|;$$

where *Y* is the value at the peak/trough of the maximum deflection closest to zero, μ is the mean of the particular cross-correlogram, and μ_{sd} is the standard deviation of μ for all cross-correlograms.

2.3.8. Significance Calculation of Functional Connections

In order to determine which neuronal connections were statistically significant, we used the Between-Sample Analysis of Connectivity (BSAC) methodology to detect spurious connections (Freeman et al., 2013). For all MEA cultures used within a single experimental condition, cross-correlograms and corresponding z-scores were calculated for every possible neuron pair consisting of isolated neurons existing in separate, physically distinct MEAs. Because the comparison is between two neurons existing in two different dishes, any correlation between their activities is not physiologically relevant. Using this paradigm, we built distributions of inter-culture z-scores, one for positive and another for negative connections, that could be used to empirically determine two z-score thresholds for statistical significance in each intra-culture distribution. We chose to use a threshold equivalent to the z-score corresponding to a false-discovery rate (FDR) of 0.05, meaning 5% of the inter-culture connection z-score data lay above the derived threshold value.

These positive and negative connection thresholds were then used on z-score distributions constructed from intra-culture comparisons. For the same MEAs used for the inter-culture analysis, cross-correlations and corresponding z-scores were calculated for every possible neuron pair consisting of spike-sorted neurons existing in the same MEA. These putative connections had the potential to be physiologically relevant. Positive and negative connection distributions were again constructed, this time from within culture comparisons. The thresholds determined from the across culture distributions were then applied to the positive and negative intra-culture distributions, respectively. Any connection with a z-score lying at the 5% FDR threshold or better was deemed significant and used in further analyses.

2.4. Results

2.4.1. Growth of ES-Derived Chx10-enriched MEA Cultures

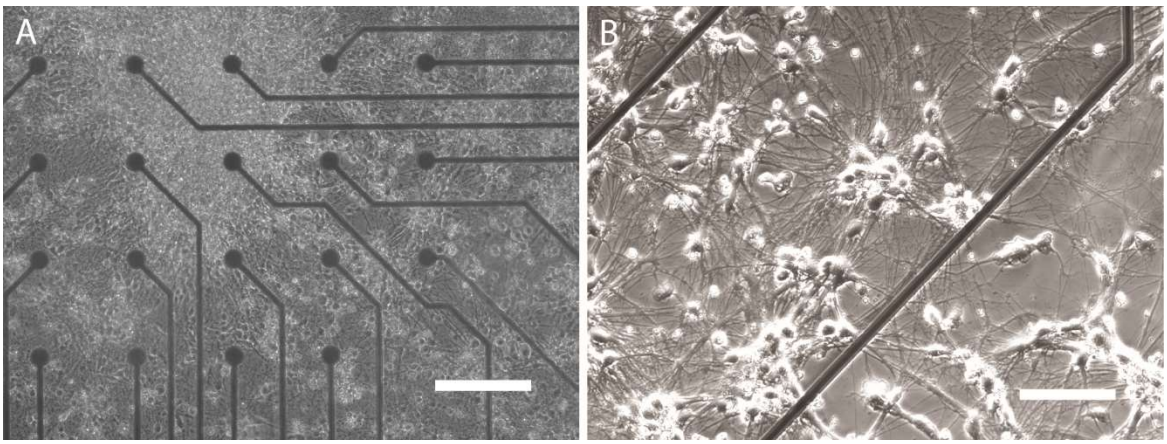

Figure 2.1. **Dissociated cultures of ES-derived Chx10-enriched populations of neurons on MEAs.** (A) 10× phase image of ES-derived dissociated neuronal cultures densely growing over the electrode contacts (black circles) at 14 days in MEA culture (B) 20× phase image of ES-derived dissociated neuronal cultures growing in small clusters on a MEA. (Scale bars = 200 μm and 100 μm respectively)

ES-derived neural populations were first driven towards increased expression of Chx10 using the six day $2^{-}/4^{+}$ induction protocol. Chx10-enriched populations were grown on MEAs in two different manners: dissociated or aggregated cultures. Dissociated Chx10-enriched populations formed a fairly uniform layer of both neurons and glia across the MEAs (**Figure 2.1**). For all of the dissociated cultures (n = 6), the majority of the 60 electrodes in each culture had cell bodies in close proximity to or on top of the electrode contacts early in development, but a subset of cultures exhibited some recession of growth that resulted in a reduction of electrode coverage. Dissociated cultures remained healthy up to the recording time points, either DIV 17 or 18. Neural aggregates of the ES-derived Chx10-enriched cells were plated on the MEAs such that the majority of the aggregates sat in the middle of the MEA dish in order to ensure coverage of the electrode contacts with neurons. Maturing aggregate cultures formed an extremely dense layer over the electrode contacts with some migration of glia radially from the main body of

aggregates (**Figure 2.2**). Aggregate cultures (n = 4) also remained healthy up to the electrophysiological recordings at DIV 17 or 18.

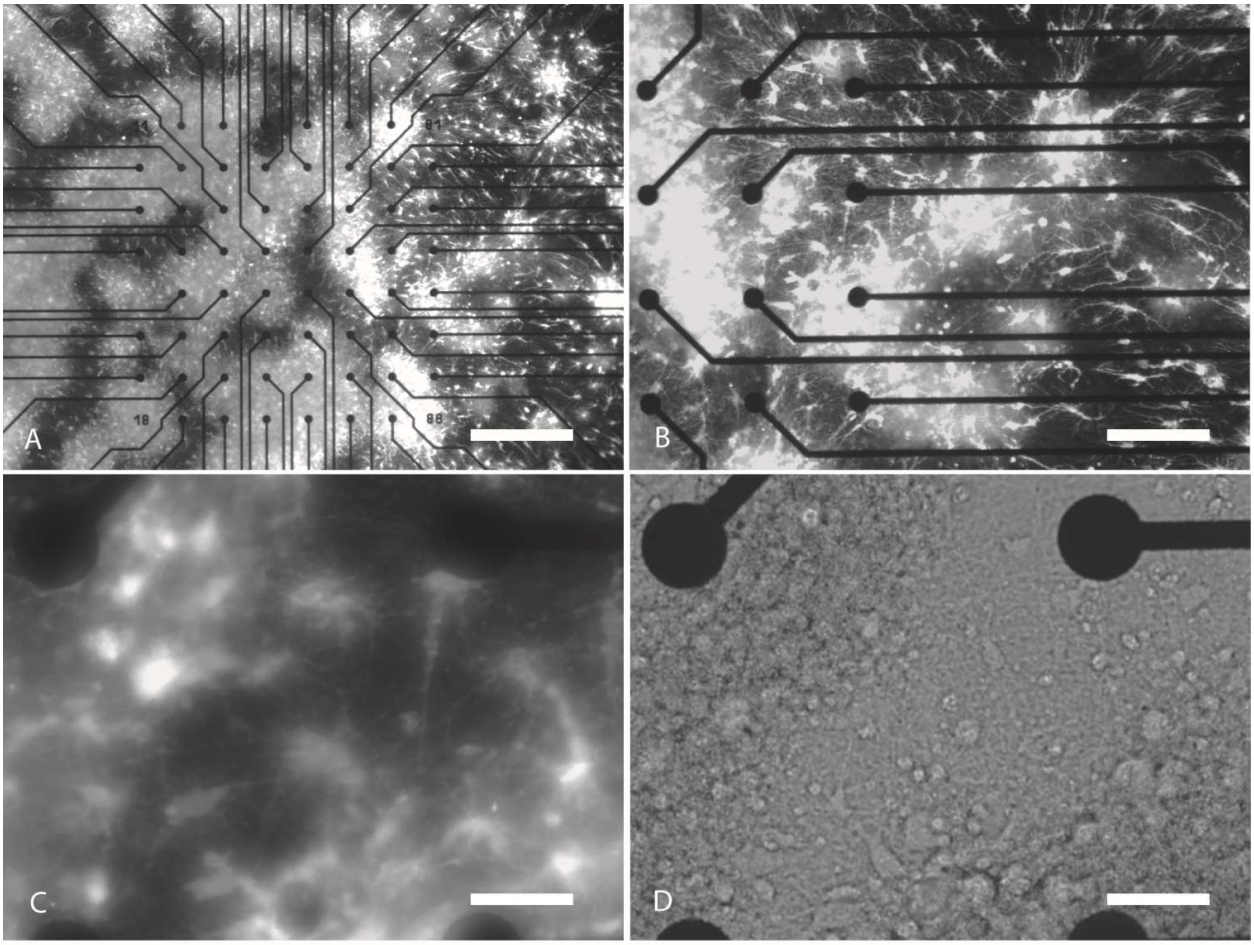

Figure 2.2 Aggregated cultures of ES-derived Chx10-enriched populations of neurons on MEAs. (A) 4× fluorescent image of ES-derived aggregated neuronal cultures densely growing over the electrode contacts (black circles) at 14 days in MEA culture. All ESC-derived cells are fluorescently labeled. (B) 10× fluorescent image of ES-derived neural aggregates clustered over the MEA electrode contacts. (C,D) 40× fluorescent and phase images, respectively, of same viewing area containing ES-derived neurons and glia in aggregate culture near MEA electrode contacts. All ESC-derived cells are fluorescently labeled. (Scale bar = 400, 200, 50 and 50 µm respectively)

2.4.2. MEAs Recorded Spontaneous Synchronized Activity

MEAs recorded spontaneous network activity in both dissociated and aggregated cultures at either DIV 17 or 18. Both culture types exhibited burst firing synchronized across MEAS,

with the synchronized bursts occurring in two groupings of firing closely positioned in time followed by long periods of silence (**Figure 2.3a**). Closer inspection of individual spike clusters showed variable levels of spike density within the bursts. **Figure 2.3b** is an exemplar of a dense burst from an electrode in a dissociated culture, while **Figure 2.3c** is an increasingly sparse burst from the same culture. Of the 6 dissociated MEA cultures and the 4 aggregated MEA cultures, all cultures displayed this double bursting behavior, which is consistent with previous investigations of MEA activity in embryonic-derived cultures between 2 and 3 weeks old (Illes et al., 2007). A small subset of electrodes in both culture types also exhibited spontaneous random firing of single action potentials interspersed amongst the bursting activity.

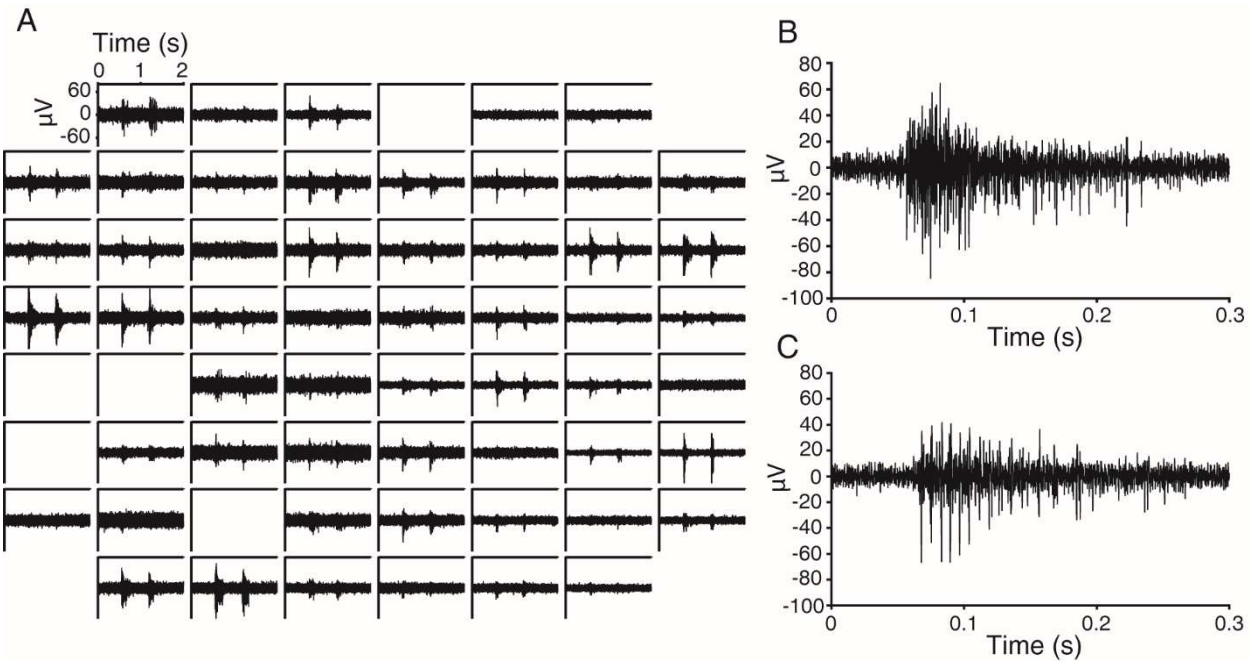

Figure 2.3 Both dissociated and aggregate cultures display synchronized bursting across MEAs. (A) 60 channel electrode arrangement from a single dissociated culture. Each square window represents the extracellular activity recorded from a single electrode over a 2 second period. The channel windows are arranged in the same configuration as the physical electrode contacts on the planar surface of the MEA. Empty windows signify noisy recordings that were set to ground in order to avoid noise interference with neighboring electrodes. (B) An enlarged display of the first neuronal burst in the activity recorded on electrode 83 (column 8, row 3). Each individual large spike represents a single action potential. (C) An enlarged display of the first neuronal burst in the activity recorded on electrode 38 (column 3, row 8). Each individual large spike represents a single action potential.

2.4.3. Identification of Individual Neurons from Spontaneous Multi-Unit Activity

Spontaneous MEA spiking activity was thresholded during recordings with a 5RMS threshold to extract the spike waveforms and spike-sorted (**Figure 2.4a**). The majority of the spike-sorted data exhibited Poisson-like spiking when the inter-spike intervals (ISI) were plotted, which is in concordance with ISI behavior in a variety of previous reports (Jones, 2004; Longtin et al., 1991; Perkel et al., 1967). **Figures 2.4b,c** show ISI histograms of two neurons spikes-

sorted from the same electrode. Both histograms are approximately exponentially distributed, implying Poisson-like behavior.

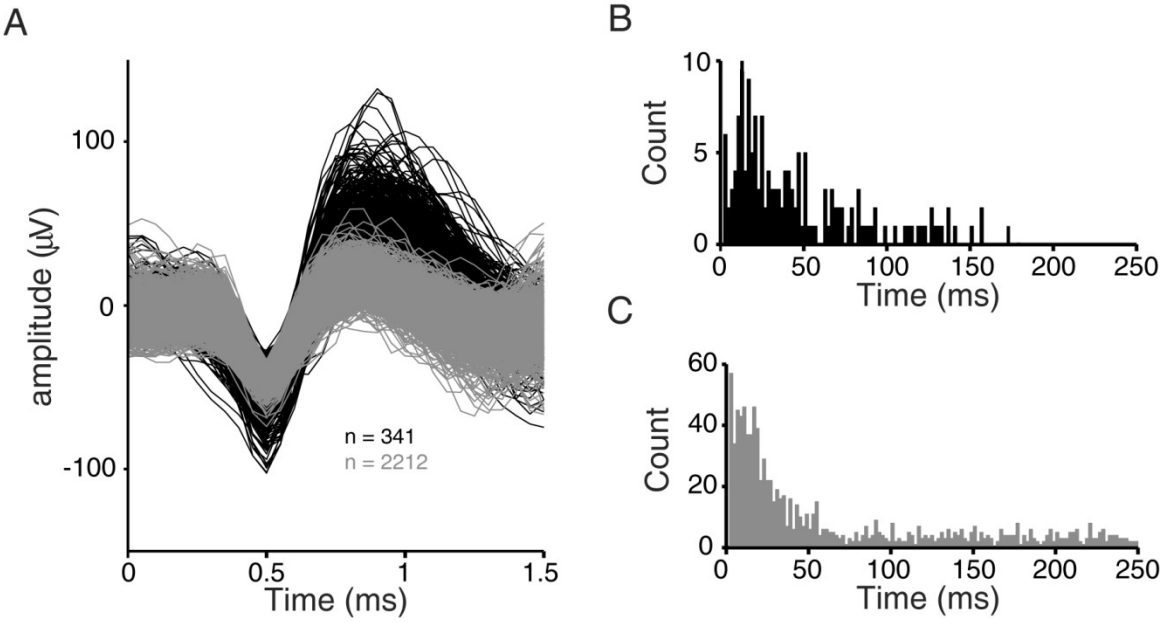

Figure 2.4 Individual neurons were isolated from single electrodes using offline PCA spike-sorting. (A) Two spike-sorted neurons recorded over a 1 hour period from the same electrode in an aggregated culture (B,C) Inter-spike intervals of the two neurons. The black and grey histograms correspond to the black and grey action potential clusters, respectively.

In total, 177 neurons were isolated across 6 dissociated MEA cultures and 162 neurons were isolated across 4 aggregated cultures. **Table 2.1** provides details about various neuron statistics from these spike-sorted units. One result that arises from the data is the difference in both the absolute number of active units per MEA between the two cultures groups as well as the difference in variability between the groups. Dissociated cultures averaged 19.7 active electrodes (electrodes with at least one neuron having over 100 action potentials during the recording period), with a standard deviation of 12.5. On the other hand, aggregated cultures averaged 32 active electrodes with a much smaller standard deviation of 4.7. The numbers of active neurons showed a similar but weaker trend with respective neuron counts of 29.5 ± 19.8 for dissociated

and 40.5 ± 9.03 for aggregated. Variability was also low in the spike rate of neurons recorded in aggregated cultures relative to dissociated cultures (**Table 2.1**). All of these neuron data suggest that the aggregate culture protocol may yield more reliable spontaneous spiking in ES-derived networks.

Table 2.1 Culture techniques drive different reliabilities in expected activity. Neurons were determined to be active if they had >100 action potentials over the hour recording period. Electrodes were signified as active if at least one active neuron was recorded from the electrode. Mean spike rate for a single MEA culture was calculated by averaging the spike rate of all active neurons within the culture.

Culture Type	MEA Culture Number	Num. Active Electrodes	Num. Active Neurons	Mean Spike Rate (sp/s)
Dissociated Cultures	1	25	37	1.3
	2	5	9	0.56
	3	29	48	0.32
	4	12	12	0.11
	5	10	16	0.28
	6	37	55	0.31
	Ave	19.7 ± 12.5	29.5 ± 19.8	0.47 ± 0.41
Aggregated Cultures	1	33	49	0.23
	2	38	47	0.32
	3	30	36	0.30
	4	27	30	0.29
	Ave	32 ± 4.7	40.5 ± 9.03	0.28 ± 0.042

Although the distributions of neurons may have varied across culture conditions, the isolated units appeared to maintain similarity in the structure of their firing patterns (**Figure 2.5**). In **Figure 2.5a**, a dissociated culture exhibits a very rigid on/off bursting structure for 45 out of the 55 neurons while 10 neurons appear to have a more spontaneous random firing structure. An aggregated culture in **Figure 2.5b** also has a synchronized bursting response, but it appears to be more widespread across all neurons in the culture, with intermittent random firing between bursts

on many of the channels. Both culture techniques yield enough neurons after spike-sorting to proceed to an assessment of connectivity in both spatial and temporal dimensions.

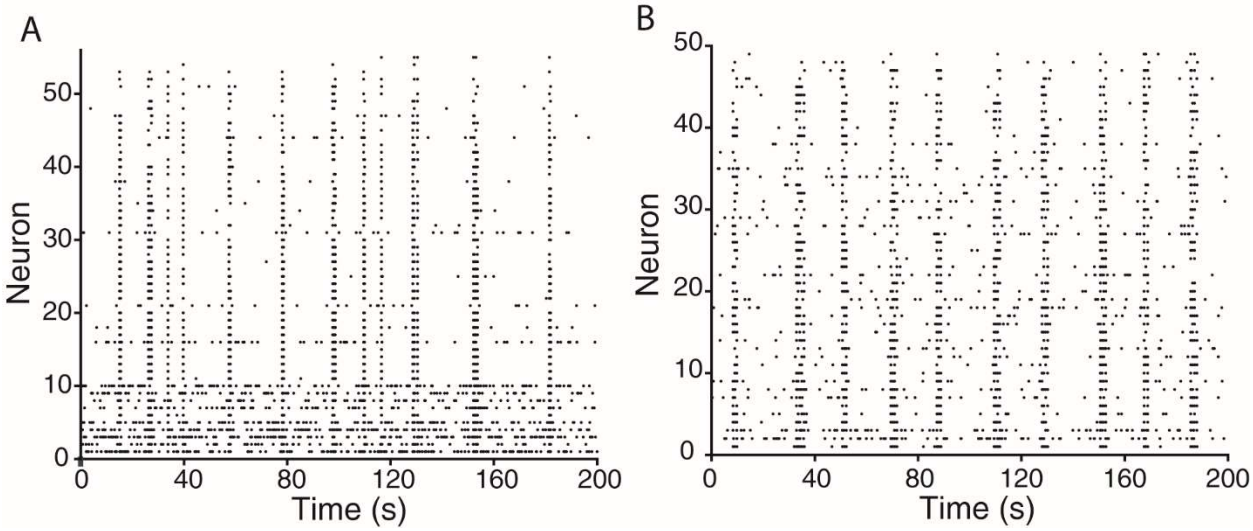

Figure 2.5 Individual neurons from MEA recordings retain synchronization observed in raw data for both types of cultures. (A) Raster plot of action potentials from all of the individual neurons (n = 55) in a single dissociated culture. Each row represents the activity of an individual neuron, where each dot represents a single action potential. Rows were sorted by the number of action potentials in the time period. (B) Raster plot of action potentials from all of the individual neurons (n = 49) in a single aggregated culture.

relative to neuron A's action potential. Essentially, these values reflect the probabilities over an entire recording period of two neurons firing at each particular time delay relative to one another. The width of the bins used in CCH can be adjusted, and in our particular application, we chose a 5 ms window to maximize the amount of neuron-level correlations captured in the analysis while minimizing network state or noise correlations that occur on broader time scales (Doiron et al., 2016). We deemed the resulting histogram the "functional connection" between a neuron pair.

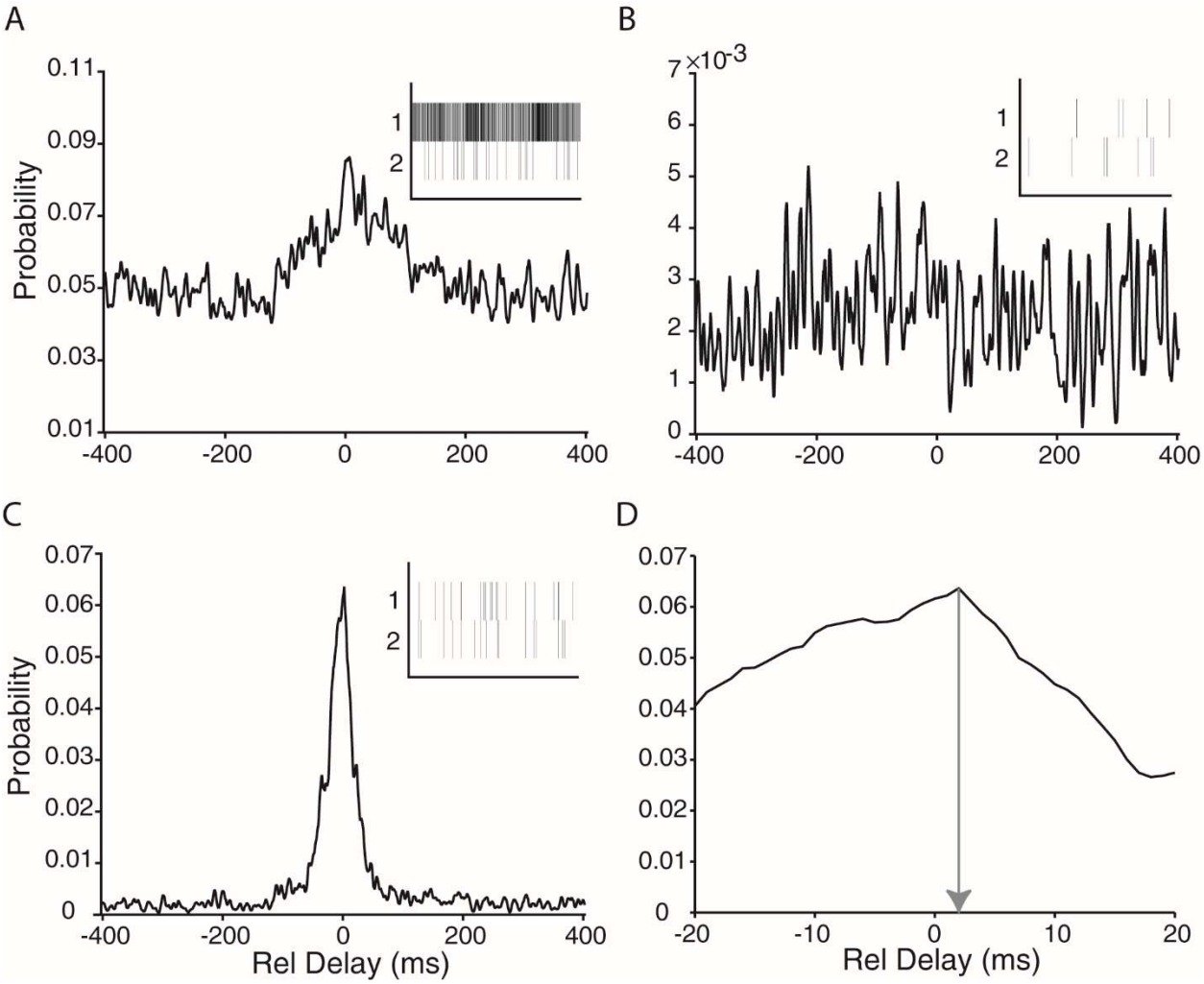

Figure 2.6 Cross-correlation histograms demonstrate different forms of connectivity between neurons. (A,B) CCHs computed from two different pairs of neurons in dissociated cultures. Inset for each figure are the raster plots of the two neurons being compared, where each row represents the activity from a single neuron for a 40 s period and the dashed lines represent action potentials. (C,D) CCHs computed between two neurons in an aggregated culture. D is a time-scaled version of C that demonstrates the peak value of this particular cross-correlogram occurs at a 2 ms connection delay, shown with the grey arrow.

Typically, peaks within the CCH signify a time relationship between neurons while a flat histogram conveys no relatedness (i.e. a uniform distribution of coincident firing probability). Depending on the firing statistics of the neurons being compared, the shape or broadness of the peaks can convey information about the underlying connection. Computing the functional

connections between neurons in both dissociated and aggregated culture conditions revealed multiple shapes of CCHs (**Figure 2.6**). **Figure 2.6a** shows two rapidly spiking neurons in a dissociated culture that are temporally related between a time delay of ±100 ms and unrelated outside of that window. In contrast, **Figure 2.6b** shows a comparison between two bursting neurons that appear to have no temporal relationship to each other. A CCH between two neurons in an aggregated culture is shown in **Figure 2.6c,d**. The histogram on the left shows a very narrow, sharp temporal relationship in the activities of the two neurons. The histogram on the right demonstrates that the peak cross-correlation value occurs at a particular relative time delay, in this case 2 ms. The time delay of the maximal (or minimal peak for negative relatedness) is one of a handful of attributes that can be derived from CCH analyses in MEAs.

2.4.5. MEAs Provide a Unique Methodology for Determining Connection Significance

In order to determine the statistical significance of putative connections between neurons, we chose a methodology that leverages the physical aspects of MEAs and has been previously validated with dissociated mouse suprachiasmatic nucleus (Freeman et al., 2013). Determining the significance of connections requires the construction of a null distribution that represents the distribution from which non-connections are drawn and deriving the significance level at which we can claim with statistical confidence that a connection was not drawn from the null distribution.

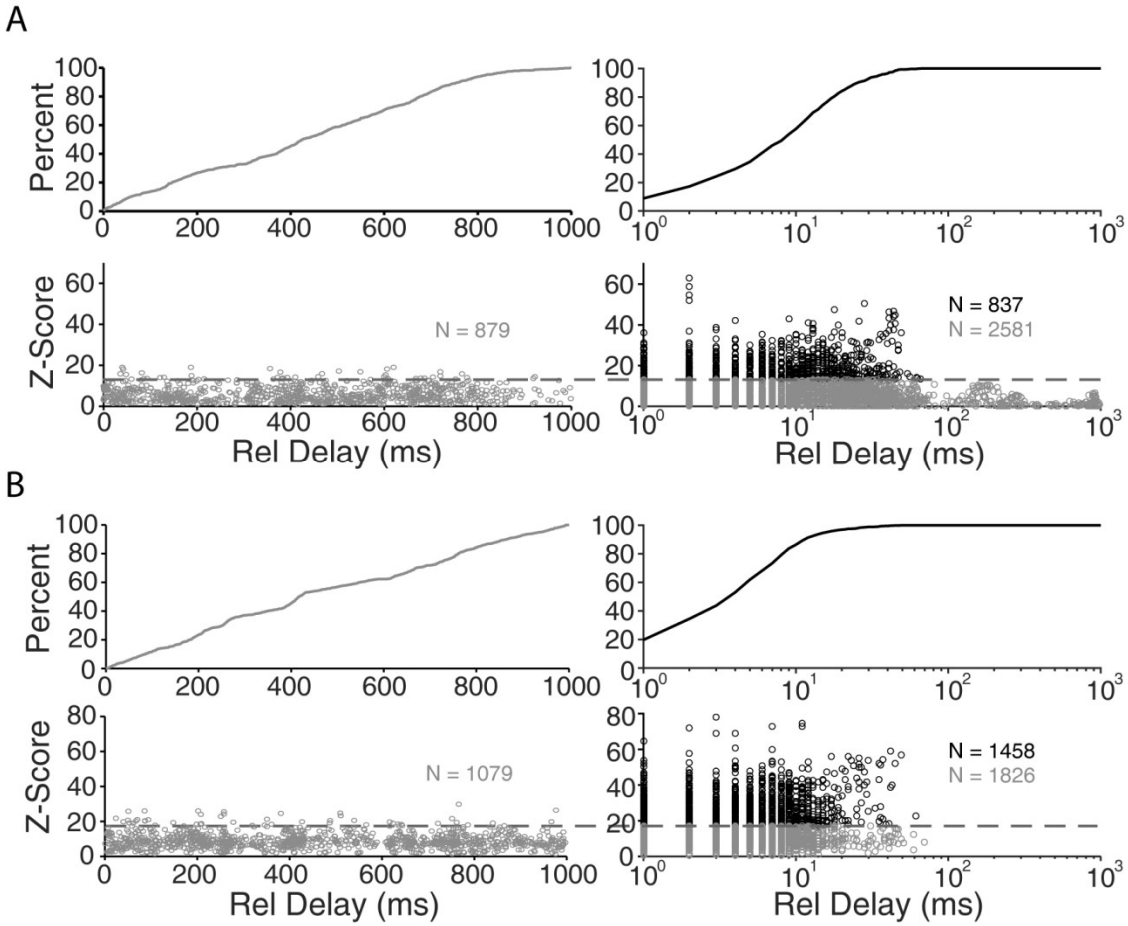

Figure 2.7 BSAC methodology allows for detection of statistically significant neuron-neuron functional connections. Black and grey circles represent the z-score of a single cross-correlogram. (A) Left-panel represents the z-score distribution of cross-correlations computed between neurons located in separate dissociated MEA cultures. These "virtual" connections were computed to serve as the chance distribution for calculating significance. A false-discovery rate of 0.05 was selected to determine the z-score significance level, 13.1, shown as the dark grey dashed line. This significance level was then applied to the distribution of cross-correlation z-scores calculated from neurons grown within the same dissociated MEA cultures, compiled across all dissociated cultures (n=6) and shown in the right panel. Altogether, 837 statistically significant connections were detected with this methodology. (B) Same methodology was applied to aggregated cultures. Significance z-score value of 17.1 was determined and 1458 significant connections were detected across all aggregated cultures (n = 4).

Figure 2.7 demonstrates not only the construction of this null distribution but also the application of the resulting significance level to the actual CCH data for both dissociated (**7a**) and aggregated (**2.7b**) cultures using BSAC. A z-score for every CCH was constructed as described in the Materials & Methods to allow for comparisons across CCH. By comparing neurons that were grown in separate MEAs, we were able to build a null distribution of 879 and 1079 peri-spike comparisons, respectively, in the bottom left panels of **Figure 2.7a-b**. As expected, these null distributions were uniform across the 1000 ms delay window, producing the diagonal cumulative curves shown in the upper left panels. The significance values at a 5% false-discovery rate, 13.1 for dissociated and 17.1 for aggregated, were applied to the z-score distributions in the bottom right panels that were derived from CCH comparisons between neurons within the same MEA culture dish. Any CCH z-score lying above the significance level was deemed a statistically significant connection.

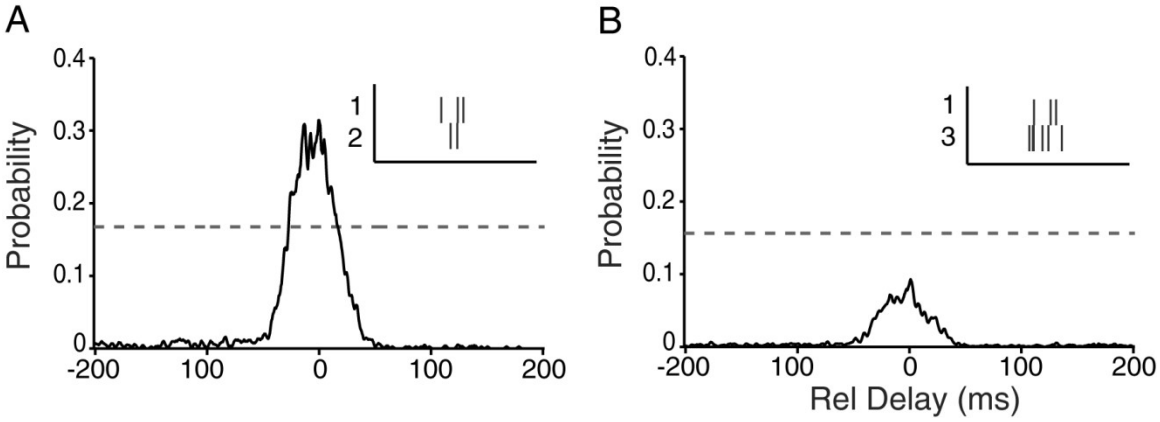

Figure 2.8 Neurons from same electrode can show different significance when compared to the same neuron on a different electrode. (A,B) Cross-correlation histograms computed from two different pairs of neurons in dissociated culture. Neuron 1 was recorded from electrode 12 while neurons 2 and 3 were recorded from electrode 14. Inset for each figure are the raster plots of the two neurons being compared, where each row represents the activity from a single neuron for a 500 ms period and the dashed lines represent action potentials. The dotted grey line in both figures represents the significance level for each respective cross-correlograms. Connections are deemed significant if at least one point in the curve meets the significance level.

For the dissociated and aggregated ES-derived cultures, 837 and 1458 significant connections were detected with the BSAC methodology, and all of the peaks of the significant connections occurred under relative delays of 66 and 61 ms, respectively. These delays are consistent with the timing that might be expected for network interactions. This method of significance detection was also sensitive enough to distinguish between multiple neuron-neuron relationships existing on a single electrode pair (**Figure 2.8**). The two neurons compared in Figure 8a were deemed statistically significant as shown by the grey dotted significance line. Even though neurons 1 and 2 had a significant connection, when neuron 1 was compared to neuron 3 (2 and 3 were recorded from the same electrode), the resulting CCH was insignificant, implying that spiking on each of these neurons did not influence spiking on the other.

2.5. Discussion

To our knowledge, this is the first comparison of the effectiveness of aggregate or neurosphere culture relative to traditional dissociated culture for the purpose of recording ESC-derived functional connectivity between identified neurons. The 3D-like structure of aggregate/neurosphere culture provide a favorable growth-promoting environment for neuronal and glial cells and have been recently used to characterize network activity in ESC-derived MEA cultures (Heikkila et al., 2009; Illes et al., 2014; Koito and Li, 2009; Lappalainen et al., 2010; Matthieu et al., 1978). Our data suggest that both culture types can support spontaneously active Chx10-enriched cultures with bursting behavior reminiscent of previous stem cell-derived MEA investigations (Ban et al., 2007; Heikkila et al., 2009; Illes et al., 2007; Illes et al., 2014; Lappalainen et al., 2010), but only aggregate cultures support repeatable electrode coverage and neuron detection compared to the high variability in dissociated MEA cultures. The

synchronized bursting activity observed in both cultures conditions is also consistent with the stem cell-derived activity characterized in previous studies (Ban et al.; Heikkila et al.; Illes et al.; Illes et al.; Lappalainen et al.). Global bursts are ubiquitous across both primary and ESC-derived cultures, but the bursting in our spinal cord ESC-derived cultures occurred at a slower burst rate compared to that of primary cultures (Maeda et al., 1995; Wagenaar et al., 2005; Wagenaar et al., 2006).

Cross-correlation histograms have been ubiquitously applied in the neuronal assembly literature to quantify the temporal relatedness between simultaneously recorded neurons (Aertsen et al., 1989; Freeman et al., 2013; Fujisawa et al., 2008; Moore et al., 1966; Perkel et al., 1967, 1967). The width of the time bins used in the calculations can also influence the type of connectivity encompassed by the histograms. State-dependent correlations in neural activity occur at longer time-scales (Doiron et al., 2016). ESC-derived MEA studies that utilize wider binning in their connectivity measures can lead to overestimates in neuron-neuron correlations (Ban et al., 2007).

Typically, these measurements are interpreted to identify the physical neural circuitry underlying the measured connectivity. For example, thin peaks can signify the existence of monosynaptic connections or shared excitatory input (Freeman et al., 2013; Fujisawa et al., 2008; Perkel et al., 1967), while broad peaks may represent shared inhibitory synaptic input (Aertsen et al., 1989; Perkel et al., 1967, 1967). Any interpretation of circuitry requires 1) the assumption of stationarity, meaning the spike rates of the simultaneously recorded neurons remain stable over various time scales (Aertsen et al., 1989; Moore et al., 1966; Perkel et al., 1967, 1967), and 2) an inspection of the auto-correlations of the individual neurons themselves (Moore et al., 1966; Perkel et al., 1967). Due to the prominent synchronized bursting and long

periods of silence in our recorded data, we cannot make a stationarity assumption, which limits what can be ascertained about each individual connection. This does not, however, diminish the utility of these statistically significant functional connections for network comparisons in the context of diagnostics. Resting state functional connectivity has become an extremely useful diagnostic tool for cortical disorders even though the circuit diagrams underlying the observed correlations between cortical areas are not well defined (Ann et al., 2016; Fox and Greicius, 2010; Woodward and Cascio, 2015). In the future, ESC-derived network functional connections could potentially be used to construct adjacency matrices and make comparisons across groups.

2.6. Conclusion

We have shown that MEAs, ESC differentiation protocols, and computational techniques can be combined to detect the network connectivity of ESC-derived neuronal populations. Our ability to leverage the nature of MEA cultures to calculate connection significance not only further validates a methodology pioneered in other systems neuroscience applications (Freeman et al., 2013), but also demonstrates its promise in characterizing the connectivity of ESC-derived transplantation candidates. Such methodologies can be expanded to explore the neurotransmitters underlying neuronal connections and the differential effects of stimulation on ESC-derived neuronal networks. Moving forward, these types of approaches, in parallel with *in vivo* transplantation studies in animal models of SCI, will provide an avenue towards generating network fingerprints of therapeutically successful ESC-relay grafting.

Chapter 3: *In Vitro* Characterization of Functional Connectivity within Stem Cell-Derived Populations of V2a Interneurons

3.1. Abstract

Recent work has suggested that stem cell-derived ventral interneuron (IN) populations may be desirable targets for transplantation therapy following spinal cord injury (SCI) due to their properties in native propriospinal circuits and favorable plasticity after the injury. One particular population, V2a INs are an intriguing candidate population due to their long, ipsilateral excitatory projections onto both IN circuits as well as motor neurons in the native spinal cord. Although highly-enriched embryonic stem cell (ESC)-derived populations of these neurons have been developed, the functional interconnectivity within these networks has yet to be ascertained with current technologies, a fundamental impediment to their therapeutic optimization for SCI. To address this limitation, we utilized a previously validated *in vitro* assay for detecting functional connectivity with ESC-derived neuronal populations. By culturing ESC-V2a INs both in various conditions and co-culture with ESC-MN/glia and modulating the network activity of the various culture groups with the application of glutamate and glycine antagonists, we were able to characterize the functional connectivity within the populations. We found that ESC-MN/glia aggregates formed active networks with a variety of activity and functional connectivity that was dependent on the transmission of glutamate. ESC-V2a INs could only survive out to the 4-week time point if they were grown in media conditioned with glial factors, but these cultures still lacked spontaneous extracellular activity. Mixed ESC-V2a/MN/glia populations formed the most active networks and had thousands of detectable connections which were also dependent on glutamate transmission. Application of glycine antagonist modulated network activity but the

underlying cause is fairly inconclusive due to possible secondary effects. High growth factor concentrations in the growth media actually decreased network activity and detectable functional connections in the mixed populations. All of these findings in this proof of concept study collectively suggest that a mixture of ESC-V2a INs and ESC-MN/glia may be the most viable candidate for transplantation and sets the stage for future investigations into the manipulability of their connectivity with electrical stimulation, as well as scaled versions of this assay performed in combination with animal studies.

3.2. Introduction

Embryonic stem cell (ESC) transplantation has become an increasingly intriguing area of pre-clinical research as a potential therapy for spinal cord injury (SCI). Stem cell-based interventions present an opportunity to enhance regeneration and rehabilitation post-injury when tailored towards injury-specific deficits. Beyond damage to existing central pattern generator networks within the cord, one of the primary drivers of the sensorimotor loss caudal to the site of injury is diminished connectivity along the damaged cord (Bunge et al., 1993; Nashmi and Fehlings, 2001; Rosenzweig et al., 2010; Takeoka et al., 2014; Zaaimi et al., 2012). Damaged axons running along the rostro-caudal axis of the spinal cord result suffer a deficit of signal transmission and overall functional connectivity across the site of injury (Donnelly and Popovich, 2008; Schwab and Bartholdi, 1996; Silver and Miller, 2004). Once transplanted post-injury, ESC-derived neurons have the potential to interconnect with one another inside the spinal cord lesion cavity, forming exogenous graft networks that have been shown to form functional bridges across the site of injury (Abematsu et al., 2010; Bonner et al., 2011; Fujimoto et al., 2012; Sharp et al., 2014).

The efficacy of ESC-derived neuronal grafts as functional relays depends heavily on the phenotypes of the graft neurons and the types of synapses they form within the graft and with host neurons. In order to achieve functional recovery, sensorimotor information must be transferred with a certain level of specificity and fidelity. Not only do ascending and descending spinal cord axons, disrupted by the injury, serve predetermined purposes due to axonal guidance cues and activity-dependent plasticity during development, but transplanted populations will exhibit specific neurotransmitter profiles as well as electrophysiological properties that will affect information transfer through the exogenous circuits (Bonner and Steward, 2015; Mothe and Tator, 2013). To this end, significant strides have been made in restricting ESC-derived neurons to particular genetically-defined subtypes (Davis-Dusenbery et al., 2014; Lippmann et al., 2015; Patani et al., 2009). Recently, specific subclasses of neurons have been generated according to transcription factor expression and shown to phenotypically resemble their *in vivo* counterparts, increasing their potential utility for therapeutic grafting (Iyer et al., 2016; McCreedy et al., 2014; McCreedy et al., 2014; Xu et al., 2015).

One ventral interneuron (IN) population defined by the expression of Chx10 in development, V2a INs, has shown to be an intriguing candidate for SCI transplantation therapy. V2a INs are ipsilaterally projecting, predominantly glutamatergic (Al-Mosawie et al., 2007; Lundfald et al., 2007) and appear to project predominantly to CPG INs as well as motor neurons (Al-Mosawie et al., 2007; Azim et al., 2014; Crone et al., 2008; Dougherty et al., 2013). For these reasons, they are prime candidates for use in creating new excitatory bridge circuits following SCI. The interconnectivity of naturally occurring V2a INs has been well examined with traditional dual whole-cell patch clamp techniques in slice preparations. For example, only electrical synapses between V2a INs have been observed in slice experiments where transverse

spinal cord slices were utilized (Zhong et al., 2010). On the other hand, $Chx10^{+}/Shox2^{+}$ neurons have been shown to have excitatory interconnections in dorsal horn-removed (longitudinal cut) patch clamp studies (Dougherty et al., 2013). Recently, highly-enriched ESC-derived populations of V2a INs were developed and characterized in dissociated cultures, exhibiting a variety of channel characteristics in response to agonist puffs and forming both excitatory and inhibitory synapses in co-culture with Olig2-positive (progenitor motorneuron) ESC-derived cells (Iyer et al., 2016) .

One shortcoming of this type of electrophysiological analysis is its low-throughput assessment of network interconnectivity due to the time-intensive aspect of *in vitro* dual patch clamp recordings (Bain et al., 1995; Buhnemann et al., 2006; Finley et al., 1996; Iyer et al., 2016; Xu et al., 2015). In vivo inquiries into graft interconnectivity with implantable electrode arrays have also been shown to under-detect neuronal connections. Lee and colleagues investigated the integration of grafted fetal spinal cord tissue neurons into rat cervical spinal cord lesions and were only able to record 23 neurons across 10 animals (Lee et al., 2014). Further characterizing the transplantation potential of ESC-derived V2a INs requires methodologies capable of simultaneously detecting the spontaneous activity of large volumes of neurons, which will allow for more accurate estimates of network functional connectivity. Better understanding of how environmental conditions and genetic identity affect functional connectivity within transplant populations is essential for optimizing graft parameters for improved information transmission through graft circuits.

Planar multi-electrode arrays (MEAs) provide an *in vitro* platform for this type of analysis by not only identifying individual neuron spiking activity, but also enabling comparison of relative spike-timing behavior of neurons across the entire array, thus allowing for reliable

identification of connectivity (Freeman et al., 2013; Fujisawa et al., 2008). We have previously shown that MEAs can be used to rapidly assay thousands of functional connections across multiple ESC-derived neuronal cultures (Chapter 2). In this present study, we apply MEAs to perform a novel large-scale characterization of the functional synaptic connectivity across highly-enriched networks of ESC-derived V2a INs which, as previously stated, is the context within which these INs will function post-transplantation. By extending our previous work to determine 1) which neurotransmitter predominantly underlies network functional connectivity observed within ES-derived V2a populations and 2) the minimal environmental conditions necessary to achieve this connectivity, we are both furthering our understanding of this particular populations' therapeutic potential, as well as establishing a general framework for extensively assaying the network properties of ESC-derived IN populations.

3.3. Methods

3.3.1. ESC Culture

A selectable Chx10-Puro mouse ESC line expressing TdTomato and a selectable Olig2-Puro mouse ESC line were developed, cultured, and differentiated for the production ESC-V2as and ESC- derived progenitor motor neurons (ESC-pMNs) as previously described (Iyer et al., 2016; McCreedy et al., 2014). Mouse ESCs were cultured on gelatin-coated T25 flasks in supplemented complete media containing Dulbelcco's Modified Eagle Medium (DMEM; Life Technologies #11965-092), 10% newborn calf serum (Life Technologies #26140-079), 1× Embryomax Nucleosides (Millipore #ES-008-D), 100 μM β-mercaptoethanol (BME; Life Technologies #21985-023) and 1000 U/mL leukemia inhibitory factor (LIF; Millipore # ESG1106). For differentiating both ESC-V2as and ESC-pMNs, a $2^{-}/4^{+}$ protocol specific to each desired neuronal population was used.

Chx10-Puro differentiation began with 10^6 cells being suspended in 10 mL of DFK5 media which consists of a DMEM/F12 base supplemented with βME, 5% knockout replacement serum (Life Technologies #10828-028), 50 μM nonessential amino acids (Life Technologies #11140-050), 1:200 100× Embryomax Nucleosides, and 100× insulin transferrin-selenium (Life Technologies #41400-045) on an agar-coated 100 mm petri dish for two days (2^-). Media was changed to DFK5 media containing 10 nM retinoic acid (RA; Sigma #R2625) and 1 μM purmorphamine (EMD Millipore #540223), and after 2 days (2^+), media was again changed to DFK5 with 10 nM RA, 1 μM purmorphamine, and 5 μM of a gamma secretase inhibitor N-[N-(3,5-difluorophenacetyl-L-alanyl)]-(S)-phenylglycine t-butyl ester (DAPT; Sigma-Aldrich #D5942) for the last two days (4^+). For the Olig2-Puro differentiation, the same 2^- portion of the protocol was used before changing the media to DFK5 supplemented with 2 μM RA and 500 nM Smoothened agonist (SAG; EMD Millipore #566660). After 2 days (2^+), media was replenished with the same supplemented DFK5 for the final 2 days (4^+) of the Olig2-Puro induction.

3.3.2. ESC Selection and Aggregate Formation

After their respective inductions, EBs of both cell lines were separately collected, dissociated with 0.25% Tryspin-EDTA (Life Technologies #25200-056), re-suspended in selection DFK5NB media consisting of DFK5 and Neurobasal (NB; Life Technologies #21103-049) at a 1:1 ratio supplemented with B-27 (Life Technologies #17504-044), glutaMAX (Life Technologies #35050-061), 5 ng/mL glial-derived neurotrophic factor (GDNF; Peprotech #450-10), 5 ng/mL brain-derived neurotrophic factor (BDNF; Peprotech #450-02), 5 ng/mL neurotrophin-3 (NT-3; Peprotech #450-03), and puromycin in water (2 μg/mL and 4 μg/mL for ESC-V2as and ESC-pMNs respectively) at a density of 5×10^5 cells/cm^2 and 5×10^4 cells/cm^2 for

ESC-V2as and ESC-pMNs, and then plated on poly-L-ornithine (Sigma-Aldrich #P4957) and laminin-coated T75 flasks. After 24 hours, were washed twice with DMEM/F12 and lifted from the flasks with a 30 minute exposure to Accutase (Sigma, #A6964) at room temperature.

Selected cells were used to create three different types of aggregates: 1) Chx10-Puro, 2) Olig2-Puro, and 3) mixed 1:1 Chx10-Puro:Olig2-Puro. For all aggregate types, 5×10^5 cells of the appropriate cell type were seeded into each well of a 400 μm Aggrewell plate (StemCell Technologies, #27845) in modified DFK5NB media (no puromycin) for 2 days of aggregate formation. Half of the media was replaced daily. Aggregates were lifted from the wells by trituration, placed in centrifuge tubes, and allowed to settle prior to being placed in MEA wells according to the relevant culture conditions for each experimental group.

3.3.3. MEA Neuronal Culture

Selected aggregates were grown on individual 8×8 electrode grid poly-L-ornithine/laminin coated S1-type MEAs with 200 μm electrode spacing and 10 μm electrode diameter (Warner Instruments #890102) in aggregated form as previously described (Chapter 2). Five types of culture groups were grown in this study: 1) Chx10-Puro 2) Glial-conditioned (GC) Chx10-Puro 3) Olig2-Puro 4) 1:1 Chx10-Puro:Olig2-Puro and 5) Growth factor (GF) optimized 1:1 Chx10-Puro:Olig2-Puro and from here-on will be respectively referred to as 1) ESC-V2a 2) GC-V2a 3) ESC-MN/glia 4) ESC-V2a/MN/glia 5) High GF ESC-V2a/MN/glia, . For ESC-V2a, ESC-MN/glia, and Mixed ESC-V2a/MN/glia MEA cultures, 1.5×10^5 cells of selected aggregates were respectively suspended in modified DFK5NB media with growth factor concentrations of 5 ng/mL GDNF, 5 ng/mL BDNF, and 5 ng/mL NT-3 and plated at the center of each MEA. For High GF ESC-V2a/MN/glia MEA cultures, 1.5×10^5 cells of selected ESC-V2a/MN/glia

aggregates were suspended in High GF DFK5NB media with GF concentrations of 200 ng/mL GDNF, 200 ng/mL BDNF, and 50 ng/mL NT-3, and 50 ng/mL PDGF and plated at the center of each MEA. For the GC-V2a MEA cultures, 1.5×10^5 cells of selected ESC-V2a aggregates were suspended in GC DFK5NB media, which consisted of modified DFKNB media with 5 ng/mL GDNF, 5 ng/mL BDNF, and 5 ng/mL NT-3 that had been used in a gelatin-plated T75 flask to support selected ESC-MN/glia dissociated progenitor MN cultures for 24 hours and prior to media collection, and were then plated at the center of each MEA. Full media changes of the appropriate modified DFKNB media were performed every two days for 6 days in MEA culture. After 6 days, the media was replaced with NB containing the same condition-appropriate supplements for the duration of culture, with a full change of media performed every two days. Images of MEA cell cultures were captured using an Olympus IX70 inverted microscope with an attached MICROfire camera.

3.3.4. MEA Recording

A Multichannel Systems MEA2100 60-channel signal amplifier (ALA Scientific Instruments, Inc) was used to amplify and record data to disk as previously described (Chapter 2). Briefly, data were recorded at 20 ksamples/s with A/D conversion at a 1200× gain. All experiments were conducted at 37^o C, and MC Rack was used as the data acquisition software. All 60 channels were filtered from 300-5000 Hz with a 4th order Butterworth filter during recordings. For all conditions, one hour of neuronal activity was recorded from all 60 channels of each MEA, where only neuronal spikes crossing a 5 standard deviation negative deflection threshold were extracted and saved to disk, along with the time stamp of the threshold crossing.

3.3.5. Pharmacology

Pharmacological agents were applied to MEA cultures through pipette bath application. For ESC-V2a/MN/glia and ESC-MN/glia cultures, 10 μM CNQX (Sigma-Aldrich #C239) and 50 μM AP-5 (Sigma-Aldrich #A5282) were added in combination in order to block glutamatergic transmission. To block glycinergic transmission, 1μM strychnine (Sigma-Aldrich #S0532) was added alone to cultures. Channel antagonists were washed out by removing the antagonist solution and rinsing cultures twice with 1 mL of NBDFK5 media prior to replacing with fresh media. After the addition or removal of channel antagonists, cultures were given 10 minutes to reach steady-state prior to the commencement of recordings.

3.3.6. Offline Spike-Sorting

Extracted waveforms were spike-sorted offline as previously described (Chapter 2). Time stamps were adjusted to correspond to the peak of the negative deflection in each spike waveform. Principal-components analysis for feature selection and k-means clustering were performed on spiking data from each individual channel on each MEA in MATLAB (Mathworks, Inc), leading to the identification of anywhere from one to six neurons recorded by a single electrode.

3.3.7. Bursting Quantification

The level of bursting in the cultures, also called “burstiness,” was quantified as described by Wagenaar and colleagues (Wagenaar et al., 2005). Recordings were divided into 1-second bins. The number of spikes across all individual neurons was counted for each 1-second bin

(summed across network). Looking at the 15% of bins with the largest number of spike counts, the fraction of spikes across the entire recording period accounted for by these top 15% bins was then computed and label f_{15}. A f_{15} close to 0.15 implies evenly distributed firing temporally, or tonic firing, across the network. Highly synchronized bursting across the network followed by periods of silence will result in a f_{15} close to 1. The burstiness index BI is then computed as

$$\text{BI} = \frac{(f_{15} - 0.15)}{0.85},$$

where BI equal to 0 implies tonic firing and BI equal to 1 implies dominating bursting.

3.3.8. Cross-Correlation Histogram

Cross-correlation histograms (CCH) were used to calculate the functional connectivity between individual neurons (Alonso and Martinez, 1998; Freeman et al., 2013; Fujisawa et al., 2008; Gerstein and Perkel, 1969; Knox, 1974; Melssen and Epping, 1987; Perkel et al., 1967). By comparing the relative timings of action potentials between two neurons, CCHs provide a measure of the relatedness of activity between two neurons. Depending on the spike train statistics of the neurons, they can be interpreted as various types of effective connectivity, i.e. monosynaptic or shared input (Aertsen et al., 1989; Herrmann and Gerstner, 2002; Kirkwood and Sears, 1978; Moore et al., 1970; Ostojic et al., 2009; Palm et al., 1988; Perkel et al., 1967). Connectivity between neurons was assessed over a 2005 ms time window with 5 ms bins sliding in 1 ms increments across the window. Histograms were then low-pass filtered with a 5-point boxcar filter. Under this framework, the strength, S, of each connection was calculated as:

$$S = \left| \frac{Y - \mu}{\mu} \right|$$

Where Y is the maximum peak or minimum trough of the deflection closest to zero and μ is the mean value of the histogram.

3.3.9. Connectivity Significance Calculations

To calculate the statistical significance of individual CCH, between-sample analysis of connectivity (BSAC) was utilized as previously described (Freeman et al., 2013). Comparisons between histograms required the calculation of connection z-scores:

$$Z = \left| \frac{Y - \mu}{\mu_{sd}} \right|$$

For each type of culture (ESC-MN/glia, GC ESC-V2a INs, etc.), each experimental condition (i.e. glutamate block) was considered separately and independently during BSAC procedures. To build the null distribution for significance calculations, z-scores were computed for CCH comparisons between every possible pair of neurons consisting of two neurons located in physically distinct MEA culture dishes for a particular condition. These inter-culture z-score distributions were used to determine the significance level corresponding to a false-discovery rate (FDR), selected according to the number of available inter-culture comparisons, for both positive and negative connections respectively. Ideally, a 0.1% FDR was selected unless the number of available samples did not permit this criterion. For example, if 1003 inter-culture comparisons existed for the positive distribution, the FDR chosen would be 0.1% for positive connections. If 103 inter-culture comparison existed for the negative distribution, the FDR chosen would be 1% for negative connections. These significance levels were then applied to intra-culture z-score distributions computed from CCH comparisons between pairs of two

neurons located within the same MEA culture dish for a particular experimental condition. Any connection z-score lying at or above the 0.1% threshold was considered significant.

3.4. Results

3.4.1. Culture Type Dictates Differential Network Activity

After differentiation and selection, all neural aggregate groups were grown on MEAs for 26-30 days prior to attempting spontaneous recordings. As can be seen in **Table 3.1**, the observed activity was determined by the culture type examined. ESC-MN/glia aggregate cultures (n = 6), consisting of motor neurons, oligodendrocytes, and astrocytes, were active across the entire cultures with an average of 30.5 ± 17.7 active neurons identified after offline spike-sorting. Bath application of CNQX and AP5 abolished spontaneous activity in these cultures such that no neurons were recorded across all cultures. Washout of glutamate antagonists recovered the number of active neurons to baseline levels. Strychnine application in the ESC-MN/glia cultures did not elicit significant changes in spike rates ($p = 0.15$, one-way ANOVA Tukey's HSD/Scheffe *post-hoc* corrected for multiple comparisons), but the excitability of the cultures does appear to trend upwards.

ESC-V2a aggregate cultures (n = 6), which consisted of nearly all Chx10-positive cells, assumed to be V2a INs, displayed no spontaneous activity across all cultures as measured by MEA recording (**Table 3.1**). On the other hand, a low-level of spontaneous activity was recorded from glial-conditioned ESC-V2a aggregate cultures (n = 5) with only 5 active neurons recorded across all cultures. A visual inspection of these both of these culture groups will be discussed later in this chapter in the context of functional connectivity.

Table 3.1 Culture identity determines neuronal activity and response to pharmacological bath conditions. Neurons were deemed active if they spiked more than 100 times in the hour recording period. Average spike rate was calculated across all neurons within a single MEA culture condition. Burstiness was calculated using 1 second bins. Average spike rate and burstiness during the application of CNQX/AP5 for ESC-MN/glia cultures were N/A because only 2 neurons were active across all cultures (n = 6). ESC-V2a statistics were N/A due to lack of any spiking active across all cultures (n = 6). Average spike rate and burstiness for glial-conditioned ESC-V2a cultures were N/A because only 5 neurons were active across all cultures (n = 5).

Culture Type	Condition	Num. Active Neurons	Ave. Spike Rate (sp/s)	Burstiness
ESC-MN/glia	Baseline	30.5 ± 17.7	1.60 ± 0.742	0.111 ± 0.032
	CNQX/AP5	N/A	N/A	N/A
	Washout	27.2 ± 13.9	1.78 ± 0.739	0.130 ± 0.057
	Strychnine	40.5 ± 15.7	3.05 ± 1.82	0.059 ± 0.020
	Washout	38.6 ± 17.6	1.38 ± 0.708	0.170 ± 0.044
ESC-V2a	Baseline	N/A	N/A	N/A
Glial-Conditioned ESC-V2a	Baseline	1.00 ± 1.41	N/A	N/A
ESC-V2a/MN/glia	Baseline	69.2 ± 32.0	4.55 ± 1.57	0.110 ± 0.057
	CNQX/AP5	14.8 ± 10.5	1.30 ± 0.874	0.175 ± 0.089
	Washout	69.0 ± 28.8	4.78 ± 1.97	0.147 ± 0.113
	Strychnine	70.2 ± 19.6	9.29 ± 4.84	0.064 ± 0.023
	Washout	81.4 ± 18.6	4.97 ± 1.96	0.165 ± 0.065
High Growth Factor ESC-V2a/MN/glia	Baseline	24.5 ± 22.2	1.33 ± 0.503	0.140 ± 0.083

ESC-V2a/MN/glia aggregate cultures (n = 6), where 50% of each neural aggregate contained V2a INs while the other 50% contained MNs and glia, were the most active of the ES-derived cultures investigated. At baseline, 69.2 ± 32.0 active neurons were detected on average across all cultures. Unlike the ESC-MN/glia cultures, the number of active neurons in the mixed 1:1 cultures was significantly reduced compared to baseline, but not completely abolished by CNQX/AP5 application ($p = 0.004$, one-way ANOVA Tukey's HSD/Scheffe *post-hoc* corrected for multiple comparisons). Spike rate was not significantly reduced during the glutamate block condition but trended downward to 1.30 ± 0.874 sp/s. Interestingly, strychnine application had no effect on the number of active neurons within the ESC-V2a/MN/glia networks but significantly increased the spike rate from both the baseline ($p = 0.0354$, one-way ANOVA

Tukey's HSD/Scheffe *post-hoc* corrected for multiple comparisons) and the washout period of glutamate blockers ($p = 0.049$, one-way ANOVA Tukey's HSD/Scheffe *post-hoc* corrected for multiple comparisons). With the average number of neurons at 24.2 ± 22.2 and average spike rates at 1.33 ± 0.503 sp/s, high GF ESC-V2a/MN/glia populations had a significantly lower number of active neurons ($p = 0.017$, paired t-test) and average spike rates ($p = 0.029$, paired t-test) than normal 1:1 mixed cultures at baseline. Differences in the morphology of these two culture groups will be discussed later in this chapter in the context of network connectivity. Burstiness, a quantification of the level of the bursting in MEA cultures, was consistently low at baseline across all culture groups with sufficient activity recorded. The only condition that appeared to significantly affect this metric by reducing synchronized network bursting was the application of strychnine for the ESC-MN/glia populations relative to both washout of CNQX/AP5 ($p = 0.031$, one-way ANOVA Tukey's HSD/Scheffe *post-hoc* corrected for multiple comparisons), washout of strychnine ($p = 0.0011$, one-way ANOVA Tukey's HSD/Scheffe *post-hoc* corrected for multiple comparisons), but not baseline ($p = 0.146$, one-way ANOVA Tukey's HSD/Scheffe *post-hoc* corrected for multiple comparisons).

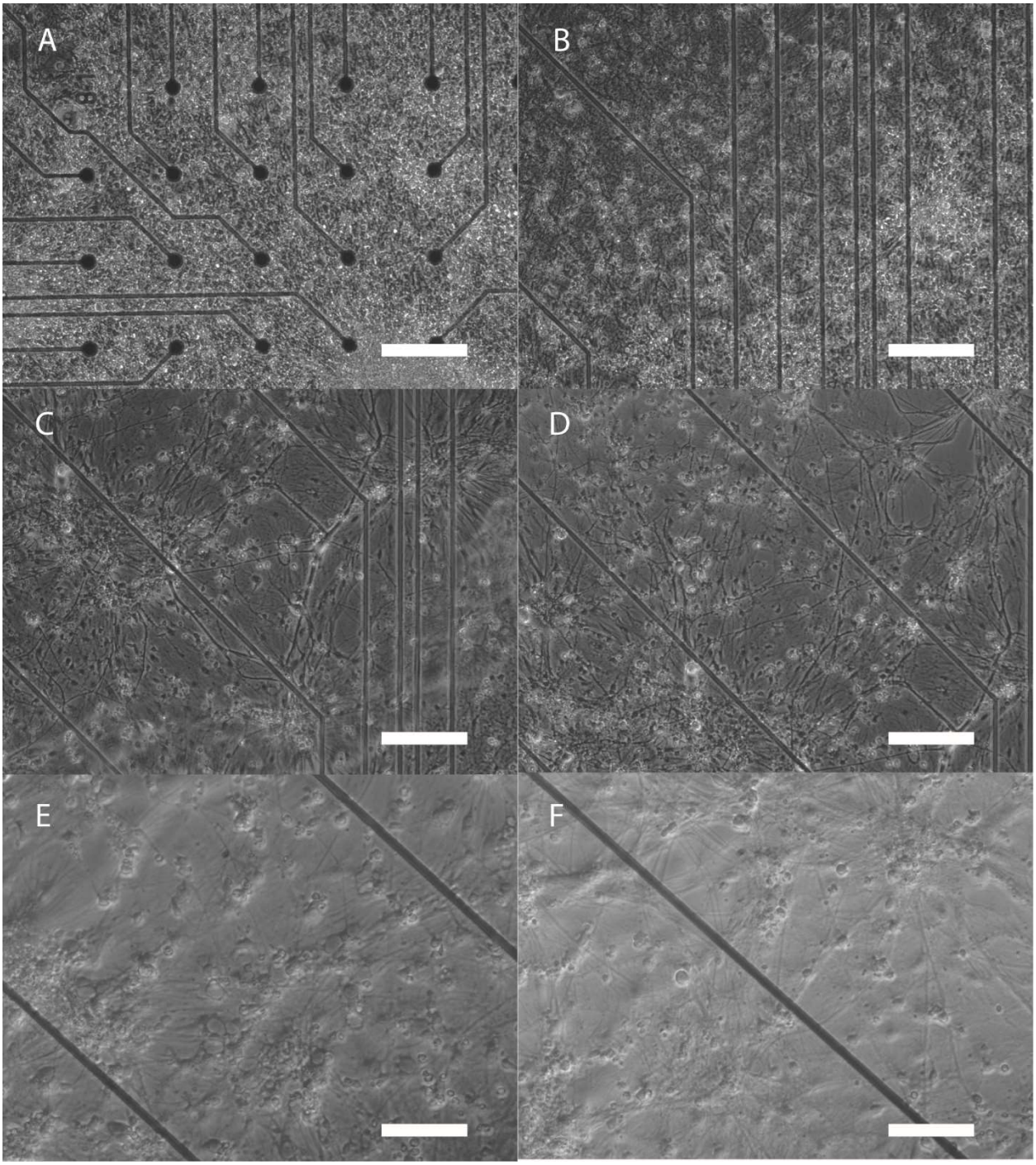

Figure 2 Aggregated cultures of ES-derived ESC-MN/glia populations proliferate on MEAs. **(A-D)** 10× phase-contrast image of ESC-MN/glia aggregate cultures growing on a planar MEA on day 28. **(E-F)** 20× phase-contrast image of ESC-MN/glia aggregate cultures growing on a planar MEA on day 28 (scale bar = 200 μm for A-D and 100 μm for E-F).

3.4.2. Robust ESC-MN/glia Networks Modulated by Glutamate Blockade

As can be seen in **Figure 3.1**, ESC-MN/glia aggregates formed dense networks when cultured on MEAs. Glia within the cultures proliferated over the time-course of the culture period and migrated outward from aggregates, which were predominantly attached near the electrode grid. At day 28, neuron morphology reflected that of healthy neuronal cultures with intact axon extensions (**Figure 3.1e-f**). ESC-MN/glia cultures exhibited both synchronized bursting and tonic firing, consistent with the type of activity that has been previously observed in MEA cultures over 4 weeks *in vitro*. **Figure 3.2** shows example segments of recordings from a

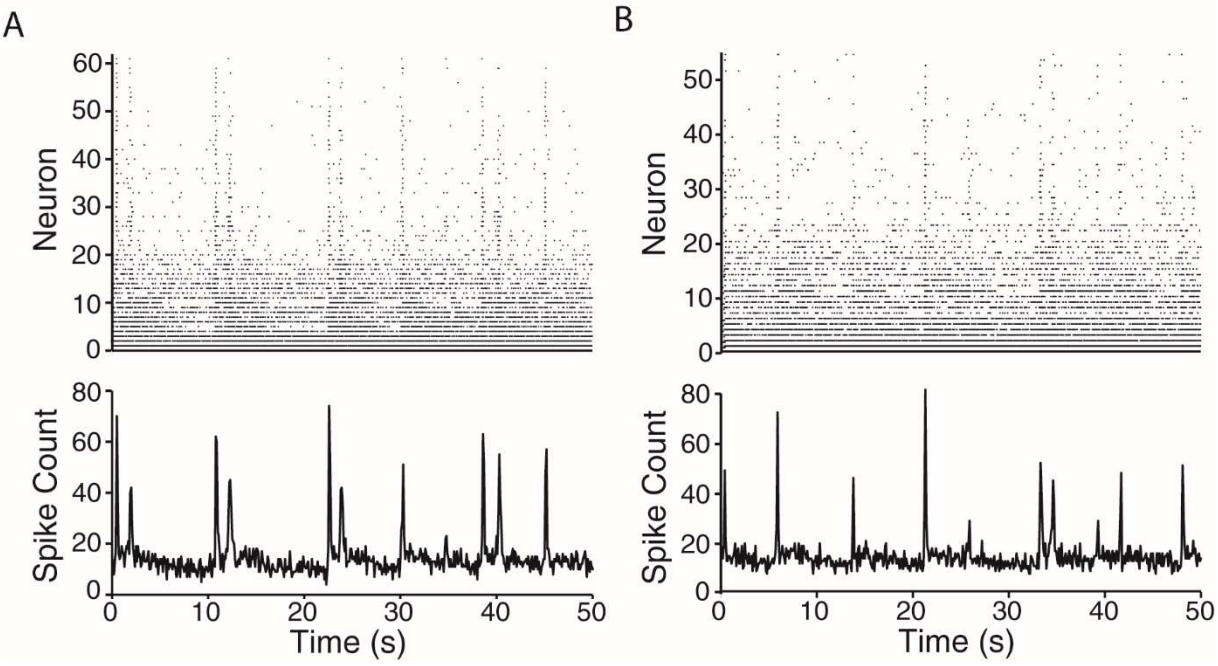

Figure 3.2 ESC-MN/glia networks exhibit both synchronized bursting and tonic activity at baseline and after washout of CNQX/AP5. **(A)** Top panel is a sorted raster plot of individual neurons recorded during baseline, and the bottom panel is the network spike count across time using 100 ms bins. **(B)** Top panel is a sorted raster plot of individual neurons recorded after washout of CNQX and AP5, and the bottom panel is the network spike count across time using 100 ms bins.

single ESC-MN/glia culture during the baseline condition and after washout of glutamate channel antagonists, CNQX and AP5. In both conditions, a subset of the isolated neurons appeared to be firing tonically throughout the segment. Another subset has prolonged spontaneous activity after each synchronized network-wide burst that slowly diminishes to silence until the next burst. The final subset of neurons was silent except for their participation in the intermittent synchronization of activity across the network. The correspondence between **Figures 3.2a** and **3.2b** suggest that the patterns of activity in ESC-MN/glia networks can be recovered through the washout procedure after bath application of CNQX and AP5.

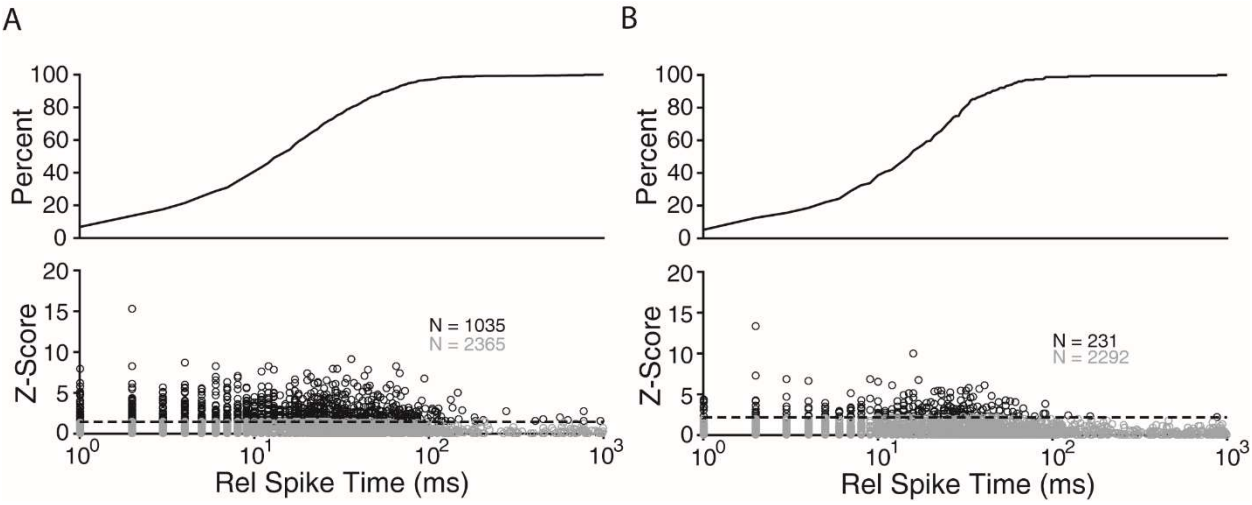

Figure 3.3 Incomplete recovery of functional connection in ESC-MN/glia cultures after washout of CNQX/AP5. **(A)** Cross-correlation z-score distribution from ESC-MN/glia cultures at baseline. At a significance level of 1.46 (black dashed line) and false discover rate of 1%, 1035 functional connections were detected (black circles) (**B**) Cross-correlation z-score distribution from ESC-MN/glia cultures after washout of CNQX and AP5. At a significance level of 2.20 (black dashed line) and false discover rate of 1%, 231 functional connections were detected (black circles).

After spike-sorting, cross-correlation histograms were computed for every pair of identified neurons within each ESC-MN/glia culture dish for the baseline and washout conditions. Cultures lacked sufficient active neurons during the CNQX/AP5 condition to compute cross-correlations and their respective significance, suggesting that 1) ESC-MN/glia

cultures may lack pacemaker neurons (or existent pacemakers didn't lie near electrodes) and 2) glutamate transmission may completely drive spontaneous activity in these cultures (or CNQX/AP5 application shifts activity towards particular regions of the culture not covering the electrodes). BSAC was used separately for each condition as originally described by Freeman and colleagues (Freeman et al., 2013) and recently validated for ESC-derived cultures (Chapter 2) to compute the significance of cross-correlations within the conditions. **Figure 3.3a** shows the resulting distribution of cross-correlation z-scores for the baseline condition. Using a false-discovery rate (FDR) of 1% (the null distribution generated from between-culture cross-correlations lacked the number of neuron pairs necessary to use a more stringent FDR), we detected 1035 statistically significant functional connections. On the other hand, a FDR of 1% led to 231 significant functional connections detected after washout of glutamate blockers (**Figure 3.3b**), thus raising the question: why only recover approximately one-fifth of the baseline number of connections.

One possible explanation is that the cultures had not completely recovered from glutamate blockade, even after three washes with fresh media and the fifteen minute waiting period prior to the start of the washout recording. A related explanation could be that washout of CNQX/AP5 does not recover the original connections but actually activates a compensatory mechanism in the network that activates a different assembly of neurons. Another explanation is further explored in **Figure 3.4**. Some specific pairs of neurons with statistically significant connectivity prior to glutamate block were able to recover that abolished connectivity after washout (**Figure 3.4a-b**). Other pairs of neurons, however, were not able to recover significant detection of their functional connectivity even though the peak of the cross-correlation histogram reached pre-blockade values (**Figure 3.4c-d**). This behavior is likely driven by the fact that

cross-correlation histograms with peaks near threshold are highly susceptible to small changes in

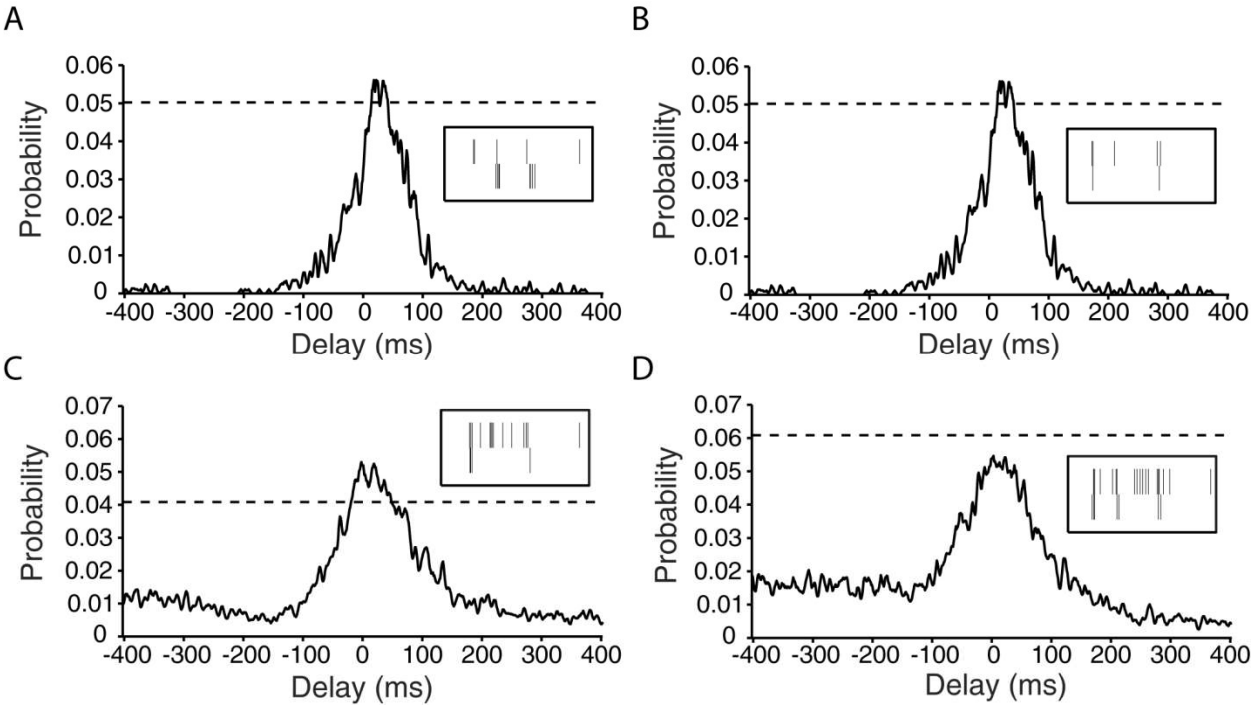

Figure 3.4 Differential significance level across conditions can lead to under-detection of connections. **(A-B)** Cross-correlation histograms of ESC-MN/glia culture functional connections between the same two neurons at baseline and after washout of CNQX/AP5, respectively, where the significance level (black dashed line) is stable across conditions. Insets are 5 second rasters of the neurons. (**C-D**) Cross-correlation histograms of ESC-MN/glia culture functional connections between the same two neurons at baseline and after washout of CNQX/AP5, respectively, where the significance level (black dashed line) is not stable across conditions. Insets are 5 second rasters of the neurons.

significance levels. As can be seen in **Figure 3.4c** and **3.4d**, the threshold level changes even though the peaks are nearly identical. These changes could potentially arise from two possible scenarios that can act independently or collectively. First, the significance level is computed in the form of a z-score before it is mapped back to the cross-correlation histogram, a mapping governed by the z-score equation described in methods (**Figure 3.3**). Assuming that the z-score significance value is equivalent between two conditions, its mapping onto each individual cross-correlation histogram is then dictated by either the individual means, μ, of the histograms in

question, or by the standard deviation of the histogram means, μ_{sd}, for each condition. If either of these values is not in agreement across conditions for the pair of neurons in consideration, the significance threshold will change for the individual histograms. The second behavior that could lead to discrepancies in between-condition probability significance levels would explain a difference in the culture condition z-score significance levels. Because the significance levels are computed from a null distribution based on between-MEA culture cross-correlation histograms (see Methods), any fluctuation in the null cross-correlation histogram distribution across culture conditions will result in a change in significance level across culture conditions.

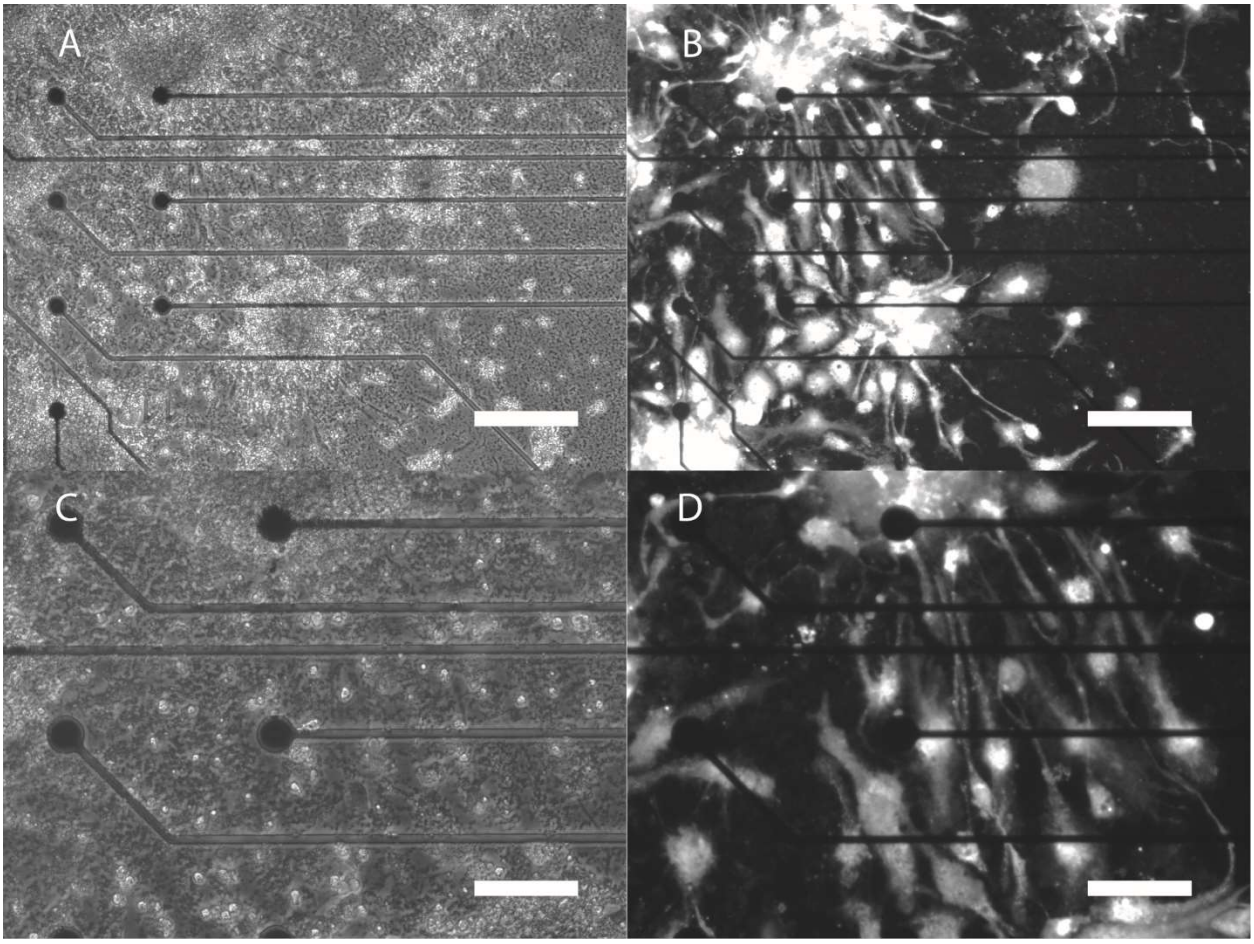

Figure 3.5 Neuronal death and glial survival in aggregated cultures of ESC-V2a populations on MEAs. **(A-B)** 10× phase-contrast image and fluorescent image, respectively, of Chx10-Puro aggregate cultures on a planar MEA on day 28. All live cells are fluorescent. **(C-D)** 20× phase-contrast image and fluorescent image, respectively, of ESC-V2a aggregate cultures growing on a planar MEA on day 28. All live cells are fluorescent (scale bar = 200 μm for A-B and 100 μm for C-D).

As discussed earlier, neurons within ESC-V2a aggregate MEA cultures did not appear to survive long enough for recordings at days 26-30 (**Figure 3.5**). Any minimal glial contamination within the cultures led to minor proliferation of the glia in the MEA cultures. Debris from axons was apparent in many of the cultures (**Figure 3.5a-c**). As expected from visual inspection of these cultures, no spontaneous activity was recorded by the MEAs (**Table 3.1**). Conditioning the growth media with glial factors released by ESC-MN/glia cultures, however, led to increased neuronal survival in the ESC-V2a aggregate cultures (**Figure 3.6**). Dense bundles of axons can

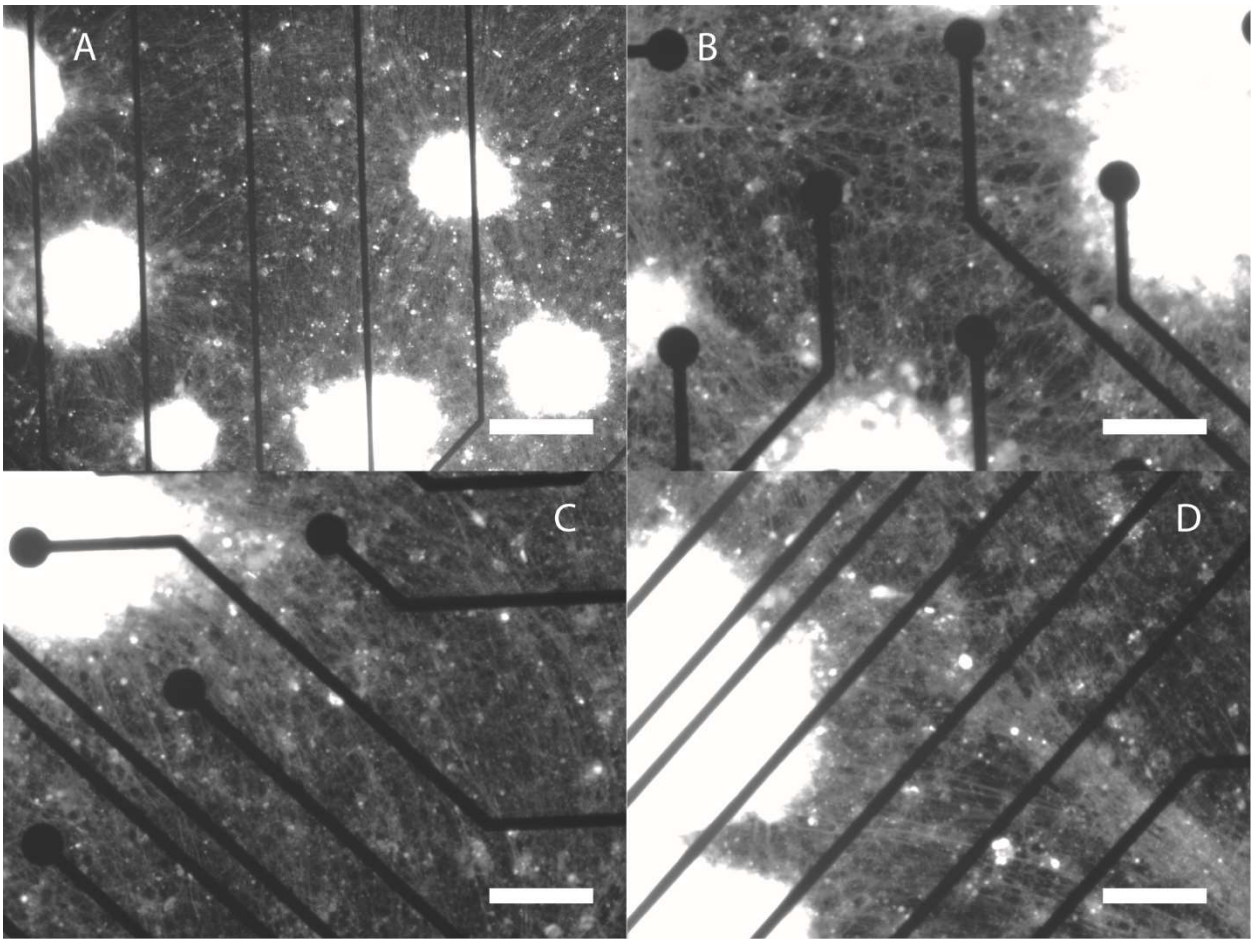

Figure 3.6 ESC-MN/glia conditioned media promotes neuronal growth and survival in aggregated cultures of GC ESC-V2a populations of neurons. (A) 10× fluorescent image of GC ESC-V2a aggregate cultures on a planar MEA on day 28 (B-D) 20× fluorescent images of GC ESC-V2a aggregate cultures growing on a planar MEA on day 28. All live cells are fluorescing in all images (scale bar = 200 μm for A and 100 μm for B-D).

be seen extending outward from the neural aggregates towards adjacent aggregates. GC media also appears to have reduced the glial contamination and proliferation within these cultures as well. This culture condition did also have an insignificant but notable effect on spontaneous activity. As mentioned earlier, five neurons were detected and deemed active across all GC ESC-V2a cultures (n = 5). Although this collection of neurons was not large enough to compute significance levels, cross-correlation histograms were still computed for the three possible unique neuron pairs, two of which are shown in **Figure 3.7**. Nothing can be stated about the statistical significance of these histograms, but they appear to have the shape typical of functional connections detected in these preparations, suggesting the potential for identifying connections if the culture conditions are further optimized in future investigations. This also suggests that these cultures may have potentially been active subthreshold of action potential generation, which the extracellular electrodes of MEAs cannot detect.

3.4.4. Individual Glutamatergic Connections Detected Throughout Mixed Cultures

MEA cultures of ESC-V2a/MN/glia aggregates were also grown out to 26-30 days *in vitro* for extracellular recordings. All cultures were healthy at the time of recording, typically with complete coverage of the electrode grid (**Figure 3.8a-b**). Aggregates clearly extended axons and contacted with adjacent aggregates, and axon bundles traveled long distances across the culture dish (**Figure 3.8c-d**). Glia derived from the ESC-MN/glia portion of the population were proliferative and remained healthy in the cultures (**Figure 3.8e**).

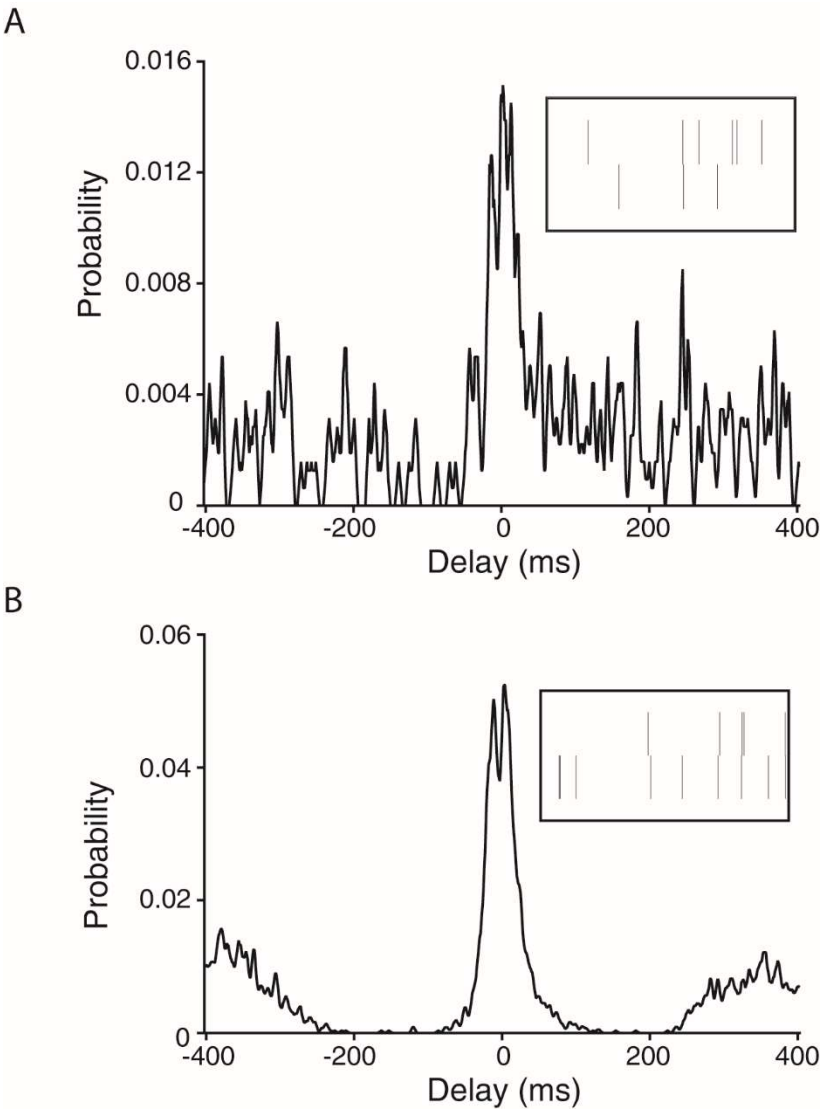

Figure 3.7 Insufficient samples to determine significance of peaks found in GC ESC-V2a culture cross-correlations. **(A-B)** Cross-correlation histograms from two different sets of neurons detected in GC ESC-V2a cultures. These represent 2 of 3 pairs detected across all cultures (n=5). Inset are the respective rasters for the neuron pairs.

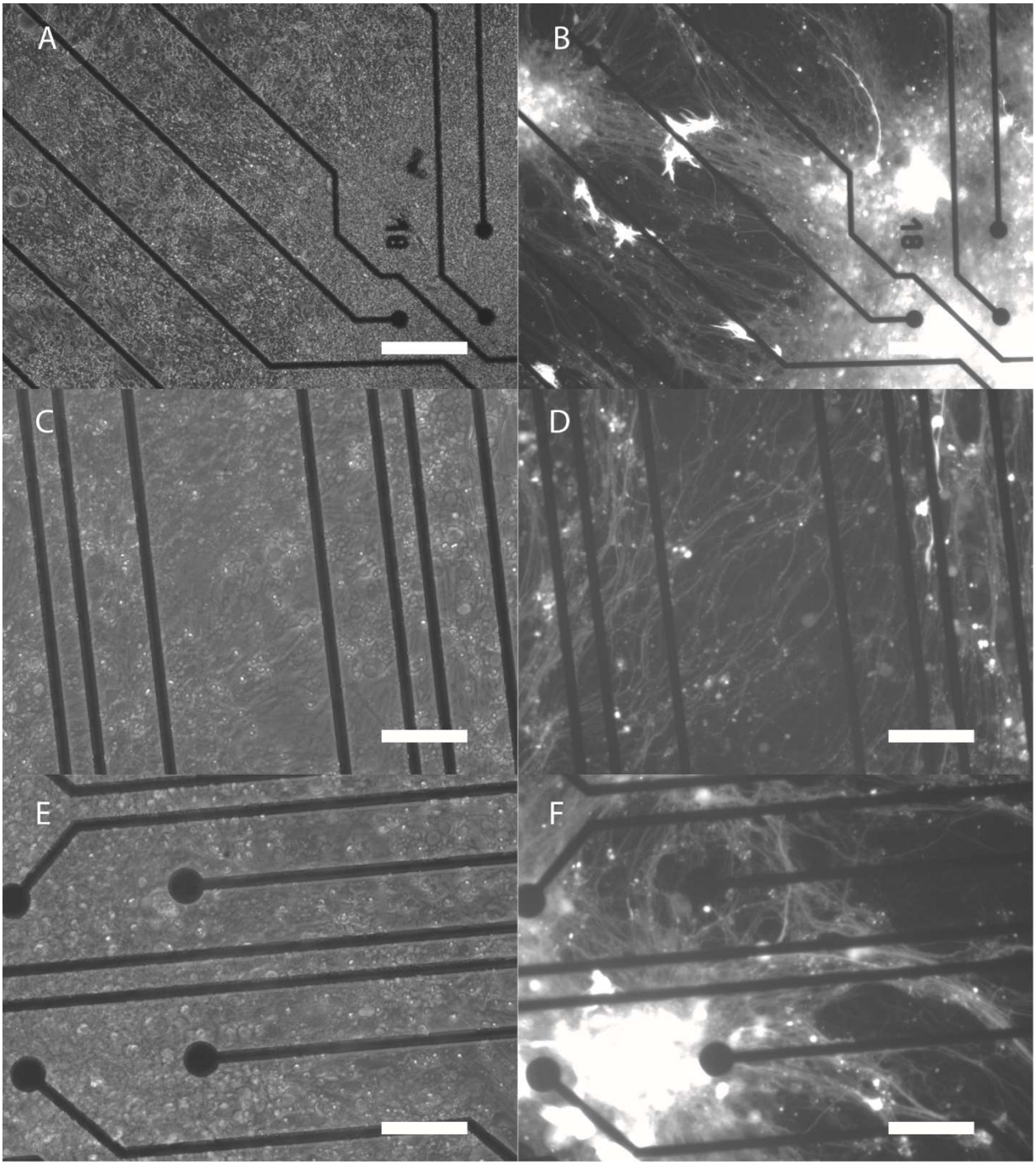

Figure 3.8 ESC-V2a/MN/glia aggregate cultures proliferate and extend axons across MEAs. **(A-B)** 10× phase-contrast and fluorescent images, respectively, of ESC-V2a/MN/glia aggregates growing near MEA electrodes on day 27 **(C-D)** 20× phase-contrast and fluorescent images, respectively, of ESC-V2a/MN/glia axons growing across an MEA on day 27 **(E-F)** 20× phase-contrast and fluorescent images, respectively, of ESC-V2a/MN/glia aggregate growing between MEA electrodes on day 27. Only cells derived from stem cells exposed to the Chx10 induction protocol are fluorescing in B, D, and F (scale bar = 200 μm for A-B and 100 μm for C-F).

Given their healthy appearance under microscopy, we then examined the spontaneous spiking behavior of mixed cultures with MEA recordings. As discussed earlier, these cultures had the most excitable networks at baseline of all of ESC-derived culture groups investigated in this study as measured by the average number of active neurons per culture (69.2 ± 32.0) and the average spike rate of active neurons (4.55 ± 1.57 sp/s). This activity-level could be seen in more detail in the baseline condition individual raster plots of these cultures (**Figure 3.9a**). For this particular culture, 95 neurons were isolated and identified as active. Similar to the behavior observed in the ESC-MN/glia group, these cultures had three categories of firing behaviors: 1) tonic, tonic bursting, and transient bursting (**Figure 3.9a**). Unlike what was sampled in the ESC-MN/glia networks, mixed aggregate network activity was not obliterated by CNQX/AP5 application (**Table 3.1, Figure 3.9b**). On average, 14.8 ± 10.5 neurons were active in this particular group. In **Figure 3.9b**, although a small subset of active neurons were was detected in this culture, bursting behavior appears to have been abolished. Their persistent activity could reveal the existence of pacemaker neurons in mixed cultures, but all fast synaptic activity would need to be blocked to confirm this speculation. A shifting of activity away from the electrode grid could also explain this phenomenon. Washout of CNQX/AP5 resulted in the resumption of the characteristic activity observed in the baseline condition, possibly suggesting full removal of glutamate blockade. (**Table 3.1, Figure 3.9c**). Similar to the ESC-MN/glia cultures, an alternative explanation could be that the effects of CNQX/AP5 persisted on the silenced neuronal assembly after washout while another assembly with different neuron membership became active.

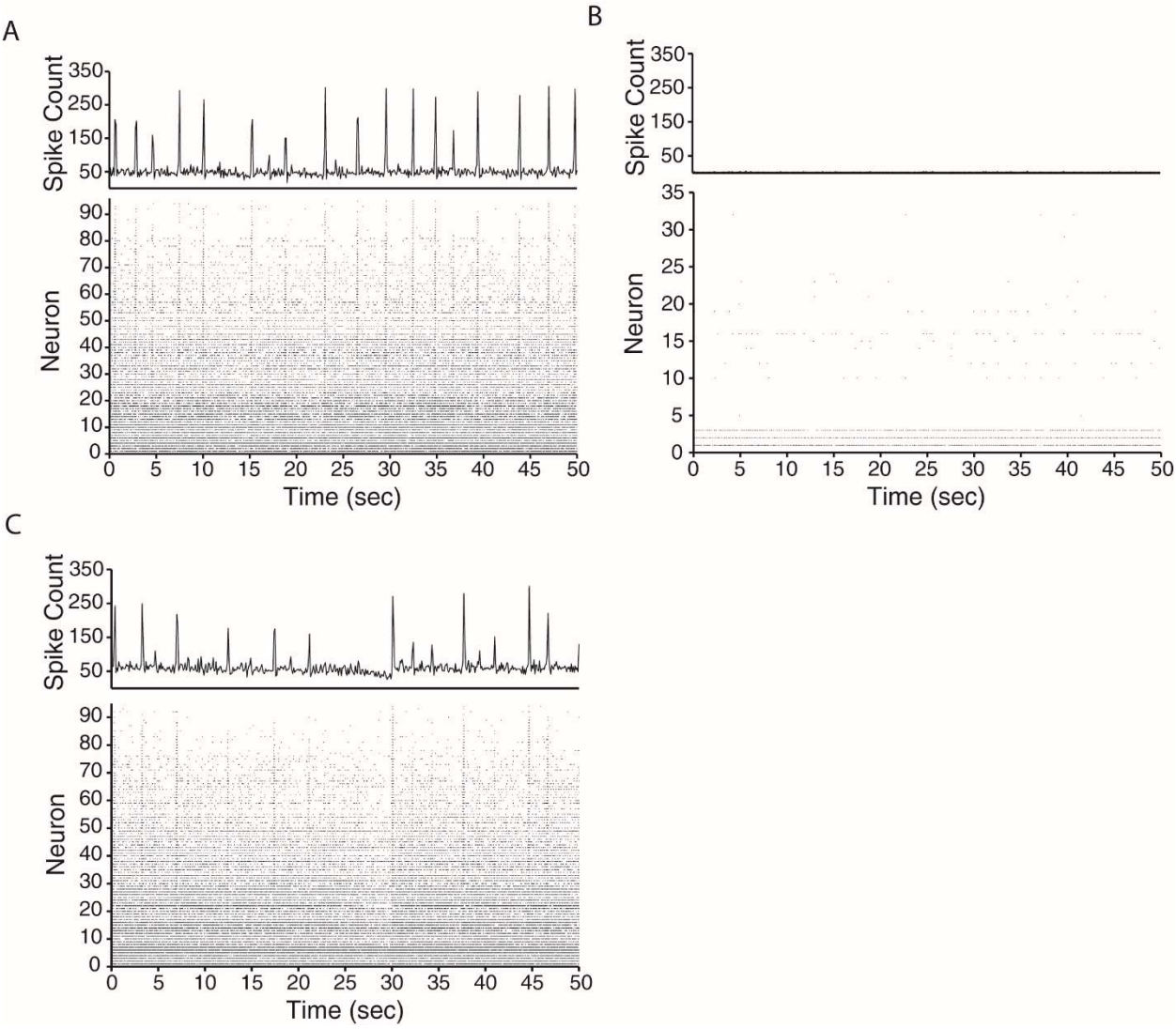

Figure 3.9 ESC-V2a/MN/glia networks exhibit high level of tonic activity with intermittent network bursts. **(A)** Bottom panel is a raster plot of spike-sorted neurons recorded during baseline, and the top panel is the network spike count across time using 100 ms bins **(B)** Bottom panel is a raster plot of the same spike-sorted neurons recorded during the application of CNQX and AP5, and the top panel is the network spike count **(C)** Bottom panel is a raster plot of the same spike-sorted neurons recorded after washout of CNQX and AP5, and the top panel is the network spike count.

After characterizing the effect of glutamate block on the network activity mixed ESC-V2a/MN/glia cultures, we used BSAC to assay the network connectivity within these cultures

(**Figure 3.10**). At a FDR of 0.1%, we detected 4219 significant functional connections in mixed cultures at baseline (**Figure 3.10a**). As expected, this number dropped drastically to 66 significant connections during glutamate block, which was assessed at a FDR of 1% due to the smaller number of active between-culture neuron pairs for building the null distribution (**Figure 3.10b**). Removal of CNQX/AP5 recovered 1653 significant connections (FDR = 0.1%), again highlighting the susceptibility of connections near threshold to shifts in the significance threshold level, similar to those seen previously in the ESC-MN/glia cultures (**Figure 3.10c**). Taken together, these data suggest that glutamate predominantly underlies the connectivity in 1:1 mixed cultures, assuming that pharmacological application is not spatially shifting activity in the culture dishes. Insets in all three sub-figures in **Figure 3.10** are the cross-correlation histograms from a single pair of neurons across the three conditions to illustrate this point. This strongly connected pair of rapidly-spiking neurons is reduced to a disconnected pair, signified by the flat cross-correlation histogram in **Figure 3.10b**. Once the receptor antagonists CNQX and AP5 are washed out of the culture, the strong connection between the pair resumes (**Figure 3.10c**).

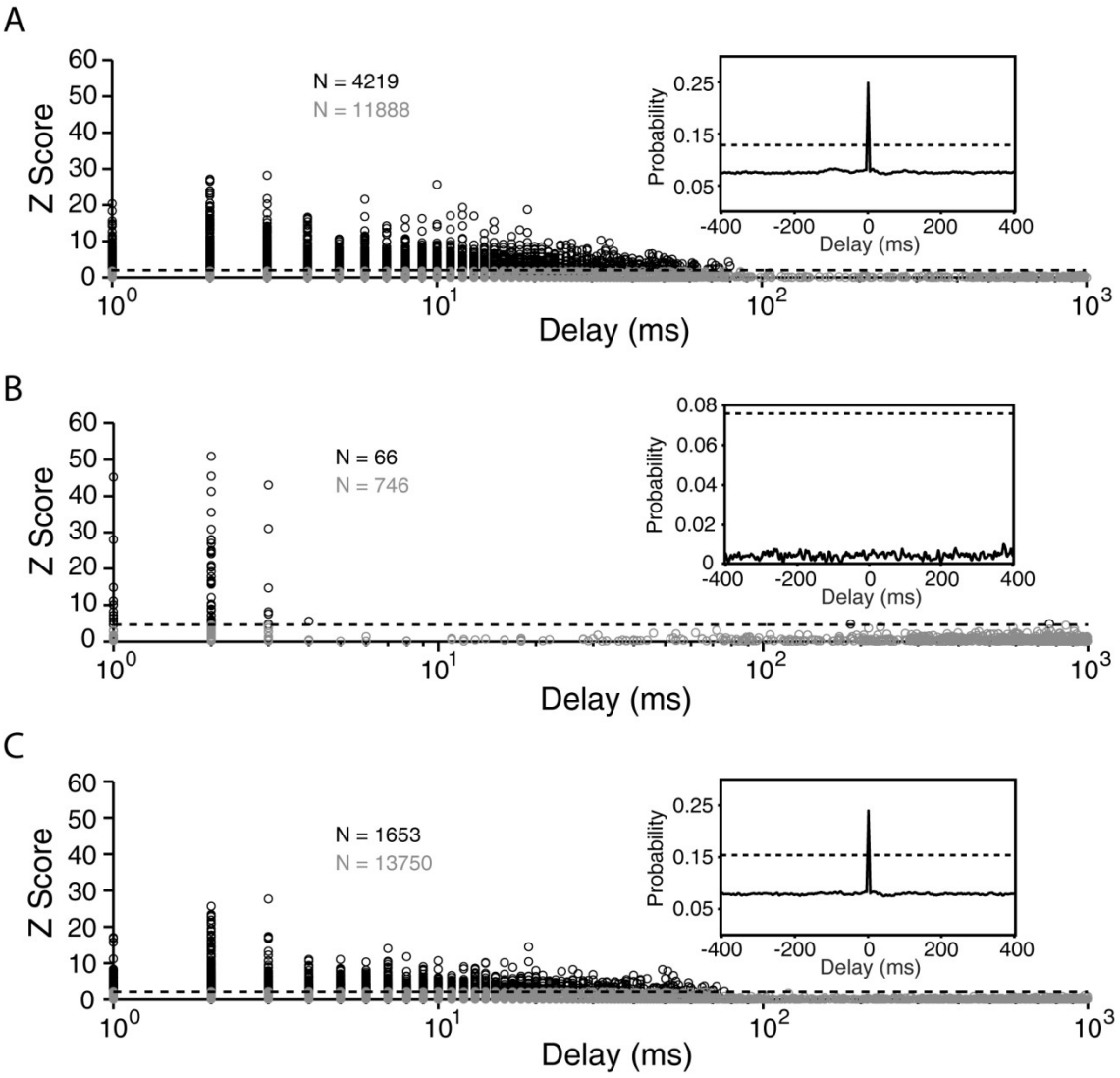

Figure 3.10 ESC-V2a/MN/glia network connections are blocked by CNQX and AP5 and recovered after washout. **(A)** Z-score distribution from mixed cultures at baseline. At a significance level of 1.71 (black dashed line) and FDR of 0.1%, 4219 functional connections were detected (black circles). Inset is an example of a significant connection between a pair of neurons **(B)** Z-score distribution from mixed cultures during CNQX/AP5 application. At a significance level of 4.60 (black dashed line) and FDR of 1%, 66 functional connections were detected (black circles). Inset is an example of the same pair of neurons unconnected during glutamate block **(C)** Z-score distribution from mixed cultures after washout of CNQX/AP5. At a significance level of 2.28 (black dashed line) and FDR of 0.1%, 1653 functional connections were recovered (black circles). Inset is an example of a significant connection between the same pair of neurons.

3.4.5. Small Quantity of Negative Connections Detected in Mixed Cultures

Mixed ESC-V2a/MN/glia cultures were also subjected to the bath application of strychnine, a competitive antagonist of the inhibitory neurotransmitter glycine to test whether glycine transmission was present in ESC-derived cultures containing V2a INs in accordance with what has been observed *in vivo* (Al-Mosawie et al., 2007; Lundfald et al., 2007). As previously mentioned, strychnine application had no significant effects on the average number of neurons detected in mixed cultures but significantly increased the average spike rate, suggesting an increase in culture excitability. To determine the effects of strychnine on network functional connectivity, BSAC was again utilized to assess the statistical significance of connections, but in this case, only cross-correlation histograms where the maximum deflection from the mean was in the negative direction i.e. a trough in the cross-correlation histogram.

Figure 3.11a shows the z-score distribution of troughs during the baseline condition. At a FDR of 0.1%, only 5 statistically significant negative connections were detected across all mixed cultures (n = 6). **Figure 3.11b** shows the z-score distribution for cross-correlation histogram troughs during strychnine application. Counterintuitively, the number of connections detected increases to 44 even though strychnine should have had the effect of blocking inhibitory transmission. To further investigate this discrepancy, we looked at individual pairs of neurons across the two conditions in question. In **Figure 3.11c** and **3.11e**, a significant trough in the cross-correlation histogram of a single pair of neurons is reduced during strychnine application such that the neurons are no longer functionally connected. The raster plots of the two neurons in **Figure 3.11d** clearly shows an inhibitory-like relationship between the neurons compared to the more complex relationship under strychnine in **Figure 3.11f**.

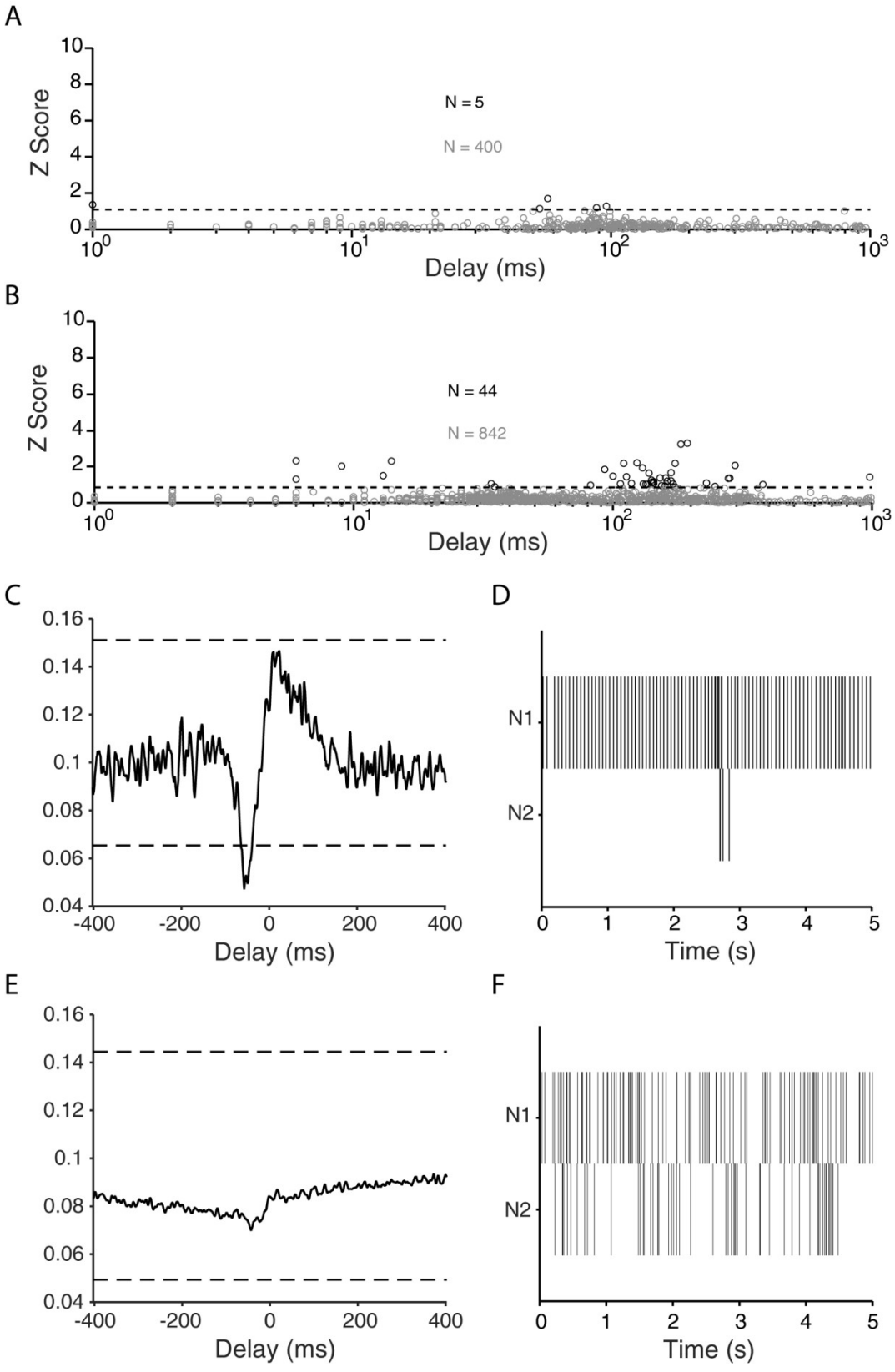
A
Z Score
N = 5
N = 400
Delay (ms)
B
Z Score
N = 44
N = 842
Delay (ms)
C
Delay (ms)
D
N1
N2
Time (s)
E
Delay (ms)
F
N1
N2
Time (s)

Figure 3.11 Inhibitory connections can be detected in ESC-V2a/MN/glia cultures and are blocked by strychnine application in some instances. **(A-B)** Negative connection z-score distributions of mixed cultures at baseline and during strychnine application, respectively. For baseline, 5 inhibitory connections are detected at a FDR of 0.1% while 44 are detected during strychnine application at an FDR of 0.1%. **(C-D)** Cross-correlation histogram of an inhibitory connection that passes the negative significance threshold alone with the raster plots of its corresponding neuron pair over a 5 s period. **(E-F)** Cross-correlation histogram of the same neuron pair during strychnine application along with the corresponding raster plots over a 5 s period.

The inconsistency between what is seen at the population level (increase in number of detected connections during strychnine) and what is seen at the individual connection level (blockade of inhibition during strychnine) could be simply explained by the low number of connections detected relative to the number of z-scores deemed insignificant. As can be seen in **Figure 3.11a-b**, the number of neuron pairs determined to be insignificant are two orders of magnitude larger than those lying above the significance threshold, suggesting the existence of a large number of comparisons near threshold relative to the number above threshold. Even miniscule shifts downward in threshold (case presented here) could potentially result in many more connections being detected. Another explanation could be the effective circuit driving the observed functional connectivity. If GABA transmission was also present in these cultures, which is plausible considering the presence of GABA in native spinal cord circuits (Malcangio and Bowery, 1996), glycine block would not remove all inhibition. Depending on the circuit, release of inhibition of a glycinergic synapse onto a GABAergic neuron could result in stronger inhibitory GABAergic connections. Strychnine has also been shown to be cooperatively allosteric at m2 and m4 muscarinic acetylcholine receptors (Gharagozloo et al., 1999; Zhang et al., 2005). Bath application could have potentially stimulated inhibitory neurons with that subset of receptors such that they became more active.

3.4.6. High Growth Factor Concentrations Reduce Network Activity of Mixed Cultures

A separate group of ESC-V2a/MN/glia cultures (n = 6) were exposed to high concentrations of GFs relevant for ESC-derived neuronal growth and maturation to test the effects of growth factor concentration on network connectivity (Calver et al., 1998; Henderson et al., 1994; Hu et al., 2008; Leitner et al., 1999). Upon examination with microscopy, there was a marked difference between the mixed networks exposed to high GF concentrations for the entire culture period relative to those with the control culture media (**Figure 3.12**). As can be seen in

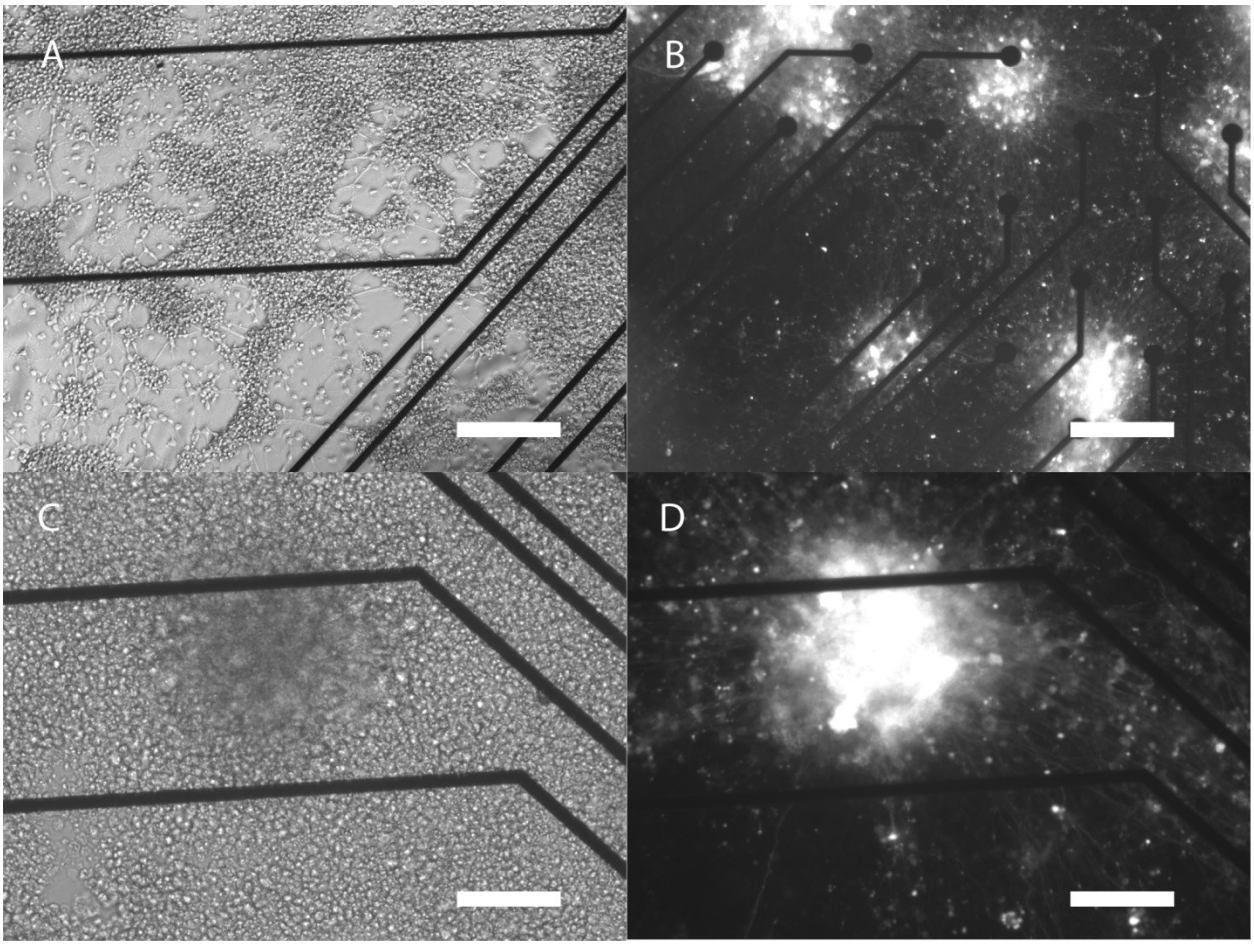

Figure 3.12 High GF ESC-V2a/MN/glia aggregate cultures extend axons across MEAs but show reduced long-term proliferation. **(A-B)** 10× phase-contrast and fluorescent images, respectively, of high GF ESC-V2a/MN/glia aggregates growing near MEA electrodes on day 28. **(C-D)** 20× phase-contrast and fluorescent images, respectively, of an aggregate in high GF ESC-V2a/MN/glia culture extending axons on day 28. Only cells derived from stem cells exposed to the Chx10 induction protocol are fluorescing (scale bar = 200 μm for A-B and 100 μm for C-D).

Figure 3.12a, high GF cultures were sparser and had increased levels debris. Axon extension density from aggregates was also visibly less in these cultures (**Figure 3.12b,d**). Spike rates in the high GF group were lower than the control mixed cultures and more comparable to those of the ESC-MN/glia cultures (**Table 3.1**). Despite the less healthy visual appearance of the cultures, spontaneous tonic and synchronized bursting activity was still observed in the networks (**Figure 3.13**). The level of bursting in these cultures was comparable to the other culture groups as quantified by the burstiness metric (**Table 3.1**).

Functional connectivity between individual neurons was then examined with cross-correlation and BSAC (**Figure 3.14**). Only 425 connections were detected at a FDR of 0.5%, which is a considerably lower quantity of connections detected relative to the control mixed populations (n = 6). This differential is readily explained by the lower number of active neurons detected in the high GF cultures. These differences may be due to negative effects being potentially associated with prolonged exposure to high concentrations of GFs. Extended periods of high-proliferation of glia may have led to cell death due to long-term overcrowding in the culture dishes. Even if the overall cell counts were similar across conditions, high GF exposure could have alternatively led to sparser connectivity due to complex interactions between GF mechanisms. Although the number of detected connections was lower, the connections that passed significance had shapes consistent with the shapes seen with the other culture groups examined in this study (**Figure 3.14 b,c**).

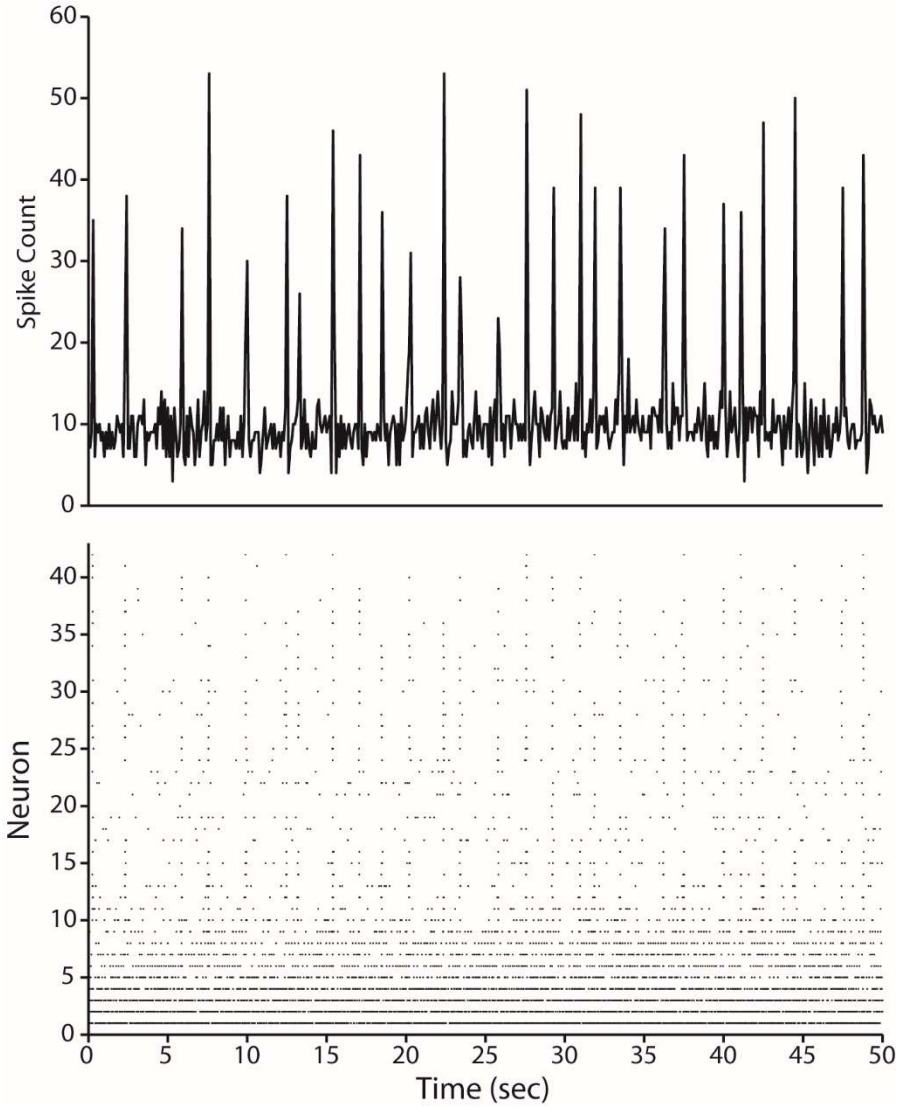

Figure 3.13 High GF ESC-V2a/MN/glia aggregates exhibit tonic activity with intermittent synchronized bursting across the network. Bottom panel is a raster plot of spike-sorted neurons recorded during baseline, and the top panel is the network spike count across time using 100 ms bins.

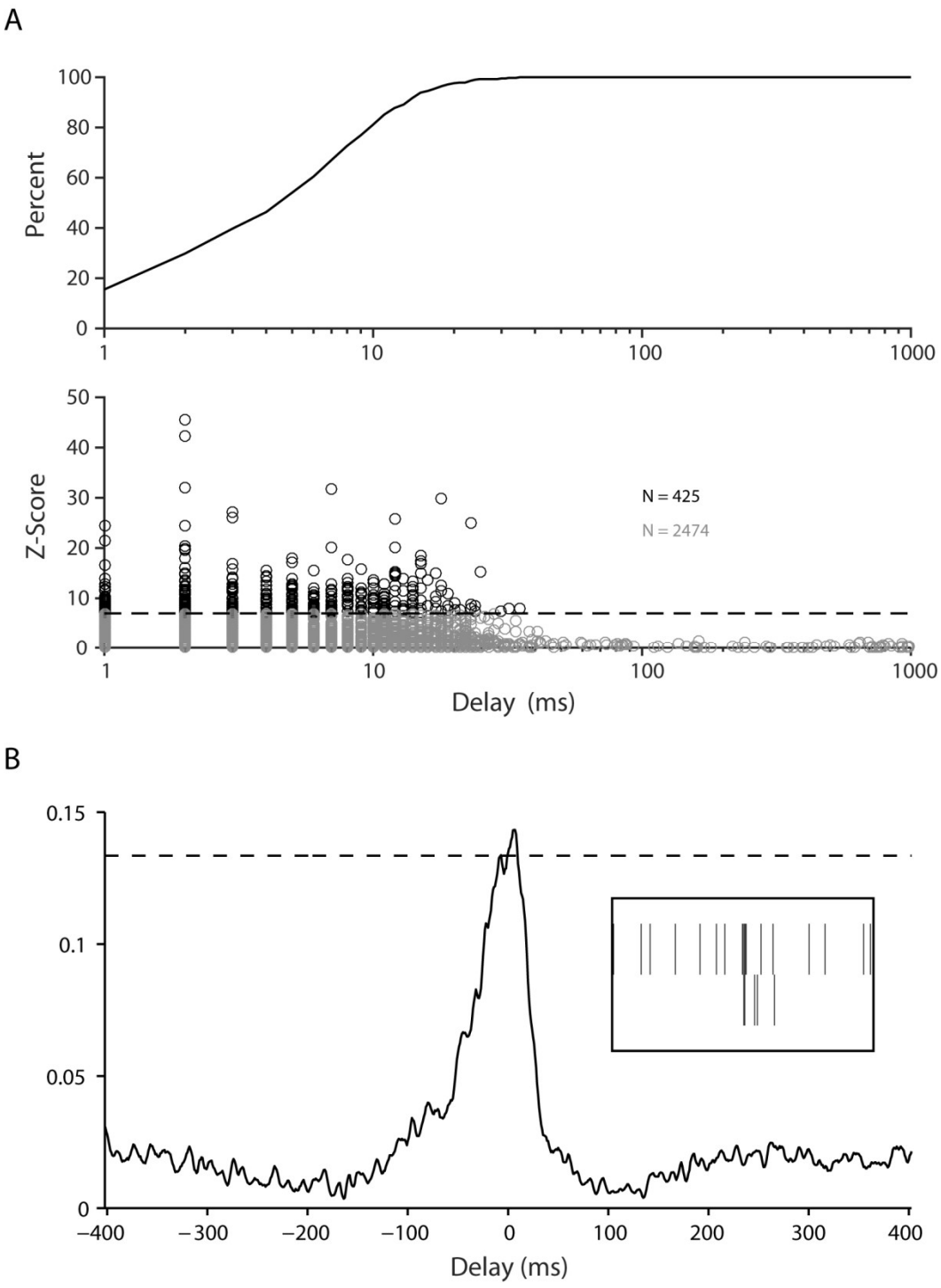

Figure 3.14 Less connectivity detected in High GF ESC-V2a/MN/glia cultures compared to control. **(A)** cross-correlation z-score distribution at baseline. At a FDR of 0.5% (dashed line), 425 functional connections were detected (black circles). (**B**) Cross-correlation histograms of a statistically significant High GF ESC-V2a/MN/glia culture functional connection between two neurons at baseline. Insets are 5 second rasters of neuron spiking.

3.5. Discussion

3.5.1. MEAs and Stem Cell Characterizations

This study presents the use of a previously developed high-throughput *in vitro* assay of functional connectivity (Chapter 2) to detect and characterize connectivity within ESC-derived V2a IN networks, a population implicated as a viable candidate for SCI transplantation therapy due to its advantageous in vivo phenotype and connectivity (Al-Mosawie et al., 2007; Azim et al., 2014; Crone et al., 2008; Dougherty et al., 2013; Lundfald et al., 2007). To our knowledge, this study represents the first attempt to rapidly detect functional connectivity between neuron pairs within purified stem cell-derived populations of transplantation candidate neurons for spinal cord injury repair. Previous studies have used dual whole-cell patch clamp to assess individual synaptic connections in purified populations of ESC-V2a and ESC-V3 interneurons, both relevant for SCI repair and were able to detect functional synapses that were modulated by application of particular neurotransmitter antagonists (Iyer et al., 2016; Xu et al., 2015). Both glutamatergic and GABAergic synapses were characterized in ESC-derived populations purified according to the L1-antibody (Jungling et al., 2003). Murine ESC-based populations have also been synaptically characterized by patch clamp both in vivo and *in vitro* (Buhnemann et al., 2006; Finley et al., 1996). Although all of these investigations provided meaningful information about synaptic formation in these ESC-derived populations, they were limited in the number of detectable connections due to the time-consuming aspects of whole-cell patch clamp, which in term prevents acquiring an overall picture of ESC-derived networks.

MEAs present in intriguing opportunity to overcome this barrier, and previous work has established MEAs as means to investigate network formation in both embryonic and induced pluripotent stem cell derived neuronal cultures (Ban et al., 2007; Heikkila et al., 2009; Illes et al.,

2007; Illes et al., 2009; Illes et al., 2014; Lappalainen et al., 2010). In particular, applications of neurotransmitter agonists and antagonists have been shown to modulate the frequency of spiking activity and bursting in stem cell-derived networks on MEAs (Heikkila et al., 2009; Illes et al., 2007; Lappalainen et al., 2010). Ban and colleagues demonstrated functional connectivity in ESC-derived cultures, but used wide time bins and multi-unit activity that can potentially average out synaptic level interactions between neurons (Ban et al., 2007). Our work utilized the cross-correlation function between every active spike-sorted neuron pair within five different purified ESC-derived populations relevant for SCI repair to detect thousands of connections between individual neurons.

3.5.2. Cross-Correlation and Functional Connectivity

This is significant considering that cross-correlation when used in such a manner is capable of capturing synaptic interactions (Bartho et al., 2004; Binder and Powers, 2001; Csicsvari et al., 1998; Fujisawa et al., 2008; Sears and Stagg, 1976; Snider et al., 1998; Turker and Powers, 2001, 2002), and these connections can be potentially used to construct topological maps of individual networks (Boehler et al., 2012; Downes et al., 2012; Marconi et al., 2012; Schroeter et al., 2015). However, there are limitations to the interpretations of the effective connectivity underlying the cross-correlation measured functional connectivity. Previous studies have stressed the importance in considering confounding factors, such as synaptic properties, background inputs, network activity, and rate correlations, which can all lead to spurious peaks in the cross-correlation function and misinterpretations of the underlying circuit diagram (Aertsen et al., 1989; Constantinidis et al., 2001; Herrmann and Gerstner, 2002; Kirkwood and Sears, 1978; Knox, 1974; Ostojic et al., 2009; Perkel et al., 1967; Veredas et al., 2005). Here, we

are limited to the information provided by the cross-correlation peak size (strength) and location (delay), as well as the distance between the electrodes being considered without any inference of the underlying neuronal circuit diagram. In the future, these attributes can still be applied to assessing functional connectivity differences between potentially therapeutic populations, such as those presented in the current study. Functional connectivity comparisons have been shown to be meaningful in diagnostics derived from resting state magnetic resonance imaging, a field with minimal understanding of the underlying structural connectivity principles (Fox and Greicius, 2010; Greicius et al., 2004; Supekar et al., 2008).

3.5.3. Glutamate Transmission Important for Isolated and Co-Cultured ESC Networks

Co-application of CNQX and AP5 obliterated network activity in ESC-MN/glia aggregate cultures, and removal of these substances returned network activity to baseline levels. CNQX and AP5 are antagonists of non-NMDA and NMDA glutamate receptors, respectively, and both receptor types have been shown to be present on the membranes of spinal MNs both in primary and ESC-derived populations (Mayer and Westbrook, 1984; McCreedy et al., 2014; Miles et al., 2004; Westbrook and Mayer, 1984). The removal of network activity suggests that glutamate underlies synaptic transmission in ESC-MN/glia cultures even though acetylcholine should be the predominant neurotransmitter according to decades-worth of previous findings (Cullheim et al., 1977; Curtis and Ryall, 1964; Eccles et al., 1954; Windhorst, 1996). Recent work, however, demonstrated the ability of spinal MNs to form glutamatergic synapses with adjacent MNs (Nishimaru et al., 2005), which could potentially explain the discrepancy. The same study also showed glutamate synapse formation between MNs and CPG interneurons, which supports the effects of CNQX/AP5 application in the ESC-V2a/MN/glia cultures as well.

These aggregate cultures had a predominant amount of activity depressed by antagonist application while a subset of neuronal activity persisted.

It should be noted that MEAs only sample a small geographic region of the larger culture network. Any conclusion has the caveat that pharmacological applications could be shifting activity to another region of the culture as opposed to silencing the entire network. Using proportionally larger grids or cultures restricted to grid regions could alleviate these concerns. V2a INs have been ubiquitously shown to be a predominantly glutamatergic population (Al-Mosawie et al., 2007; Lundfald et al., 2007), which coincides with the reduction and recovery in ESC-V2a network activity. Pacemaker behavior has been previously observed in both spinal cultures (Streit et al., 2001) and ESC-derived cultures (Illes et al., 2014) under fast synaptic blockade which may explain the persistent activity under CNQX/AP5 bath application. Blocking glutamate synapses may also just not be enough to prevent excitatory transmission in cultures containing V2a INs. Zhong and colleagues were only able to identify gap junctions between $Chx10^{+}$ INs, suggesting excitatory connectivity in the presence of neurotransmitter blockade (Zhong et al., 2010).

Testing for glycinergic synapses with strychnine application may be an even more complicated narrative for both the ESC-MN/glia and ESC-V2a/MN/glia cultures. As stated earlier, strychnine, an antagonist of glycine transmission, generated a significant increase in firing rate for ESC-V2a/MN/glia cultures and an upwards trending firing rate with ESC-MN/glia cultures. Because of the expression of glycine receptors in both ESC-derived populations (Iyer et al., 2016; McCreedy et al., 2014) and the previous finding that a small percentage of the V2a IN population is glycinergic (Al-Mosawie et al., 2007; Lundfald et al., 2007), a simple conclusion would be increased excitability resulting from glycine blockade-induced disinhibition, which

would also be supported by the knockout and recovery of individual inhibitory functional connections found in this study (**Figure 3.11**). Contradictory to this interpretation are findings that strychnine also acts as a cooperative agonist of muscarinic (acetylcholine) receptors (Gharagozloo et al., 1999; Lazareno and Birdsall, 1995; Lysikova et al., 2001; Zhang et al., 2005). Parsing the behavior observed in this study would require another set of experiments where picrotoxin was used as opposed to strychnine to block glycine transmission.

3.5.4. ESC-V2a INs Need Optimal Culture Conditions

The longevity of ESC-V2a MEA cultures appears to be dependent on the presence of glial factors in the growth media, suggesting neurons alone cannot support long-term survival. A previous protocol for highly-enriched V3 spinal interneurons similarly showed a dependence on glial-conditioned media to promote survival and synaptic formation at 2-3 weeks in culture (Xu et al., 2015). Both of these studies are in accordance with previous work that have highlighted the importance of the presence of glia to provide trophic support, neurotransmitter reuptake, and physical support in synapse formation (Brustle et al., 1999; Clarke and Barres, 2013; Keirstead et al., 2005; Sharp et al., 2010; Zhang et al., 2006). Although GC ESC-V2a cultures survived out to the 4 week time point at which electrophysiology was conducted, spontaneous extracellular activity was only recorded from five neurons total across five cultures. This does not imply, however, that these cultures were not spontaneously active. Healthy V2a INs in CPG circuits can maintain subthreshold spontaneous activity only detectable as membrane potential oscillations with the use of patch clamp (Dougherty and Kiehn, 2010; Zhong et al., 2010). Future studies may need to apply excitatory agonists, such as NMDA and/or serotonin, to promote suprathreshold activity readily identifiable by MEAs for calculation of connectivity. Electrical

stimulation may provide another means to elicit spiking activity, but the connectivity measured will not necessarily coincide with that measured with spontaneous activity (Goel and Buonomano, 2013; Kohn and Smith, 2005).

3.5.5. Diverse Neuronal Activity in Cultured and Native Circuits

Individual neurons across ESC-MN/glia, ESC-V2a/MN/glia, and High GF ESC-V2a/MN/glia exhibited a diversity of firing characteristics, including transient bursting, tonic bursting, and tonic firing, suggesting healthy maturation of the electrophysiological properties of these aggregate cultures. Synchronized bursting accompanied by more tonic forms of spiking activity have been observed across many different types stem cell-derived neuronal cultures grown on MEAs (Ban et al., 2007; Heikkila et al., 2009; Illes et al., 2007; Illes et al., 2009; Illes et al., 2014; Lappalainen et al., 2010), with activity increasing and shifting towards a mixture over the course of culture maturation (Heikkila et al., 2009; Illes et al., 2007; Lappalainen et al., 2010). Patch clamp studies have shown diverse firing characteristics for individual ESC-V2a and ESC-MN neurons (Iyer et al., 2016; McCreedy et al., 2014), which are also present in primary populations of V2a INs and MNs (Kernell et al., 1983; Martin-Caraballo and Greer, 1999; Zhong et al., 2010). Differences in the network activity phenotypes between different types of cultures are typically observed after 3-4 weeks in vitro (Bettencourt et al., 2007; Wagenaar et al., 2006). Noticeable differences in the overall activity levels of the different culture groups investigated in this study may have been driven by different proportions of genetically-defined spinal cord neurons, which was recently shown to drive differences in network speed and segmentation (Sternfeld et al., 2017).

3.6. Conclusion

In summary, we have combined planar multi-electrode arrays, transgenic stem cell technology, and functional connectivity metrics to rapidly detect and characterize network functional connectivity in transplantation candidate populations for spinal cord injury repair. In particular, stem cell-derived V2a interneurons appear to require, at bare minimum, glial trophic factors to survive out to four weeks, but may require physical glial support to form functional networks. Stem cell-derived motor neuron cultures containing glia form active networks with diverse firing characteristics and functional connectivity susceptible to modulation of glutamate transmission. Co-culture of stem cell-derived V2a INs, MNs and glia are highly active with thousands of detectable connections, the vast majority of which appear to be affected by glutamate transmission. As expected strychnine application increases neuronal excitability in both MN and mixed cultures, but the causes may be either disinhibition or activation of muscarinic receptors. Prolonged exposure to high concentrations of growth factors has detrimental effects on the robustness of the co-cultured networks. Taken together, these findings suggest 1) ESC-V2a INs may require co-culture with glia to form functional networks after transplantation 2) ESC-V2a/MN/glia aggregates may provide a robust means to graft healthy, excitatory neuronal networks and 3) Growth factor concentration may need to be variable over the time course of network development after grafting. In the future, this work can be extended towards examining the effects of stimulation on network connectivity, characterizing topological functional network differences between culture groups, and in vivo studies that investigate graft efficacy in parallel.

Chapter 4: Summary and Future Directions

4.1. Summary of Findings

Chapters 2 and 3 present a proof of concept for an *in vitro* assay capable of detecting and characterizing functional connections in transplantation candidate ESC-derived populations for spinal cord injury intervention. Developing this assay is essential for characterizing graft network formation due to the current limitations of *in vivo* and other *in vitro* methodologies. In Chapter 2, we combined multi-electrode arrays, stem cell differentiation protocols, and connectivity metrics to validate a high-throughput assay of individual function connections in ESC-derived neuronal populations enriched for Chx10-expressing V2a INs. We compared two types of culture methods, dissociation and aggregation, to determine which allowed for the most optimal electrode coverage and individual neuron detection and found that aggregate culture greatly reduced the variability in the number of covered electrodes and neurons detected. Both types of cultures resulted in actively bursting networks at days 16 and 17 *in vitro* with activity that could be readily spike-sorted. In both cases, the combination of the cross-correlation function and BSAC, a methodology previously established for studying circadian rhythm networks, was able to detect hundreds of statistically significant positive functional connections across a small sample of cultures.

The validation study in Chapter 2 opened the door for Chapter 3, which presented the characterizing of functional connectivity in a particularly intriguing transplantation candidate ESC-derived population, ESC-V2a INs, due to their excitatory, long projecting connections in native propriospinal circuits. In this particular study, we combined multi-electrode arrays, transgenic stem cell technology, and the cross-correlation function to do an in-depth comparison

of the functional connectivity in three purified ESC-derived populations developed by the Sakiyama-Elbert group: ESC-V2a INs, ESC-MN/glia, and mixed ESC-V2a/MN/glia. By exposing aggregate cultures of these groups to various culture conditions, we could compare their effects on connectivity. The control population, ESC-MN/glia, exhibited robust bursting and tonic activity that was completely abolished by the application of glutamate antagonists CNQX and AP5 and recovered after antagonist washout, suggesting glutamate transmission underlying connectivity in these cultures. The glycine antagonist strychnine increased network excitability as expected but may have resulted from excitation of muscarinic receptors as opposed to reduced network inhibition. In all of these conditions except glutamate blockade, hundreds of functional connections could be robustly detected. In ESC-V2a IN cultures, we found that conditioning the media with trophic factors released from glia was necessary for neuronal survival but generally did not produce spontaneous extracellular activity, suggesting the need for further culture condition optimization or application of excitatory pharmacological agents in order to test for functional connectivity.

ESC-V2a/MN/glia aggregate cultures, by far the most active culture group, exhibited spontaneous bursting and tonic activity at high spiking rates compared to the other populations. BSAC detected thousands of functional connections in this group, and although CNQX and AP5 application significantly reduced the number of active neurons, many of those remaining active became disconnected. Glutamate antagonist washout recovered a comparable number of active neurons, but a different experimental setup would be needed to definitively parse whether these were the same neurons or a different neural assembly that becomes more active after CNQX/AP5 washout. Results from strychnine application were again complicated in this group as well. Excitability increases may not have been attributable to disinhibition, but upon inspection of

detected individual negative connections, strychnine application did abolish these connections even if the neurons remained active. Finally, ESC-V2a/MN/glia cultures were also grown in high growth factor concentrations to determine if this condition positively affected network functional connectivity. In actuality, network activity and the number of detected functional connections were much lower in this group compared to the normal mixed cultures.

Five main conclusions can be drawn from this work as a whole: 1) This assay can reliably detect positive functional connections. 2) Assuming that an excitation:inhibition ratio of 100:1 is unlikely in stable networks (which is what was observed in the ESC-V2a/MN/glia group), this assay may be less sensitive to negative functional connections. 3) ESC-V2a INs are not viable unmodified as transplantation candidates. 4) Mixed ESC-V2a/MN/glia appear to be the most viable candidate population in terms of the robust activity and connectivity detected in this study. 5) Prolonged exposure to high growth factor concentrations may be detrimental to the long-term survival and viability of ESC-derived networks. All of these conclusions must be taken in the context of the undersampling of the overall network in neuronal cultures due to the limitations of MEAs.

4.2. Recommendations for Future Directions

This technology and initial research will lay the foundation for efficient modeling and characterization of the functional connectivity within ES-derived neuronal grafts *in vitro*, with the expectation that this will inform strategies for their transplantation after SCI. The proof of concept presented in this thesis will allow increasingly accurate tracking of network connectivity in candidate neuronal subtypes, both those used in these aims and others, during the application of growth factors, pharmacological agents, and possibly electrical stimulation. Data gathered

from this reduced and controlled biological assay will help to generate informed hypotheses about how ES-derived neurons within the graft may interact with each other *in vivo*. Developing optimal manipulations to alter the intrinsic functional connectivity within ES-derived networks *in vitro* will directly inform similar protocols to promote recovery through transplantation therapies in animal models of SCI. The following sections further elaborate on future directions for the work carried out in this thesis.

4.2.1. Quantifying Topological Differences Across Populations

This thesis strictly focused on the high-throughput detection of connections between individual neuron pairs. Although this alone allows for a characterization of the functional connectivity observed in various types of ESC-derived transplantation candidates, such as ESC-V2a INs, it could potentially be extended to examine whole-network topological differences between populations. Network theory provides a mathematical framework to do so by treating connections between neurons as edges between nodes in a graph. This graph can then be represented as an adjacency matrix (A_{ij} equals 1 if nodes *i* and *j* have a direct connection, A_{ij} equals 0 otherwise), which opens the door for a plethora of analytical avenues to characterize network topology.

One such avenue, graph theory, has been extensively explored in the resting state fMRI literature and allows for statistical measures to be applied to adjacency matrix representations of graphs or networks (Bullmore and Bassett, 2011). In recent years, this methodology has also been utilized to characterize functional connectivity topology in MEA cultures (Boehler et al., 2012; Downes et al., 2012; Marconi et al., 2012; Schroeter et al., 2015). Common statistical measures such as node degree, average cluster coefficient, average path length, and small-world

index allow for topology comparisons across groups or conditions (Poli et al., 2015). Fundamental caveats exist, though, when considering applications for these statistical metrics in MEA functional network topology: graphs must have the same number of nodes to be compared using conventional graph theory statistics (Bollobas, 2001), and the statistical measures tend to be correlated to each other (Meskaldji et al., 2013). Graph transformations have been developed to attempt to overcome this restriction, but none of them appear to be consistently reliable and unbiased (van Wijk et al., 2010). The number of detected nodes (neurons) in MEA functional connectivity studies is inherently going to be variable across cultures, meaning future studies must take this into account when designing experiments and choosing metrics.

One emerging field of parametric network statistics, object-oriented data analysis (OODA), appears to overcome some of the limitations of graph theory when comparing across populations (Marron and Alonso, 2014). This framework typically maps sets of networks or trees into a Euclidean space, models their underlying distributions, and then uses various metrics to calculate whether graphs drawn from one population are statistically different than graphs drawn from the other population. Recently, a variant of OODA was applied to networks computed from resting state fMRI data and was able to detect statistical differences between populations of graphs modeled with a Gibbs mixture model while traditional graph theory metrics could not detect significance (La Rosa et al., 2016). Although this suggests OODA with Gibbs distributions as a promising avenue for population functional connectivity comparisons in ESC-derived networks grown on MEAs, this study, too, was limited to graphs with equal numbers of nodes.

Graph kernels, a mathematical framework developed to convert graphs into vectors for machine learning classification schemes or graph comparisons, may be suitable for overcoming

restrictions pertaining to the number of nodes in networks. Graph kernels were originally developed to only handle graphs where information was limited to the existence of edges between nodes, but more recently, graph kernels have been developed to incorporate incomplete node label information as well as continuous attributes associated with each node (Borgwardt and Kriegel, 2005; Feragen et al., 2013). One particularly recent graph kernel algorithm, propagation kernels, can efficiently handle incomplete node label and attribute information and has been used to compare and learn chemical compound structure (Neumann et al., 2016). At a fundamental level, propagation kernels propagate information along the edges of a graph and maintain label and attribute distributions that can be compared between individual graphs after each iteration of the algorithm. This scheme appears to be an intuitive application for the functional connections detected in this thesis due to the continuous attributes associated with each connection (delay, distance, and strength). Because propagation kernels are 1) not limited to comparisons of graphs of equal size, 2) can incorporate node or edge information and 3) convert networks (graphs) into vectors, they may allow for topological comparisons across ESC-derived populations and set a foundation for classification schemes to be applied with the use of machine learning.

4.2.2. Different Neuron-Pair Connectivity Metrics

As discussed in throughout this thesis, the cross-correlation function has been extensively used to study connectivity between individual neurons for half a century, and multiple investigations have explored the limitations of this methodology for determining underlying effective connectivity (Ashby and Zilm, 1982; Constantinidis et al., 2001; Fujisawa et al., 2008; Gerstein and Perkel, 1969, 1972; Kirkwood and Sears, 1978; Knox, 1974; Moore et al., 1966;

Moore et al., 1970; Ostojic et al., 2009; Perkel et al., 1967; Snider et al., 1998). Many other metrics have been developed over the years and applied to neural data. Cutts and Eglen recently performed a comparison study using over 30 metrics and elegantly described both ideal and desirable properties for a metric to accurately detect synaptic level interactions (Cutts and Eglen, 2014). For ideal properties, metrics should be 1) symmetric 2) invariant to firing rate 3) invariant to quantity of spikes 4) bounded and 5) invariant to small changes in time bin width. Desirable properties were 1) ignoring periods of simultaneous inactivity 2) making no assumptions about underlying spike distributions and 3) having minimal parameters beyond the time bin width (Cutts and Eglen, 2014). All of these properties, along with computational time, should be taken into consideration when choosing a metric because interpretations and sensitivities to population differences will depend on the criteria the metric meets. Distance metrics (Kreuz et al., 2007; Victor and Purpura, 1997), synchrony metrics (Joris et al., 2006; Wong et al., 1993), information theory metrics (Garofalo et al., 2009), and more complex measures like Granger causality (Kaminski et al., 2001; Nedungadi et al., 2009; Pourzanjani et al., 2015) all have their own advantages and drawbacks and should be explored on a theoretical level prior to large scale applications in the assay developed in this thesis.

4.2.3. MEA-Microfluidic Studies

After transplantation, ES-derived populations form novel networks that interface with native neuronal networks spared after SCI. However, growth and migration of the grafted neurons into the spared endogenous tissue creates spatial mixing of cells that acts as a serious impediment to the investigation of functional connections between the graft and spared native circuits (Ikegami et al., 2005). Characterization of graft-host connectivity has been limited to

molecular assays and gross measures of electrophysiological input/output, which miss the cellular level functional connectivity between individual ES-derived and primary neurons (Abematsu et al., 2010; Bonner et al., 2011; Bonner and Steward, 2015; Fujimoto et al., 2012; Nori et al., 2011; Sharp et al., 2014). This gap in knowledge must be addressed before transplantable populations can be rationally integrated into native circuits as synaptic relays.

Polydimethylsiloxane (PDMS) microfluidic devices are a useful technology for consistently segregating populations of cultured neurons while allowing directed interconnectivity between them (Kim et al., 2009; Lu et al., 2012; Taylor et al., 2005; Taylor et al., 2006). MEAs interfaced with microchannels have been used to quantify the proportion of action potentials propagating in a particular direction between neuronal populations and also the propagation of bursting activity from one well to another (Pan et al., 2011). Cross-correlation has already been applied to such culture systems to quantify the functional connectivity between populations of neurons located in the different compartments (Kanagasabapathi et al., 2012). Combining this technology with the transgenic stem cell lines characterized in this thesis would allow a characterization of the functional connectivity between these populations and primary CPG neurons, simulating synaptic connectivity between graft and host CPG neurons spared by the injury. Descending axons from higher motor centers re-sprout after SCI and form and maintain synaptic connections adjacent to incomplete injuries (Bareyre et al., 2004; Courtine et al., 2008; Rosenzweig et al., 2010; Takeoka et al., 2014; van den Brand et al., 2012; Zaaimi et al., 2012). Graft circuits may potentially receive synaptic connections from these tracts, making this novel assay also essential for studying functional connectivity between cortical neurons and transgenic populations via microchannel-MEA co-culture. Data gathered from the reduced and controlled biological environment enabled by this new technology will provide an assay capable

of developing informed hypotheses about how the neurons within the graft may interact with the neurons of native spinal cord circuits and how to manipulate this intrinsic functional connectivity for *in vivo* SCI studies.

4.2.4. Induced Plasticity with Electrical Stimulation

Previously attempted transplanted circuit relays in rodents showed limited to moderate electrophysiological signal transduction across the site of injury, suggesting the need to modulate the synaptic efficacy of these feed-forward polysynaptic pathways (Bonner et al., 2011; Fujimoto et al., 2012; Sharp et al., 2014). Besides physical training, electrical stimulation provides an avenue to inducing synaptic changes at the host-graft interface as well as within the graft circuits. Synaptic plasticity has previously been induced in descending corticospinal connections in healthy monkeys by enforcing Hebbian rules of neuronal activation with electrical stimulation (Nishimura et al., 2013), but optimizing this type of strategy for multi-synaptic relay circuits would be extremely challenging, especially in the context of the poor molecular environment of the SCI.

MEAs have been used to demonstrate functional plasticity in dissociated mammalian cultures for twenty years (Jimbo et al., 1998; Maeda et al., 1998; Massobrio et al., 2015). In order to consistently detect changes induced by stimulation protocols, culture activity must have low variability temporally (Chiappalone et al., 2008), and spatiotemporal patterns must persist for at least an hour (Marder and Buonomano, 2004; Wagenaar et al., 2006). Different types of electrical stimulation have been applied to cultures to evoke recorded changes, both in terms of faster high frequency and slower low frequency tetanic stimulation (Chao et al., 2007; Jimbo et al., 1998; Maeda et al., 1998). However, it should be noted that inducing plasticity in pseudo-

random dissociated cultures can be potentially difficult due to the dense synaptic connectivity and persistent bursting dynamics (Corner et al., 2002; Zhou and Poo, 2004).

The system presented in this thesis is perfectly positioned to test the effects of electrical stimulation on plasticity induction in ESC-derived transplantation candidate cultures. Because cross-correlation in this thesis represents the average connectivity over the course of an hour, this type of measure is well-suited to overcome stability caveats. A variety of plasticity-inducing paradigms could be used to determine the capacity of ESC-derived neurons to modify synaptic efficacy whether those previously used in the context of MEAs (Chao et al., 2007; Jimbo et al., 1998; Maeda et al., 1998) or those investigated by the Barbour group *in silico* (Sinha et al., 2014). This system will allow for the optimization of stimulation parameters as well as test for plasticity susceptibility between ESC-derived population groups. Considering the plastic behavior of ventral interneuron populations after SCI (Bareyre et al., 2004; Courtine et al., 2008), observing changes in network functional connectivity after electrical stimulation is very likely in ESC-derived ventral populations, such as the ESC-V2a and ESC-MN/glia characterized in this thesis.

4.2.5. Neuroprotective Screening

This thesis serves as a proof of concept of detecting functional connectivity in candidate populations of ESC-derived neurons in the most reduced culture conditions. In reality, these neurons would need to functionally interconnect in the non-permissive acute environment of spinal cord injuries (Okada et al., 2005; Tarasenko et al., 2007). The effects of such environmental conditions on ESC-derived network formation could potentially be analyzed in the assay presented in this thesis. Previous work by Taccola and colleagues replicated the toxic

conditions of the acute injury and assessed the damage on neonatal rat locomotor networks in *vitro* (Taccola et al., 2008). Not only could culture conditions such as these be used to test for changes in the detection of functional connections in populations such as ESC-V2a or ESC-MN/glia relative to baseline conditions, but this functional connectivity toxicity assay could also serve as a means to characterize the neuroprotective properties of various potential molecular interventions. Previous *in vitro* models of acute SCI conditions have been established as model-systems for preclinical screening of the properties of neuroprotective drugs on neuronal and glial survival (Margaryan et al., 2010; Nasrabady et al., 2011; Nasrabady et al., 2011). Extending the work documented in this thesis towards toxicology screening will enhance the field's knowledge about potential ways to promote functional connectivity in populations grafted into the non-permissive SCI environment.

4.2.6. Paired *In Vivo* Studies

Although *in vitro* studies are essential for understanding or observing phenomena at a more fundament level, we must be careful about extrapolating these findings into the realm of intact *in vivo* systems. The proof of concept presented in this thesis and follow-up *in vitro* studies are paramount to assessing functional connectivity formation, maintenance, and manipulability in candidate populations of ESC-derived neurons due to the difficulty in rapidly assessing network functional connectivity after transplantation therapy for SCI, but are less meaningful than conducted in parallel with in vivo transplantation studies comparable to those mentioned in this thesis but at scale (Bonner et al., 2011; Fujimoto et al., 2012; Nori et al., 2011; Sharp et al., 2014). In order to collect the most repeatable and informative data from such studies, the experimental setup of the animal studies would need to reduce variability in as many ways as

possible. Animal strain, injury location, behavioral measures, immunosuppressants, transplantation time point, molecular assays, and electrophysiological assessments should be held constant across multiple laboratory research locations. Increasing sample number and reducing experimental variability in animal SCI studies using transplantation candidates such as ESC-V2a INs in parallel with the functional connectivity *in vitro* assay presented here would provide both validation opportunities for *in vitro* findings and equally important in vivo data points to correlate with *in vitro* functional connectivity fingerprints.

4.2.7. Improving High-Throughput Screening

The 60-channel MEAs used in this thesis provided high-throughput assessments of individual functional connections in ESC-derived neuronal populations on the order of thousands of functional relationships, which may be sufficient to detect population differences. Other MEA technologies exist that can provide an even more accurate picture of the network topology while also rapidly scaling the sample size of the populations being considered. High-density arrays (~1000 electrodes) more densely detect functional connections between individual neurons and have been used in various studies of network functional interactions (Berdondini et al., 2009; Frey et al., 2009; Maccione et al., 2012). Compared to the 60-channel systems, these can approach 1:1 coupling between electrodes and neurons depending on the density of the culture. Multi-well MEA systems provide the opportunity to rapidly increase population samples by allowing simultaneous recordings from multiple culture wells. The Axion Maestro Multi-well system, for example, has 768 simultaneous recording channels and supports 12-, 48-, or 96-well MEA plates. This means that the 12-well plate is equivalent to 12 simultaneous 64-electrode

culture recordings, an order of magnitude scale-up from the types of recordings performed in this thesis.

It should be noted that both high-density and multi-well recordings will drive up both analysis computational and time requirements. In chapter 3, computing the functional connectivity for a single ESC-V2a/MN/glia condition across 6 cultures required a week of processing on a single 16 GB RAM, 3.4 GHz Intel Core CPU. Computational time scales fairly linearly with a multi-well system while a high-density array increases the number of possible neuron pairs combinatorially. Spike-sorting also must be taken into account, considering that neurons are typically sorted manually by experts. Some automated spike-sorting algorithms such as SPLIT and AMPLITUDE have been shown to perform at par with expert spike-sorting when used in neural decoding tasks, suggesting these methods are a possible consideration depending on the required fidelity of the task at hand (Todorova et al., 2014).

4.3. Concluding Remarks

Collaboration across fields of expertise is paramount to optimizing stem cell therapy as a viable intervention for SCI in humans. Generating phenotypically predictable populations of stem cell-derived neurons alone has required interdisciplinary approaches. The proof of concept in thesis lays the foundation for future inquiries to build upon in terms of accurately and reliably detecting and characterizing functional connectivity within ESC-derived populations. Future endeavors will require the borrowing of computational and statistical metrics mastered in other fields of study to apply them in the appropriate manner for the optimization of stem cell therapy. Every new metric and experimental design has caveats associated with them that are imperative to consider before scalable application. No matter what design is used *in vitro*, little meaning can

be derived from these investigations until they are paired with well-designed, low-variability *in vivo* studies at scale. Translating this work to the clinic will continue to require creative cooperation and presents an exciting and achievable goal moving forward.

References

1. Abematsu M, Tsujimura K, Yamano M, Saito M, Kohno K, et al. (2010) Neurons derived from transplanted neural stem cells restore disrupted neuronal circuitry in a mouse model of spinal cord injury. J Clin Invest 120: 3255-3266.
2. Aertsen A, Vaadia E, Abeles M, Ahissar E, Bergman H, et al. (1991) Neural interactions in the frontal cortex of a behaving monkey: signs of dependence on stimulus context and behavioral state. J Hirnforsch 32: 735-743.
3. Aertsen AM, Gerstein GL, Habib MK, Palm G (1989) Dynamics of neuronal firing correlation: modulation of "effective connectivity". J Neurophysiol 61: 900-917.
4. Al-Mosawie A, Wilson JM, Brownstone RM (2007) Heterogeneity of V2-derived interneurons in the adult mouse spinal cord. Eur J Neurosci 26: 3003-3015.
5. Alexander GE, Crutcher MD (1990) Functional architecture of basal ganglia circuits: neural substrates of parallel processing. Trends Neurosci 13: 266-271.
6. Alonso JM, Usrey WM, Reid RC (1996) Precisely correlated firing in cells of the lateral geniculate nucleus. Nature 383: 815-819.
7. Alonso JM, Martinez LM (1998) Functional connectivity between simple cells and complex cells in cat striate cortex. Nat Neurosci 1: 395-403.
8. Alvarez FJ, Jonas PC, Sapir T, Hartley R, Berrocal MC, et al. (2005) Postnatal phenotype and localization of spinal cord V1 derived interneurons. J Comp Neurol 493: 177-192.
9. Ampatzis K, Song J, Ausborn J, El Manira A (2014) Separate microcircuit modules of distinct v2a interneurons and motoneurons control the speed of locomotion. Neuron 83: 934-943.
10. Anderson D, Self T, Mellor IR, Goh G, Hill SJ, et al. (2007) Transgenic enrichment of cardiomyocytes from human embryonic stem cells. Mol Ther 15: 2027-2036.
11. Anderson KD (2004) Targeting recovery: priorities of the spinal cord-injured population. J Neurotrauma 21: 1371-1383.
12. Ann HW, Jun S, Shin NY, Han S, Ahn JY, et al. (2016) Characteristics of Resting-State Functional Connectivity in HIV-Associated Neurocognitive Disorder. PLoS One 11: e0153493.
13. Arber S (2012) Motor circuits in action: specification, connectivity, and function. Neuron 74: 975-989.
14. Ashby P, Zilm D (1982) Relationship between EPSP shape and cross-correlation profile explored by computer simulation for studies on human motoneurons. Exp Brain Res 47: 33-40.
15. Averbeck BB, Latham PE, Pouget A (2006) Neural correlations, population coding and computation. Nat Rev Neurosci 7: 358-366.
16. Azim E, Jiang J, Alstermark B, Jessell TM (2014) Skilled reaching relies on a V2a propriospinal internal copy circuit. Nature 508: 357-363.
17. Bain G, Kitchens D, Yao M, Huettner JE, Gottlieb DI (1995) Embryonic stem cells express neuronal properties in vitro. Dev Biol 168: 342-357.
18. Bair W, Zohary E, Newsome WT (2001) Correlated firing in macaque visual area MT: time scales and relationship to behavior. J Neurosci 21: 1676-1697.
19. Bakkum DJ, Chao ZC, Potter SM (2008) Spatio-temporal electrical stimuli shape behavior of an embodied cortical network in a goal-directed learning task. J Neural Eng 5: 310-323.

20. Bakkum DJ, Radivojevic M, Frey U, Franke F, Hierlemann A, et al. (2013) Parameters for burst detection. Front Comput Neurosci 7: 193.
21. Bamford JA, Mushahwar VK (2011) Intraspinal microstimulation for the recovery of function following spinal cord injury. Prog Brain Res 194: 227-239.
22. Ban J, Bonifazi P, Pinato G, Broccard FD, Studer L, et al. (2007) Embryonic stem cell-derived neurons form functional networks in vitro. Stem Cells 25: 738-749.
23. Banati RB, Gehrmann J, Schubert P, Kreutzberg GW (1993) Cytotoxicity of microglia. Glia 7: 111-118.
24. Barbeau H, Rossignol S (1987) Recovery of locomotion after chronic spinalization in the adult cat. Brain Res 412: 84-95.
25. Bareyre FM, Kerschensteiner M, Raineteau O, Mettenleiter TC, Weinmann O, et al. (2004) The injured spinal cord spontaneously forms a new intraspinal circuit in adult rats. Nat Neurosci 7: 269-277.
26. Bargmann CI, Marder E (2013) From the connectome to brain function. Nat Methods 10: 483-490.
27. Bartho P, Hirase H, Monconduit L, Zugaro M, Harris KD, et al. (2004) Characterization of neocortical principal cells and interneurons by network interactions and extracellular features. J Neurophysiol 92: 600-608.
28. Basso DM (2000) Neuroanatomical substrates of functional recovery after experimental spinal cord injury: implications of basic science research for human spinal cord injury. Phys Ther 80: 808-817.
29. Belhaj-Saif A, Cheney PD (2000) Plasticity in the distribution of the red nucleus output to forearm muscles after unilateral lesions of the pyramidal tract. J Neurophysiol 83: 3147-3153.
30. Benito-Gonzalez A, Alvarez FJ (2012) Renshaw cells and Ia inhibitory interneurons are generated at different times from p1 progenitors and differentiate shortly after exiting the cell cycle. J Neurosci 32: 1156-1170.
31. Berdondini L, Imfeld K, Maccione A, Tedesco M, Neukom S, et al. (2009) Active pixel sensor array for high spatio-temporal resolution electrophysiological recordings from single cell to large scale neuronal networks. Lab Chip 9: 2644-2651.
32. Berry M, Maxwell WL, Logan A, Mathewson A, McConnell P, et al. (1983) Deposition of scar tissue in the central nervous system. Acta Neurochir Suppl (Wien) 32: 31-53.
33. Bettencourt LM, Stephens GJ, Ham MI, Gross GW (2007) Functional structure of cortical neuronal networks grown in vitro. Phys Rev E Stat Nonlin Soft Matter Phys 75: 021915.
34. Binder MD, Powers RK (2001) Relationship between simulated common synaptic input and discharge synchrony in cat spinal motoneurons. J Neurophysiol 86: 2266-2275.
35. Boehler MD, Leondopulos SS, Wheeler BC, Brewer GJ (2012) Hippocampal networks on reliable patterned substrates. J Neurosci Methods 203: 344-353.
36. Bollobas B (2001) Random Graphs. New York City: Cambridge University Press.
37. Bomstein Y, Marder JB, Vitner K, Smirnov I, Lisaey G, et al. (2003) Features of skin-coincubated macrophages that promote recovery from spinal cord injury. J Neuroimmunol 142: 10-16.
38. Bonner JF, Connors TM, Silverman WF, Kowalski DP, Lemay MA, et al. (2011) Grafted neural progenitors integrate and restore synaptic connectivity across the injured spinal cord. J Neurosci 31: 4675-4686.

39. Bonner JF, Steward O (2015) Repair of spinal cord injury with neuronal relays: From fetal grafts to neural stem cells. Brain Res 1619: 115-123.
40. Borgwardt KM, Kriegel HP (2005) Shortest-path kernels on graphs. Proceedings of international conference on data mining (ICDM-05): 74-81.
41. Borowska J, Jones CT, Zhang H, Blacklaws J, Goulding M, et al. (2013) Functional subpopulations of V3 interneurons in the mature mouse spinal cord. J Neurosci 33: 18553-18565.
42. Bregman BS, Kunkel-Bagden E, Schnell L, Dai HN, Gao D, et al. (1995) Recovery from spinal cord injury mediated by antibodies to neurite growth inhibitors. Nature 378: 498-501.
43. Brindley GS, Polkey CE, Rushton DN (1982) Sacral anterior root stimulators for bladder control in paraplegia. Paraplegia 20: 365-381.
44. Britz O, Zhang J, Grossmann KS, Dyck J, Kim JC, et al. (2015) A genetically defined asymmetry underlies the inhibitory control of flexor-extensor locomotor movements. Elife 4.
45. Brocard F, Tazerart S, Vinay L (2010) Do pacemakers drive the central pattern generator for locomotion in mammals? Neuroscientist 16: 139-155.
46. Brodin L, Grillner S, Rovainen CM (1985) N-Methyl-D-aspartate (NMDA), kainate and quisqualate receptors and the generation of fictive locomotion in the lamprey spinal cord. Brain Res 325: 302-306.
47. Brown CR, Butts JC, McCreedy DA, Sakiyama-Elbert SE (2014) Generation of v2a interneurons from mouse embryonic stem cells. Stem Cells Dev 23: 1765-1776.
48. Bruehlmeier M, Dietz V, Leenders KL, Roelcke U, Missimer J, et al. (1998) How does the human brain deal with a spinal cord injury? Eur J Neurosci 10: 3918-3922.
49. Brustle O, Jones KN, Learish RD, Karram K, Choudhary K, et al. (1999) Embryonic stem cell-derived glial precursors: a source of myelinating transplants. Science 285: 754-756.
50. Buhnemann C, Scholz A, Bernreuther C, Malik CY, Braun H, et al. (2006) Neuronal differentiation of transplanted embryonic stem cell-derived precursors in stroke lesions of adult rats. Brain 129: 3238-3248.
51. Bullmore ET, Bassett DS (2011) Brain graphs: graphical models of the human brain connectome. Annu Rev Clin Psychol 7: 113-140.
52. Bunge RP, Puckett WR, Becerra JL, Marcillo A, Quencer RM (1993) Observations on the pathology of human spinal cord injury. A review and classification of 22 new cases with details from a case of chronic cord compression with extensive focal demyelination. Adv Neurol 59: 75-89.
53. Buzsaki G, Anastassiou CA, Koch C (2012) The origin of extracellular fields and currents--EEG, ECoG, LFP and spikes. Nat Rev Neurosci 13: 407-420.
54. Calver AR, Hall AC, Yu WP, Walsh FS, Heath JK, et al. (1998) Oligodendrocyte population dynamics and the role of PDGF in vivo. Neuron 20: 869-882.
55. Cao Q, Xu XM, Devries WH, Enzmann GU, Ping P, et al. (2005) Functional recovery in traumatic spinal cord injury after transplantation of multineurotrophin-expressing glial-restricted precursor cells. J Neurosci 25: 6947-6957.
56. Capogrosso M, Milekovic T, Borton D, Wagner F, Moraud EM, et al. (2016) A brain-spine interface alleviating gait deficits after spinal cord injury in primates. Nature 539: 284-288.

57. Carmel JB, Berrol LJ, Brus-Ramer M, Martin JH (2010) Chronic electrical stimulation of the intact corticospinal system after unilateral injury restores skilled locomotor control and promotes spinal axon outgrowth. J Neurosci 30: 10918-10926.
58. Carmel JB, Kimura H, Berrol LJ, Martin JH (2013) Motor cortex electrical stimulation promotes axon outgrowth to brain stem and spinal targets that control the forelimb impaired by unilateral corticospinal injury. Eur J Neurosci 37: 1090-1102.
59. Carpenter MK, Inokuma MS, Denham J, Mujtaba T, Chiu CP, et al. (2001) Enrichment of neurons and neural precursors from human embryonic stem cells. Exp Neurol 172: 383-397.
60. Cazalets JR, Sqalli-Houssaini Y, Clarac F (1992) Activation of the central pattern generators for locomotion by serotonin and excitatory amino acids in neonatal rat. J Physiol 455: 187-204.
61. Chao ZC, Bakkum DJ, Potter SM (2007) Region-specific network plasticity in simulated and living cortical networks: comparison of the center of activity trajectory (CAT) with other statistics. J Neural Eng 4: 294-308.
62. Charrier V, Cabelguen JM (2013) Fictive rhythmic motor patterns produced by the tail spinal cord in salamanders. Neuroscience 255: 191-202.
63. Chiappalone M, Massobrio P, Martinoia S (2008) Network plasticity in cortical assemblies. Eur J Neurosci 28: 221-237.
64. Chiasson BJ, Tropepe V, Morshead CM, van der Kooy D (1999) Adult mammalian forebrain ependymal and subependymal cells demonstrate proliferative potential, but only subependymal cells have neural stem cell characteristics. J Neurosci 19: 4462-4471.
65. Christie AE, Skiebe P, Marder E (1995) Matrix of neuromodulators in neurosecretory structures of the crab Cancer borealis. J Exp Biol 198: 2431-2439.
66. Christie KJ, Whelan PJ (2005) Monoaminergic establishment of rostrocaudal gradients of rhythmicity in the neonatal mouse spinal cord. J Neurophysiol 94: 1554-1564.
67. Clarac F, Pearlstein E, Pflieger JF, Vinay L (2004) The in vitro neonatal rat spinal cord preparation: a new insight into mammalian locomotor mechanisms. J Comp Physiol A Neuroethol Sens Neural Behav Physiol 190: 343-357.
68. Clarke LE, Barres BA (2013) Emerging roles of astrocytes in neural circuit development. Nat Rev Neurosci 14: 311-321.
69. Clovis YM, Seo SY, Kwon JS, Rhee JC, Yeo S, et al. (2016) Chx10 Consolidates V2a Interneuron Identity through Two Distinct Gene Repression Modes. Cell Rep 16: 1642-1652.
70. Constantinidis C, Franowicz MN, Goldman-Rakic PS (2001) Coding specificity in cortical microcircuits: a multiple-electrode analysis of primate prefrontal cortex. J Neurosci 21: 3646-3655.
71. Corner MA, van Pelt J, Wolters PS, Baker RE, Nuytinck RH (2002) Physiological effects of sustained blockade of excitatory synaptic transmission on spontaneously active developing neuronal networks--an inquiry into the reciprocal linkage between intrinsic biorhythms and neuroplasticity in early ontogeny. Neurosci Biobehav Rev 26: 127-185.
72. Courtine G, Song B, Roy RR, Zhong H, Herrmann JE, et al. (2008) Recovery of supraspinal control of stepping via indirect propriospinal relay connections after spinal cord injury. Nat Med 14: 69-74.

73. Crone SA, Quinlan KA, Zagoraiou L, Droho S, Restrepo CE, et al. (2008) Genetic ablation of V2a ipsilateral interneurons disrupts left-right locomotor coordination in mammalian spinal cord. Neuron 60: 70-83.
74. Crone SA, Zhong G, Harris-Warrick R, Sharma K (2009) In mice lacking V2a interneurons, gait depends on speed of locomotion. J Neurosci 29: 7098-7109.
75. Csicsvari J, Hirase H, Czurko A, Buzsaki G (1998) Reliability and state dependence of pyramidal cell-interneuron synapses in the hippocampus: an ensemble approach in the behaving rat. Neuron 21: 179-189.
76. Cullheim S, Kellerth JO, Conradi S (1977) Evidence for direct synaptic interconnections between cat spinal alpha-motoneurons via the recurrent axon collaterals: a morphological study using intracellular injection of horseradish peroxidase. Brain Res 132: 1-10.
77. Curtis DR, Ryall RW (1964) Nicotinic and Muscarinic Receptors of Renshaw Cells. Nature 203: 652-653.
78. Cutts CS, Eglen SJ (2014) Detecting pairwise correlations in spike trains: an objective comparison of methods and application to the study of retinal waves. J Neurosci 34: 14288-14303.
79. Dai X, Noga BR, Douglas JR, Jordan LM (2005) Localization of spinal neurons activated during locomotion using the c-fos immunohistochemical method. J Neurophysiol 93: 3442-3452.
80. Davies JE, Huang C, Proschel C, Noble M, Mayer-Proschel M, et al. (2006) Astrocytes derived from glial-restricted precursors promote spinal cord repair. J Biol 5: 7.
81. Davis-Dusenbery BN, Williams LA, Klim JR, Eggan K (2014) How to make spinal motor neurons. Development 141: 491-501.
82. deCharms RC, Merzenich MM (1996) Primary cortical representation of sounds by the coordination of action-potential timing. Nature 381: 610-613.
83. Delcomyn F (1980) Neural basis of rhythmic behavior in animals. Science 210: 492-498.
84. Demarse TB, Wagenaar DA, Blau AW, Potter SM (2001) The Neurally Controlled Animat: Biological Brains Acting with Simulated Bodies. Auton Robots 11: 305-310.
85. Dergham P, Ellezam B, Essagian C, Avedissian H, Lubell WD, et al. (2002) Rho signaling pathway targeted to promote spinal cord repair. J Neurosci 22: 6570-6577.
86. Dietz S, Husch A, Harris-Warrick RM (2012) A comparison of serotonin neuromodulation of mouse spinal V2a interneurons using perforated patch and whole cell recording techniques. Front Cell Neurosci 6: 39.
87. Dietz V (2006) G. Heiner Sell memorial lecture: neuronal plasticity after spinal cord injury: significance for present and future treatments. J Spinal Cord Med 29: 481-488.
88. Dietz V, Sinkjaer T (2007) Spastic movement disorder: impaired reflex function and altered muscle mechanics. Lancet Neurol 6: 725-733.
89. Dietz V (2008) Body weight supported gait training: from laboratory to clinical setting. Brain Res Bull 76: 459-463.
90. DiMarco AF, Onders RP, Ignagni A, Kowalski KE (2006) Inspiratory muscle pacing in spinal cord injury: case report and clinical commentary. J Spinal Cord Med 29: 95-108.
91. Doiron B, Litwin-Kumar A, Rosenbaum R, Ocker GK, Josic K (2016) The mechanics of state-dependent neural correlations. Nat Neurosci 19: 383-393.
92. Donnelly DJ, Popovich PG (2008) Inflammation and its role in neuroprotection, axonal regeneration and functional recovery after spinal cord injury. Exp Neurol 209: 378-388.

93. Donoghue JP, Suner S, Sanes JN (1990) Dynamic organization of primary motor cortex output to target muscles in adult rats. II. Rapid reorganization following motor nerve lesions. Exp Brain Res 79: 492-503.
94. Dougherty KJ, Kiehn O (2010) Firing and cellular properties of V2a interneurons in the rodent spinal cord. J Neurosci 30: 24-37.
95. Dougherty KJ, Kiehn O (2010) Functional organization of V2a-related locomotor circuits in the rodent spinal cord. Ann N Y Acad Sci 1198: 85-93.
96. Dougherty KJ, Zagoraiou L, Satoh D, Rozani I, Doobar S, et al. (2013) Locomotor rhythm generation linked to the output of spinal shox2 excitatory interneurons. Neuron 80: 920-933.
97. Downes JH, Hammond MW, Xydas D, Spencer MC, Becerra VM, et al. (2012) Emergence of a small-world functional network in cultured neurons. PLoS Comput Biol 8: e1002522.
98. Droge MH, Gross GW, Hightower MH, Czisny LE (1986) Multielectrode analysis of coordinated, multisite, rhythmic bursting in cultured CNS monolayer networks. J Neurosci 6: 1583-1592.
99. Duncan ID, Aguayo AJ, Bunge RP, Wood PM (1981) Transplantation of rat Schwann cells grown in tissue culture into the mouse spinal cord. J Neurol Sci 49: 241-252.
100. Eccles JC, Fatt P, Koketsu K (1954) Cholinergic and inhibitory synapses in a pathway from motor-axon collaterals to motoneurones. J Physiol 126: 524-562.
101. Eddleston M, Mucke L (1993) Molecular profile of reactive astrocytes--implications for their role in neurologic disease. Neuroscience 54: 15-36.
102. Edgerton VR, Kim SJ, Ichiyama RM, Gerasimenko YP, Roy RR (2006) Rehabilitative therapies after spinal cord injury. J Neurotrauma 23: 560-570.
103. Eklof-Ljunggren E, Haupt S, Ausborn J, Dehnisch I, Uhlen P, et al. (2012) Origin of excitation underlying locomotion in the spinal circuit of zebrafish. Proc Natl Acad Sci U S A 109: 5511-5516.
104. Elson RC, Sillar KT, Bush BM (1992) Identified proprioceptive afferents and motor rhythm entrainment in the crayfish walking system. J Neurophysiol 67: 530-546.
105. Engesser-Cesar C, Anderson AJ, Basso DM, Edgerton VR, Cotman CW (2005) Voluntary wheel running improves recovery from a moderate spinal cord injury. J Neurotrauma 22: 157-171.
106. Ericson J, Rashbass P, Schedl A, Brenner-Morton S, Kawakami A, et al. (1997) Pax6 controls progenitor cell identity and neuronal fate in response to graded Shh signaling. Cell 90: 169-180.
107. Eytan D, Brenner N, Marom S (2003) Selective adaptation in networks of cortical neurons. J Neurosci 23: 9349-9356.
108. Feldman JL, Del Negro CA, Gray PA (2013) Understanding the rhythm of breathing: so near, yet so far. Annu Rev Physiol 75: 423-452.
109. Feragen A, Kasenburg N, Petersen J, de Bruijne M, Borgwardt KM (2013) Scalable kernels for graphs with continuous attributes. Advances in Neural Information Processing Systems 26: 216-224.
110. Fetz EE, Gustafsson B (1983) Relation between shapes of post-synaptic potentials and changes in firing probability of cat motoneurones. J Physiol 341: 387-410.

111. Filli L, Engmann AK, Zorner B, Weinmann O, Moraitis T, et al. (2014) Bridging the gap: a reticulo-propriospinal detour bypassing an incomplete spinal cord injury. J Neurosci 34: 13399-13410.
112. Finley MF, Kulkarni N, Huettner JE (1996) Synapse formation and establishment of neuronal polarity by P19 embryonic carcinoma cells and embryonic stem cells. J Neurosci 16: 1056-1065.
113. Fleming JC, Norenberg MD, Ramsay DA, Dekaban GA, Marcillo AE, et al. (2006) The cellular inflammatory response in human spinal cords after injury. Brain 129: 3249-3269.
114. Forssberg H, Grillner S, Rossignol S (1975) Phase dependent reflex reversal during walking in chronic spinal cats. Brain Res 85: 103-107.
115. Fouad K, Schnell L, Bunge MB, Schwab ME, Liebscher T, et al. (2005) Combining Schwann cell bridges and olfactory-ensheathing glia grafts with chondroitinase promotes locomotor recovery after complete transection of the spinal cord. J Neurosci 25: 1169-1178.
116. Fox MD, Snyder AZ, Zacks JM, Raichle ME (2006) Coherent spontaneous activity accounts for trial-to-trial variability in human evoked brain responses. Nat Neurosci 9: 23-25.
117. Fox MD, Raichle ME (2007) Spontaneous fluctuations in brain activity observed with functional magnetic resonance imaging. Nat Rev Neurosci 8: 700-711.
118. Fox MD, Greicius M (2010) Clinical applications of resting state functional connectivity. Front Syst Neurosci 4: 19.
119. Freeman GM, Jr., Krock RM, Aton SJ, Thaben P, Herzog ED (2013) GABA networks destabilize genetic oscillations in the circadian pacemaker. Neuron 78: 799-806.
120. Frey U, Egert U, Heer F, Hafizovic S, Hierlemann A (2009) Microelectronic system for high-resolution mapping of extracellular electric fields applied to brain slices. Biosens Bioelectron 24: 2191-2198.
121. Friston KJ, Frith CD, Liddle PF, Frackowiak RS (1993) Functional connectivity: the principal-component analysis of large (PET) data sets. J Cereb Blood Flow Metab 13: 5-14.
122. Friston KJ (1994) Functional and Effective Connectivity in Neuroimaging: A Synthesis. Human Brain Mapping: 56-78.
123. Friston KJ (2011) Functional and effective connectivity: a review. Brain Connect 1: 13-36.
124. Fujimoto Y, Abematsu M, Falk A, Tsujimura K, Sanosaka T, et al. (2012) Treatment of a mouse model of spinal cord injury by transplantation of human induced pluripotent stem cell-derived long-term self-renewing neuroepithelial-like stem cells. Stem Cells 30: 1163-1173.
125. Fujisawa S, Amarasingham A, Harrison MT, Buzsaki G (2008) Behavior-dependent short-term assembly dynamics in the medial prefrontal cortex. Nat Neurosci 11: 823-833.
126. Garofalo M, Nieus T, Massobrio P, Martinoia S (2009) Evaluation of the performance of information theory-based methods and cross-correlation to estimate the functional connectivity in cortical networks. PLoS One 4: e6482.
127. Gerstein GL, Perkel DH (1969) Simultaneously recorded trains of action potentials: analysis and functional interpretation. Science 164: 828-830.
128. Gerstein GL, Perkel DH (1972) Mutual temporal relationships among neuronal spike trains. Statistical techniques for display and analysis. Biophys J 12: 453-473.

129. Gerstein GL, Bloom MJ, Espinosa IE, Evanczuk S, Turner MR (1983) Design of a Laboratory for Multineuron Studies. IEEE Transactions on Systems, Man, and Cybernetics SMC-13.
130. Gerstein GL, Bedenbaugh P, Aertsen MH (1989) Neuronal assemblies. IEEE Trans Biomed Eng 36: 4-14.
131. Gharagozloo P, Lazareno S, Popham A, Birdsall NJ (1999) Allosteric interactions of quaternary strychnine and brucine derivatives with muscarinic acetylcholine receptors. J Med Chem 42: 438-445.
132. Giroux N, Rossignol S, Reader TA (1999) Autoradiographic study of alpha1- and alpha2-noradrenergic and serotonin1A receptors in the spinal cord of normal and chronically transected cats. J Comp Neurol 406: 402-414.
133. Goel A, Buonomano DV (2013) Chronic electrical stimulation homeostatically decreases spontaneous activity, but paradoxically increases evoked network activity. J Neurophysiol 109: 1824-1836.
134. Gosgnach S, Lanuza GM, Butt SJ, Saueressig H, Zhang Y, et al. (2006) V1 spinal neurons regulate the speed of vertebrate locomotor outputs. Nature 440: 215-219.
135. Goulding M (2009) Circuits controlling vertebrate locomotion: moving in a new direction. Nat Rev Neurosci 10: 507-518.
136. Greicius MD, Srivastava G, Reiss AL, Menon V (2004) Default-mode network activity distinguishes Alzheimer's disease from healthy aging: evidence from functional MRI. Proc Natl Acad Sci U S A 101: 4637-4642.
137. Griener A, Zhang W, Kao H, Wagner C, Gosgnach S (2015) Probing diversity within subpopulations of locomotor-related V0 interneurons. Dev Neurobiol 75: 1189-1203.
138. Griffiths IR, Miller R (1974) Vascular permeability to protein and vasogenic oedema in experimental concussive injuries to the canine spinal cord. J Neurol Sci 22: 291-304.
139. Grillner S, Zangger P (1979) On the central generation of locomotion in the low spinal cat. Exp Brain Res 34: 241-261.
140. Grillner S, McClellan A, Perret C (1981) Entrainment of the spinal pattern generators for swimming by mechano-sensitive elements in the lamprey spinal cord in vitro. Brain Res 217: 380-386.
141. Grillner S, Wallen P (2002) Cellular bases of a vertebrate locomotor system-steering, intersegmental and segmental co-ordination and sensory control. Brain Res Brain Res Rev 40: 92-106.
142. Grillner S (2003) The motor infrastructure: from ion channels to neuronal networks. Nat Rev Neurosci 4: 573-586.
143. Grillner S, Wallen P, Saitoh K, Kozlov A, Robertson B (2008) Neural bases of goal-directed locomotion in vertebrates--an overview. Brain Res Rev 57: 2-12.
144. Gris D, Marsh DR, Oatway MA, Chen Y, Hamilton EF, et al. (2004) Transient blockade of the CD11d/CD18 integrin reduces secondary damage after spinal cord injury, improving sensory, autonomic, and motor function. J Neurosci 24: 4043-4051.
145. Gritti A, Parati EA, Cova L, Frolichsthal P, Galli R, et al. (1996) Multipotential stem cells from the adult mouse brain proliferate and self-renew in response to basic fibroblast growth factor. J Neurosci 16: 1091-1100.
146. Gross GW, Rieske E, Kreutzberg GW, Meyer A (1977) A new fixed-array multi-microelectrode system designed for long-term monitoring of extracellular single unit neuronal activity in vitro. Neurosci Lett 6: 101-105.

147. Gross GW (1979) Simultaneous single unit recording in vitro with a photoetched laser deinsulated gold multimicroelectrode surface. IEEE Trans Biomed Eng 26: 273-279.
148. Gross GW, Williams AN, Lucas JH (1982) Recording of spontaneous activity with photoetched microelectrode surfaces from mouse spinal neurons in culture. J Neurosci Methods 5: 13-22.
149. Gross GW, Wen WY, Lin JW (1985) Transparent indium-tin oxide electrode patterns for extracellular, multisite recording in neuronal cultures. J Neurosci Methods 15: 243-252.
150. Guo X, Zahir T, Mothe A, Shoichet MS, Morshead CM, et al. (2012) The effect of growth factors and soluble Nogo-66 receptor protein on transplanted neural stem/progenitor survival and axonal regeneration after complete transection of rat spinal cord. Cell Transplant 21: 1177-1197.
151. Hafizovic S, Heer F, Ugniwenko T, Frey U, Blau A, et al. (2007) A CMOS-based microelectrode array for interaction with neuronal cultures. J Neurosci Methods 164: 93-106.
152. Hains BC, Yucra JA, Eaton MJ, Hulsebosch CE (2002) Intralesion transplantation of serotonergic precursors enhances locomotor recovery but has no effect on development of chronic central pain following hemisection injury in rats. Neurosci Lett 324: 222-226.
153. Hall ED, Springer JE (2004) Neuroprotection and acute spinal cord injury: a reappraisal. NeuroRx 1: 80-100.
154. Hampson M, Olson IR, Leung HC, Skudlarski P, Gore JC (2004) Changes in functional connectivity of human MT/V5 with visual motion input. Neuroreport 15: 1315-1319.
155. Hao ZZ, Meier ML, Berkowitz A (2014) Rostral spinal cord segments are sufficient to generate a rhythm for both locomotion and scratching but affect their hip extensor phases differently. J Neurophysiol 112: 147-155.
156. Harkema SJ, Hurley SL, Patel UK, Requejo PS, Dobkin BH, et al. (1997) Human lumbosacral spinal cord interprets loading during stepping. J Neurophysiol 77: 797-811.
157. Harris-Warrick R, Marder E, Selverston A, Mouling M (1992) Dynamic Biological Networks. Cambridge, MA: MIT Press.
158. Harris-Warrick RM (2002) Voltage-sensitive ion channels in rhythmic motor systems. Curr Opin Neurobiol 12: 646-651.
159. Heikkila TJ, Yla-Outinen L, Tanskanen JM, Lappalainen RS, Skottman H, et al. (2009) Human embryonic stem cell-derived neuronal cells form spontaneously active neuronal networks in vitro. Exp Neurol 218: 109-116.
160. Henderson CE, Phillips HS, Pollock RA, Davies AM, Lemeulle C, et al. (1994) GDNF: a potent survival factor for motoneurons present in peripheral nerve and muscle. Science 266: 1062-1064.
161. Herrmann A, Gerstner W (2001) Noise and the PSTH response to current transients: I. General theory and application to the integrate-and-fire neuron. J Comput Neurosci 11: 135-151.
162. Herrmann A, Gerstner W (2002) Noise and the PSTH response to current transients: II. Integrate-and-fire model with slow recovery and application to motoneuron data. J Comput Neurosci 12: 83-95.
163. Herrmann JE, Imura T, Song B, Qi J, Ao Y, et al. (2008) STAT3 is a critical regulator of astrogliosis and scar formation after spinal cord injury. J Neurosci 28: 7231-7243.

164. Hill CE, Beattie MS, Bresnahan JC (2001) Degeneration and sprouting of identified descending supraspinal axons after contusive spinal cord injury in the rat. Exp Neurol 171: 153-169.
165. Honey CJ, Sporns O, Cammoun L, Gigandet X, Thiran JP, et al. (2009) Predicting human resting-state functional connectivity from structural connectivity. Proc Natl Acad Sci U S A 106: 2035-2040.
166. Hooper SL, Moulins M (1989) Switching of a neuron from one network to another by sensory-induced changes in membrane properties. Science 244: 1587-1589.
167. Hooshmand MJ, Sontag CJ, Uchida N, Tamaki S, Anderson AJ, et al. (2009) Analysis of host-mediated repair mechanisms after human CNS-stem cell transplantation for spinal cord injury: correlation of engraftment with recovery. PLoS One 4: e5871.
168. Hou S, Tom VJ, Graham L, Lu P, Blesch A (2013) Partial restoration of cardiovascular function by embryonic neural stem cell grafts after complete spinal cord transection. J Neurosci 33: 17138-17149.
169. Houle JD, Reier PJ (1989) Regrowth of calcitonin gene-related peptide (CGRP) immunoreactive axons from the chronically injured rat spinal cord into fetal spinal cord tissue transplants. Neurosci Lett 103: 253-258.
170. Houweling DA, van Asseldonk JT, Lankhorst AJ, Hamers FP, Martin D, et al. (1998) Local application of collagen containing brain-derived neurotrophic factor decreases the loss of function after spinal cord injury in the adult rat. Neurosci Lett 251: 193-196.
171. Hu JG, Fu SL, Wang YX, Li Y, Jiang XY, et al. (2008) Platelet-derived growth factor-AA mediates oligodendrocyte lineage differentiation through activation of extracellular signal-regulated kinase signaling pathway. Neuroscience 151: 138-147.
172. Hunter DD, Cashman N, Morris-Valero R, Bulock JW, Adams SP, et al. (1991) An LRE (leucine-arginine-glutamate)-dependent mechanism for adhesion of neurons to S-laminin. J Neurosci 11: 3960-3971.
173. Husch A, Van Patten GN, Hong DN, Scaperotti MM, Cramer N, et al. (2012) Spinal cord injury induces serotonin supersensitivity without increasing intrinsic excitability of mouse V2a interneurons. J Neurosci 32: 13145-13154.
174. Hutchinson KJ, Gomez-Pinilla F, Crowe MJ, Ying Z, Basso DM (2004) Three exercise paradigms differentially improve sensory recovery after spinal cord contusion in rats. Brain 127: 1403-1414.
175. Ichiyama RM, Gerasimenko YP, Zhong H, Roy RR, Edgerton VR (2005) Hindlimb stepping movements in complete spinal rats induced by epidural spinal cord stimulation. Neurosci Lett 383: 339-344.
176. Ikegami T, Nakamura M, Yamane J, Katoh H, Okada S, et al. (2005) Chondroitinase ABC combined with neural stem/progenitor cell transplantation enhances graft cell migration and outgrowth of growth-associated protein-43-positive fibers after rat spinal cord injury. Eur J Neurosci 22: 3036-3046.
177. Illes S, Fleischer W, Siebler M, Hartung HP, Dihne M (2007) Development and pharmacological modulation of embryonic stem cell-derived neuronal network activity. Exp Neurol 207: 171-176.
178. Illes S, Theiss S, Hartung HP, Siebler M, Dihne M (2009) Niche-dependent development of functional neuronal networks from embryonic stem cell-derived neural populations. BMC Neurosci 10: 93.

179. Illes S, Jakab M, Beyer F, Gelfert R, Couillard-Despres S, et al. (2014) Intrinsically active and pacemaker neurons in pluripotent stem cell-derived neuronal populations. Stem Cell Reports 2: 323-336.
180. Imfeld K, Neukom S, Maccione A, Bornat Y, Martinoia S, et al. (2008) Large-scale, high-resolution data acquisition system for extracellular recording of electrophysiological activity. IEEE Trans Biomed Eng 55: 2064-2073.
181. Iyer NR, Huettner JE, Butts JC, Brown CR, Sakiyama-Elbert SE (2016) Generation of highly enriched V2a interneurons from mouse embryonic stem cells. Exp Neurol 277: 305-316.
182. Iyer NR, Wilems TS, Sakiyama-Elbert SE (2017) Stem cells for spinal cord injury: Strategies to inform differentiation and transplantation. Biotechnol Bioeng 114: 245-259.
183. Jakeman LB, Reier PJ (1991) Axonal projections between fetal spinal cord transplants and the adult rat spinal cord: a neuroanatomical tracing study of local interactions. J Comp Neurol 307: 311-334.
184. Jakeman LB, Wei P, Guan Z, Stokes BT (1998) Brain-derived neurotrophic factor stimulates hindlimb stepping and sprouting of cholinergic fibers after spinal cord injury. Exp Neurol 154: 170-184.
185. Jessell TM (2000) Neuronal specification in the spinal cord: inductive signals and transcriptional codes. Nat Rev Genet 1: 20-29.
186. Jiang T, He Y, Zang Y, Weng X (2004) Modulation of functional connectivity during the resting state and the motor task. Hum Brain Mapp 22: 63-71.
187. Jimbo Y, Robinson HP, Kawana A (1998) Strengthening of synchronized activity by tetanic stimulation in cortical cultures: application of planar electrode arrays. IEEE Trans Biomed Eng 45: 1297-1304.
188. Jimbo Y, Tateno T, Robinson HP (1999) Simultaneous induction of pathway-specific potentiation and depression in networks of cortical neurons. Biophys J 76: 670-678.
189. Johnson PJ, Tatara A, McCreedy DA, Shiu A, Sakiyama-Elbert SE (2010) Tissue-engineered fibrin scaffolds containing neural progenitors enhance functional recovery in a subacute model of SCI. Soft Matter 6: 5127-5137.
190. Johnstone AF, Gross GW, Weiss DG, Schroeder OH, Gramowski A, et al. (2010) Microelectrode arrays: a physiologically based neurotoxicity testing platform for the 21st century. Neurotoxicology 31: 331-350.
191. Jones BE (2004) Activity, modulation and role of basal forebrain cholinergic neurons innervating the cerebral cortex. Prog Brain Res 145: 157-169.
192. Joris PX, Louage DH, Cardoen L, van der Heijden M (2006) Correlation index: a new metric to quantify temporal coding. Hear Res 216-217: 19-30.
193. Jungling K, Nagler K, Pfrieger FW, Gottmann K (2003) Purification of embryonic stem cell-derived neurons by immunoisolation. FASEB J 17: 2100-2102.
194. Kalil K, Reh T (1979) Regrowth of severed axons in the neonatal central nervous system: establishment of normal connections. Science 205: 1158-1161.
195. Kaminski M, Ding M, Truccolo WA, Bressler SL (2001) Evaluating causal relations in neural systems: granger causality, directed transfer function and statistical assessment of significance. Biol Cybern 85: 145-157.
196. Kanagasabapathi TT, Massobrio P, Barone RA, Tedesco M, Martinoia S, et al. (2012) Functional connectivity and dynamics of cortical-thalamic networks co-cultured in a dual compartment device. J Neural Eng 9: 036010.

197. Karimi-Abdolrezaee S, Eftekharpour E, Wang J, Morshead CM, Fehlings MG (2006) Delayed transplantation of adult neural precursor cells promotes remyelination and functional neurological recovery after spinal cord injury. J Neurosci 26: 3377-3389.
198. Karunaratne A, Hargrave M, Poh A, Yamada T (2002) GATA proteins identify a novel ventral interneuron subclass in the developing chick spinal cord. Dev Biol 249: 30-43.
199. Keirstead HS, Nistor G, Bernal G, Totoiu M, Cloutier F, et al. (2005) Human embryonic stem cell-derived oligodendrocyte progenitor cell transplants remyelinate and restore locomotion after spinal cord injury. J Neurosci 25: 4694-4705.
200. Kernell D, Eerbeek O, Verhey BA (1983) Relation between isometric force and stimulus rate in cat's hindlimb motor units of different twitch contraction time. Exp Brain Res 50: 220-227.
201. Kiehn O, Kjaerulff O (1998) Distribution of central pattern generators for rhythmic motor outputs in the spinal cord of limbed vertebrates. Ann N Y Acad Sci 860: 110-129.
202. Kiehn O, Kjaerulff O, Tresch MC, Harris-Warrick RM (2000) Contributions of intrinsic motor neuron properties to the production of rhythmic motor output in the mammalian spinal cord. Brain Res Bull 53: 649-659.
203. Kiehn O, Butt SJ (2003) Physiological, anatomical and genetic identification of CPG neurons in the developing mammalian spinal cord. Prog Neurobiol 70: 347-361.
204. Kiehn O (2006) Locomotor circuits in the mammalian spinal cord. Annu Rev Neurosci 29: 279-306.
205. Kiehn O (2011) Development and functional organization of spinal locomotor circuits. Curr Opin Neurobiol 21: 100-109.
206. Kiehn O (2016) Decoding the organization of spinal circuits that control locomotion. Nat Rev Neurosci 17: 224-238.
207. Kim H, Zahir T, Tator CH, Shoichet MS (2011) Effects of dibutyryl cyclic-AMP on survival and neuronal differentiation of neural stem/progenitor cells transplanted into spinal cord injured rats. PLoS One 6: e21744.
208. Kim YT, Karthikeyan K, Chirvi S, Dave DP (2009) Neuro-optical microfluidic platform to study injury and regeneration of single axons. Lab Chip 9: 2576-2581.
209. Kimura Y, Okamura Y, Higashijima S (2006) alx, a zebrafish homolog of Chx10, marks ipsilateral descending excitatory interneurons that participate in the regulation of spinal locomotor circuits. J Neurosci 26: 5684-5697.
210. Kimura Y, Satou C, Higashijima S (2008) V2a and V2b neurons are generated by the final divisions of pair-producing progenitors in the zebrafish spinal cord. Development 135: 3001-3005.
211. Kimura Y, Satou C, Fujioka S, Shoji W, Umeda K, et al. (2013) Hindbrain V2a neurons in the excitation of spinal locomotor circuits during zebrafish swimming. Curr Biol 23: 843-849.
212. Kirkwood PA, Sears TA (1978) The synaptic connexions to intercostal motoneurones as revealed by the average common excitation potential. J Physiol 275: 103-134.
213. Kirwan P, Turner-Bridger B, Peter M, Momoh A, Arambepola D, et al. (2015) Development and function of human cerebral cortex neural networks from pluripotent stem cells in vitro. Development 142: 3178-3187.
214. Kjaerulff O, Barajon I, Kiehn O (1994) Sulphorhodamine-labelled cells in the neonatal rat spinal cord following chemically induced locomotor activity in vitro. J Physiol 478 (Pt 2): 265-273.

215. Knox CK (1974) Cross-correlation functions for a neuronal model. Biophys J 14: 567-582.
216. Kohn A, Smith MA (2005) Stimulus dependence of neuronal correlation in primary visual cortex of the macaque. J Neurosci 25: 3661-3673.
217. Koito H, Li J (2009) Preparation of rat brain aggregate cultures for neuron and glia development studies. J Vis Exp.
218. Kreuz T, Haas JS, Morelli A, Abarbanel HDI, Politi A (2007) Measuring spike train synchrony. Journal of Neuroscience Methods 165: 151-161.
219. Kulbatski I, Mothe AJ, Keating A, Hakamata Y, Kobayashi E, et al. (2007) Oligodendrocytes and radial glia derived from adult rat spinal cord progenitors: morphological and immunocytochemical characterization. J Histochem Cytochem 55: 209-222.
220. La Rosa PS, Brooks TL, Deych E, Shands B, Prior F, et al. (2016) Gibbs distribution for statistical analysis of graphical data with a sample application to fcMRI brain images. Stat Med 35: 566-580.
221. Lanuza GM, Gosgnach S, Pierani A, Jessell TM, Goulding M (2004) Genetic identification of spinal interneurons that coordinate left-right locomotor activity necessary for walking movements. Neuron 42: 375-386.
222. Lappalainen RS, Salomaki M, Yla-Outinen L, Heikkila TJ, Hyttinen JA, et al. (2010) Similarly derived and cultured hESC lines show variation in their developmental potential towards neuronal cells in long-term culture. Regen Med 5: 749-762.
223. Lavdas AA, Chen J, Papastefanaki F, Chen S, Schachner M, et al. (2010) Schwann cells engineered to express the cell adhesion molecule L1 accelerate myelination and motor recovery after spinal cord injury. Exp Neurol 221: 206-216.
224. Lawrence DG, Kuypers HG (1968) The functional organization of the motor system in the monkey. II. The effects of lesions of the descending brain-stem pathways. Brain 91: 15-36.
225. Lazareno S, Birdsall NJ (1995) Detection, quantitation, and verification of allosteric interactions of agents with labeled and unlabeled ligands at G protein-coupled receptors: interactions of strychnine and acetylcholine at muscarinic receptors. Mol Pharmacol 48: 362-378.
226. Lee KZ, Lane MA, Dougherty BJ, Mercier LM, Sandhu MS, et al. (2014) Intraspinal transplantation and modulation of donor neuron electrophysiological activity. Exp Neurol 251: 47-57.
227. Lee YS, Hsiao I, Lin VW (2002) Peripheral nerve grafts and aFGF restore partial hindlimb function in adult paraplegic rats. J Neurotrauma 19: 1203-1216.
228. Lee YS, Lin CY, Robertson RT, Hsiao I, Lin VW (2004) Motor recovery and anatomical evidence of axonal regrowth in spinal cord-repaired adult rats. J Neuropathol Exp Neurol 63: 233-245.
229. Leitner ML, Molliver DC, Osborne PA, Vejsada R, Golden JP, et al. (1999) Analysis of the retrograde transport of glial cell line-derived neurotrophic factor (GDNF), neurturin, and persephin suggests that in vivo signaling for the GDNF family is GFRalpha coreceptor-specific. J Neurosci 19: 9322-9331.
230. Lepore AC, Fischer I (2005) Lineage-restricted neural precursors survive, migrate, and differentiate following transplantation into the injured adult spinal cord. Exp Neurol 194: 230-242.

231. Levy WJ, Jr., Amassian VE, Traad M, Cadwell J (1990) Focal magnetic coil stimulation reveals motor cortical system reorganized in humans after traumatic quadriplegia. Brain Res 510: 130-134.
232. Li M, Pevny L, Lovell-Badge R, Smith A (1998) Generation of purified neural precursors from embryonic stem cells by lineage selection. Curr Biol 8: 971-974.
233. Li Q, Brus-Ramer M, Martin JH, McDonald JW (2010) Electrical stimulation of the medullary pyramid promotes proliferation and differentiation of oligodendrocyte progenitor cells in the corticospinal tract of the adult rat. Neurosci Lett 479: 128-133.
234. Li SJ, Li Z, Wu G, Zhang MJ, Franczak M, et al. (2002) Alzheimer Disease: evaluation of a functional MR imaging index as a marker. Radiology 225: 253-259.
235. Lima C, Pratas-Vital J, Escada P, Hasse-Ferreira A, Capucho C, et al. (2006) Olfactory mucosa autografts in human spinal cord injury: a pilot clinical study. J Spinal Cord Med 29: 191-203; discussion 204-196.
236. Lima C, Escada P, Pratas-Vital J, Branco C, Arcangeli CA, et al. (2010) Olfactory mucosal autografts and rehabilitation for chronic traumatic spinal cord injury. Neurorehabil Neural Repair 24: 10-22.
237. Lippmann ES, Williams CE, Ruhl DA, Estevez-Silva MC, Chapman ER, et al. (2015) Deterministic HOX patterning in human pluripotent stem cell-derived neuroectoderm. Stem Cell Reports 4: 632-644.
238. Liu ZH, Yip PK, Adams L, Davies M, Lee JW, et al. (2015) A Single Bolus of Docosahexaenoic Acid Promotes Neuroplastic Changes in the Innervation of Spinal Cord Interneurons and Motor Neurons and Improves Functional Recovery after Spinal Cord Injury. J Neurosci 35: 12733-12752.
239. Logothetis NK (2003) The underpinnings of the BOLD functional magnetic resonance imaging signal. J Neurosci 23: 3963-3971.
240. Longtin A, Bulsara A, Moss F (1991) Time-interval sequences in bistable systems and the noise-induced transmission of information by sensory neurons. Phys Rev Lett 67: 656-659.
241. Lotze M, Laubis-Herrmann U, Topka H (2006) Combination of TMS and fMRI reveals a specific pattern of reorganization in M1 in patients after complete spinal cord injury. Restor Neurol Neurosci 24: 97-107.
242. Lovely RG, Gregor RJ, Roy RR, Edgerton VR (1986) Effects of training on the recovery of full-weight-bearing stepping in the adult spinal cat. Exp Neurol 92: 421-435.
243. Lowe MJ, Dzemidzic M, Lurito JT, Mathews VP, Phillips MD (2000) Correlations in low-frequency BOLD fluctuations reflect cortico-cortical connections. Neuroimage 12: 582-587.
244. Lu P, Yang H, Jones LL, Filbin MT, Tuszynski MH (2004) Combinatorial therapy with neurotrophins and cAMP promotes axonal regeneration beyond sites of spinal cord injury. J Neurosci 24: 6402-6409.
245. Lu P, Wang Y, Graham L, McHale K, Gao M, et al. (2012) Long-distance growth and connectivity of neural stem cells after severe spinal cord injury. Cell 150: 1264-1273.
246. Lu X, Kim-Han JS, O'Malley KL, Sakiyama-Elbert SE (2012) A microdevice platform for visualizing mitochondrial transport in aligned dopaminergic axons. J Neurosci Methods 209: 35-39.

247. Lundfald L, Restrepo CE, Butt SJ, Peng CY, Droho S, et al. (2007) Phenotype of V2-derived interneurons and their relationship to the axon guidance molecule EphA4 in the developing mouse spinal cord. Eur J Neurosci 26: 2989-3002.
248. Lysikova M, Havlas Z, Tucek S (2001) Interactions between allosteric modulators and 4-DAMP and other antagonists at muscarinic receptors: potential significance of the distance between the N and carboxyl C atoms in the molecules of antagonists. Neurochem Res 26: 383-394.
249. Maccione A, Gandolfo M, Tedesco M, Nieus T, Imfeld K, et al. (2010) Experimental Investigation on Spontaneously Active Hippocampal Cultures Recorded by Means of High-Density MEAs: Analysis of the Spatial Resolution Effects. Front Neuroeng 3: 4.
250. Maccione A, Garofalo M, Nieus T, Tedesco M, Berdondini L, et al. (2012) Multiscale functional connectivity estimation on low-density neuronal cultures recorded by high-density CMOS Micro Electrode Arrays. J Neurosci Methods 207: 161-171.
251. Maeda E, Robinson HP, Kawana A (1995) The mechanisms of generation and propagation of synchronized bursting in developing networks of cortical neurons. J Neurosci 15: 6834-6845.
252. Maeda E, Kuroda Y, Robinson HP, Kawana A (1998) Modification of parallel activity elicited by propagating bursts in developing networks of rat cortical neurones. Eur J Neurosci 10: 488-496.
253. Malcangio M, Bowery NG (1996) GABA and its receptors in the spinal cord. Trends Pharmacol Sci 17: 457-462.
254. Marconi E, Nieus T, Maccione A, Valente P, Simi A, et al. (2012) Emergent functional properties of neuronal networks with controlled topology. PLoS One 7: e34648.
255. Marder CP, Buonomano DV (2004) Timing and balance of inhibition enhance the effect of long-term potentiation on cell firing. J Neurosci 24: 8873-8884.
256. Marder E, Bucher D (2001) Central pattern generators and the control of rhythmic movements. Curr Biol 11: R986-996.
257. Margaryan G, Mattioli C, Mladinic M, Nistri A (2010) Neuroprotection of locomotor networks after experimental injury to the neonatal rat spinal cord in vitro. Neuroscience 165: 996-1010.
258. Marron JS, Alonso AM (2014) Rejoinder to the discussion of: Overview of object-oriented data analysis. Biom J 56: 790-791.
259. Martin-Caraballo M, Greer JJ (1999) Electrophysiological properties of rat phrenic motoneurons during perinatal development. J Neurophysiol 81: 1365-1378.
260. Massobrio P, Tessadori J, Chiappalone M, Ghirardi M (2015) In vitro studies of neuronal networks and synaptic plasticity in invertebrates and in mammals using multielectrode arrays. Neural Plast 2015: 196195.
261. Matthieu JM, Honegger P, Trapp BD, Cohen SR, Webster HF (1978) Myelination in rat brain aggregating cell cultures. Neuroscience 3: 565-572.
262. Mayer ML, Westbrook GL (1984) Mixed-agonist action of excitatory amino acids on mouse spinal cord neurones under voltage clamp. J Physiol 354: 29-53.
263. McCrea DA (1998) Neuronal basis of afferent-evoked enhancement of locomotor activity. Ann N Y Acad Sci 860: 216-225.
264. McCrea DA, Rybak IA (2007) Modeling the mammalian locomotor CPG: insights from mistakes and perturbations. Prog Brain Res 165: 235-253.

265. McCreedy DA, Rieger CR, Gottlieb DI, Sakiyama-Elbert SE (2012) Transgenic enrichment of mouse embryonic stem cell-derived progenitor motor neurons. Stem Cell Res 8: 368-378.
266. McCreedy DA, Brown CR, Butts JC, Xu H, Huettner JE, et al. (2014) A New Method for Generating High Purity Motoneurons From Mouse Embryonic Stem Cells. Biotechnol Bioeng 111: 2041-2055.
267. McCreedy DA, Wilems TS, Xu H, Butts JC, Brown CR, et al. (2014) Survival, Differentiation, and Migration of High-Purity Mouse Embryonic Stem Cell-derived Progenitor Motor Neurons in Fibrin Scaffolds after Sub-Acute Spinal Cord Injury. Biomater Sci 2: 1672-1682.
268. McDonald JW, Sadowsky C (2002) Spinal-cord injury. Lancet 359: 417-425.
269. McKeehan WL, Ham RG (1976) Stimulation of clonal growth of normal fibroblasts with substrata coated with basic polymers. J Cell Biol 71: 727-734.
270. McLean DL, Merrywest SD, Sillar KT (2000) The development of neuromodulatory systems and the maturation of motor patterns in amphibian tadpoles. Brain Res Bull 53: 595-603.
271. McLean DL, Fan J, Higashijima S, Hale ME, Fetcho JR (2007) A topographic map of recruitment in spinal cord. Nature 446: 71-75.
272. McLean DL, Fetcho JR (2009) Spinal interneurons differentiate sequentially from those driving the fastest swimming movements in larval zebrafish to those driving the slowest ones. J Neurosci 29: 13566-13577.
273. Melssen WJ, Epping WJ (1987) Detection and estimation of neural connectivity based on crosscorrelation analysis. Biol Cybern 57: 403-414.
274. Mentel T, Cangiano L, Grillner S, Buschges A (2008) Neuronal substrates for state-dependent changes in coordination between motoneuron pools during fictive locomotion in the lamprey spinal cord. J Neurosci 28: 868-879.
275. Menzler J, Zeck G (2011) Network oscillations in rod-degenerated mouse retinas. J Neurosci 31: 2280-2291.
276. Meskaldji DE, Fischi-Gomez E, Griffa A, Hagmann P, Morgenthaler S, et al. (2013) Comparing connectomes across subjects and populations at different scales. Neuroimage 80: 416-425.
277. Metz GA, Curt A, van de Meent H, Klusman I, Schwab ME, et al. (2000) Validation of the weight-drop contusion model in rats: a comparative study of human spinal cord injury. J Neurotrauma 17: 1-17.
278. Meyrand P, Simmers J, Moulins M (1991) Construction of a pattern-generating circuit with neurons of different networks. Nature 351: 60-63.
279. Michel ME, Reier PJ (1979) Axonal-ependymal associations during early regeneration of the transected spinal cord in Xenopus laevis tadpoles. J Neurocytol 8: 529-548.
280. Miles GB, Yohn DC, Wichterle H, Jessell TM, Rafuse VF, et al. (2004) Functional properties of motoneurons derived from mouse embryonic stem cells. J Neurosci 24: 7848-7858.
281. Moon LD, Leasure JL, Gage FH, Bunge MB (2006) Motor enrichment sustains hindlimb movement recovered after spinal cord injury and glial transplantation. Restor Neurol Neurosci 24: 147-161.
282. Moore GP, Perkel DH, Segundo JP (1966) Statistical analysis and functional interpretation of neuronal spike data. Annu Rev Physiol 28: 493-522.

283. Moore GP, Segundo JP, Perkel DH, Levitan H (1970) Statistical signs of synaptic interaction in neurons. Biophys J 10: 876-900.
284. Moran-Rivard L, Kagawa T, Saueressig H, Gross MK, Burrill J, et al. (2001) Evx1 is a postmitotic determinant of v0 interneuron identity in the spinal cord. Neuron 29: 385-399.
285. Morgan VL, Price RR (2004) The effect of sensorimotor activation on functional connectivity mapping with MRI. Magn Reson Imaging 22: 1069-1075.
286. Mortin LI, Stein PS (1989) Spinal cord segments containing key elements of the central pattern generators for three forms of scratch reflex in the turtle. J Neurosci 9: 2285-2296.
287. Mothe AJ, Tator CH (2012) Advances in stem cell therapy for spinal cord injury. J Clin Invest 122: 3824-3834.
288. Mothe AJ, Tam RY, Zahir T, Tator CH, Shoichet MS (2013) Repair of the injured spinal cord by transplantation of neural stem cells in a hyaluronan-based hydrogel. Biomaterials 34: 3775-3783.
289. Mothe AJ, Tator CH (2013) Review of transplantation of neural stem/progenitor cells for spinal cord injury. Int J Dev Neurosci 31: 701-713.
290. Murray KC, Nakae A, Stephens MJ, Rank M, D'Amico J, et al. (2010) Recovery of motoneuron and locomotor function after spinal cord injury depends on constitutive activity in 5-HT2C receptors. Nat Med 16: 694-700.
291. Murre JM, Sturdy DP (1995) The connectivity of the brain: multi-level quantitative analysis. Biol Cybern 73: 529-545.
292. Nashmi R, Fehlings MG (2001) Mechanisms of axonal dysfunction after spinal cord injury: with an emphasis on the role of voltage-gated potassium channels. Brain Res Brain Res Rev 38: 165-191.
293. Nasrabady SE, Kuzhandaivel A, Mladinic M, Nistri A (2011) Effects of 6(5H)-phenanthridinone, an inhibitor of poly(ADP-ribose)polymerase-1 activity (PARP-1), on locomotor networks of the rat isolated spinal cord. Cell Mol Neurobiol 31: 503-508.
294. Nasrabady SE, Kuzhandaivel A, Nistri A (2011) Studies of locomotor network neuroprotection by the selective poly(ADP-ribose) polymerase-1 inhibitor PJ-34 against excitotoxic injury to the rat spinal cord in vitro. Eur J Neurosci 33: 2216-2227.
295. Nedungadi AG, Rangarajan G, Jain N, Ding M (2009) Analyzing multiple spike trains with nonparametric Granger causality. J Comput Neurosci 27: 55-64.
296. Neumann M, Garnett R, Bauckhage C, Kersting K (2016) Propagation kernels: efficient graph kernels from propagated information. Machine Learning 102: 209-245.
297. Nishimaru H, Restrepo CE, Ryge J, Yanagawa Y, Kiehn O (2005) Mammalian motor neurons corelease glutamate and acetylcholine at central synapses. Proc Natl Acad Sci U S A 102: 5245-5249.
298. Nishimura Y, Perlmutter SI, Eaton RW, Fetz EE (2013) Spike-timing-dependent plasticity in primate corticospinal connections induced during free behavior. Neuron 80: 1301-1309.
299. Noble LJ, Wrathall JR (1989) Distribution and time course of protein extravasation in the rat spinal cord after contusive injury. Brain Res 482: 57-66.
300. Norenberg MD, Smith J, Marcillo A (2004) The pathology of human spinal cord injury: defining the problems. J Neurotrauma 21: 429-440.

301. Nori S, Okada Y, Yasuda A, Tsuji O, Takahashi Y, et al. (2011) Grafted human-induced pluripotent stem-cell-derived neurospheres promote motor functional recovery after spinal cord injury in mice. Proc Natl Acad Sci U S A 108: 16825-16830.
302. Norton WT, Aquino DA, Hozumi I, Chiu FC, Brosnan CF (1992) Quantitative aspects of reactive gliosis: a review. Neurochem Res 17: 877-885.
303. O'Donovan MJ (1989) Motor activity in the isolated spinal cord of the chick embryo: synaptic drive and firing pattern of single motoneurons. J Neurosci 9: 943-958.
304. Obien ME, Deligkaris K, Bullmann T, Bakkum DJ, Frey U (2014) Revealing neuronal function through microelectrode array recordings. Front Neurosci 8: 423.
305. Ogawa Y, Sawamoto K, Miyata T, Miyao S, Watanabe M, et al. (2002) Transplantation of in vitro-expanded fetal neural progenitor cells results in neurogenesis and functional recovery after spinal cord contusion injury in adult rats. J Neurosci Res 69: 925-933.
306. Okada S, Ishii K, Yamane J, Iwanami A, Ikegami T, et al. (2005) In vivo imaging of engrafted neural stem cells: its application in evaluating the optimal timing of transplantation for spinal cord injury. FASEB J 19: 1839-1841.
307. Ostojic S, Brunel N, Hakim V (2009) How connectivity, background activity, and synaptic properties shape the cross-correlation between spike trains. J Neurosci 29: 10234-10253.
308. Palm G, Aertsen AM, Gerstein GL (1988) On the significance of correlations among neuronal spike trains. Biol Cybern 59: 1-11.
309. Palmer TD, Takahashi J, Gage FH (1997) The adult rat hippocampus contains primordial neural stem cells. Mol Cell Neurosci 8: 389-404.
310. Pan L, Alagapan S, Franca E, Brewer GJ, Wheeler BC (2011) Propagation of action potential activity in a predefined microtunnel neural network. J Neural Eng 8: 046031.
311. Panayi H, Panayiotou E, Orford M, Genethliou N, Mean R, et al. (2010) Sox1 is required for the specification of a novel p2-derived interneuron subtype in the mouse ventral spinal cord. J Neurosci 30: 12274-12280.
312. Pancrazio JJ, Whelan JP, Borkholder DA, Ma W, Stenger DA (1999) Development and application of cell-based biosensors. Ann Biomed Eng 27: 697-711.
313. Park E, Velumian AA, Fehlings MG (2004) The role of excitotoxicity in secondary mechanisms of spinal cord injury: a review with an emphasis on the implications for white matter degeneration. J Neurotrauma 21: 754-774.
314. Pastore VP, Poli D, Godjoski A, Martinoia S, Massobrio P (2016) ToolConnect: A Functional Connectivity Toolbox for In vitro Networks. Front Neuroinform 10: 13.
315. Patani R, Compston A, Puddifoot CA, Wyllie DJ, Hardingham GE, et al. (2009) Activin/Nodal inhibition alone accelerates highly efficient neural conversion from human embryonic stem cells and imposes a caudal positional identity. PLoS One 4: e7327.
316. Pearson KG, Collins DF (1993) Reversal of the influence of group Ib afferents from plantaris on activity in medial gastrocnemius muscle during locomotor activity. J Neurophysiol 70: 1009-1017.
317. Peng CY, Yajima H, Burns CE, Zon LI, Sisodia SS, et al. (2007) Notch and MAML signaling drives Scl-dependent interneuron diversity in the spinal cord. Neuron 53: 813-827.
318. Perkel DH, Gerstein GL, Moore GP (1967) Neuronal spike trains and stochastic point processes. II. Simultaneous spike trains. Biophys J 7: 419-440.
319. Perkel DH, Gerstein GL, Moore GP (1967) Neuronal spike trains and stochastic point processes. I. The single spike train. Biophys J 7: 391-418.

320. Pierani A, Moran-Rivard L, Sunshine MJ, Littman DR, Goulding M, et al. (2001) Control of interneuron fate in the developing spinal cord by the progenitor homeodomain protein Dbx1. Neuron 29: 367-384.
321. Pillow JW, Shlens J, Paninski L, Sher A, Litke AM, et al. (2008) Spatio-temporal correlations and visual signalling in a complete neuronal population. Nature 454: 995-999.
322. Pine J (1980) Recording action potentials from cultured neurons with extracellular microcircuit electrodes. J Neurosci Methods 2: 19-31.
323. Poli D, Pastore VP, Massobrio P (2015) Functional connectivity in in vitro neuronal assemblies. Front Neural Circuits 9: 57.
324. Poliakov AV, Powers RK, Sawczuk A, Binder MD (1996) Effects of background noise on the response of rat and cat motoneurones to excitatory current transients. J Physiol 495 (Pt 1): 143-157.
325. Potter SM, DeMarse TB (2001) A new approach to neural cell culture for long-term studies. J Neurosci Methods 110: 17-24.
326. Pourzanjani A, Herzog ED, Petzold LR (2015) On the Inference of Functional Circadian Networks Using Granger Causality. PLoS One 10: e0137540.
327. Priebe MM, Chiodo AE, Scelza WM, Kirshblum SC, Wuermser LA, et al. (2007) Spinal cord injury medicine. 6. Economic and societal issues in spinal cord injury. Arch Phys Med Rehabil 88: S84-88.
328. Qiu J, Cai D, Dai H, McAtee M, Hoffman PN, et al. (2002) Spinal axon regeneration induced by elevation of cyclic AMP. Neuron 34: 895-903.
329. Rabchevsky AG, Weinitz JM, Coulpier M, Fages C, Tinel M, et al. (1998) A role for transforming growth factor alpha as an inducer of astrogliosis. J Neurosci 18: 10541-10552.
330. Ragnarsson KT (2008) Functional electrical stimulation after spinal cord injury: current use, therapeutic effects and future directions. Spinal Cord 46: 255-274.
331. Raichle ME, Mintun MA (2006) Brain work and brain imaging. Annu Rev Neurosci 29: 449-476.
332. Raichman N, Ben-Jacob E (2008) Identifying repeating motifs in the activation of synchronized bursts in cultured neuronal networks. J Neurosci Methods 170: 96-110.
333. Rapalino O, Lazarov-Spiegler O, Agranov E, Velan GJ, Yoles E, et al. (1998) Implantation of stimulated homologous macrophages results in partial recovery of paraplegic rats. Nat Med 4: 814-821.
334. Rawe SE, Roth RH, Collins WF (1977) Norepinephrine levels in experimental spinal cord trauma. Part 2: Histopathological study of hemorrhagic necrosis. J Neurosurg 46: 350-357.
335. Renshaw B (1946) Central effects of centripetal impulses in axons of spinal ventral roots. J Neurophysiol 9: 191-204.
336. Roberts A, Soffe SR, Wolf ES, Yoshida M, Zhao FY (1998) Central circuits controlling locomotion in young frog tadpoles. Ann N Y Acad Sci 860: 19-34.
337. Rosenzweig ES, Courtine G, Jindrich DL, Brock JH, Ferguson AR, et al. (2010) Extensive spontaneous plasticity of corticospinal projections after primate spinal cord injury. Nat Neurosci 13: 1505-1510.

338. Rowland JW, Hawryluk GW, Kwon B, Fehlings MG (2008) Current status of acute spinal cord injury pathophysiology and emerging therapies: promise on the horizon. Neurosurg Focus 25: E2.
339. Ruff CA, Wilcox JT, Fehlings MG (2012) Cell-based transplantation strategies to promote plasticity following spinal cord injury. Exp Neurol 235: 78-90.
340. Rybak IA, Shevtsova NA, Lafreniere-Roula M, McCrea DA (2006) Modelling spinal circuitry involved in locomotor pattern generation: insights from deletions during fictive locomotion. J Physiol 577: 617-639.
341. Rybak IA, Stecina K, Shevtsova NA, McCrea DA (2006) Modelling spinal circuitry involved in locomotor pattern generation: insights from the effects of afferent stimulation. J Physiol 577: 641-658.
342. Salgado-Ceballos H, Guizar-Sahagun G, Feria-Velasco A, Grijalva I, Espitia L, et al. (1998) Spontaneous long-term remyelination after traumatic spinal cord injury in rats. Brain Res 782: 126-135.
343. Sanes JN, Suner S, Donoghue JP (1990) Dynamic organization of primary motor cortex output to target muscles in adult rats. I. Long-term patterns of reorganization following motor or mixed peripheral nerve lesions. Exp Brain Res 79: 479-491.
344. Satou C, Kimura Y, Higashijima S (2012) Generation of multiple classes of V0 neurons in zebrafish spinal cord: progenitor heterogeneity and temporal control of neuronal diversity. J Neurosci 32: 1771-1783.
345. Schmidt BJ, Jordan LM (2000) The role of serotonin in reflex modulation and locomotor rhythm production in the mammalian spinal cord. Brain Res Bull 53: 689-710.
346. Schneidman E, Berry MJ, 2nd, Segev R, Bialek W (2006) Weak pairwise correlations imply strongly correlated network states in a neural population. Nature 440: 1007-1012.
347. Schnell L, Schwab ME (1993) Sprouting and regeneration of lesioned corticospinal tract fibres in the adult rat spinal cord. Eur J Neurosci 5: 1156-1171.
348. Schnell L, Schneider R, Kolbeck R, Barde YA, Schwab ME (1994) Neurotrophin-3 enhances sprouting of corticospinal tract during development and after adult spinal cord lesion. Nature 367: 170-173.
349. Schroeter MS, Charlesworth P, Kitzbichler MG, Paulsen O, Bullmore ET (2015) Emergence of rich-club topology and coordinated dynamics in development of hippocampal functional networks in vitro. J Neurosci 35: 5459-5470.
350. Schwab ME, Bartholdi D (1996) Degeneration and regeneration of axons in the lesioned spinal cord. Physiol Rev 76: 319-370.
351. Sears TA, Stagg D (1976) Short-term synchronization of intercostal motoneurone activity. J Physiol 263: 357-381.
352. Segev R, Shapira Y, Benveniste M, Ben-Jacob E (2001) Observations and modeling of synchronized bursting in two-dimensional neural networks. Phys Rev E Stat Nonlin Soft Matter Phys 64: 011920.
353. Sharp J, Frame J, Siegenthaler M, Nistor G, Keirstead HS (2010) Human embryonic stem cell-derived oligodendrocyte progenitor cell transplants improve recovery after cervical spinal cord injury. Stem Cells 28: 152-163.
354. Sharp KG, Yee KM, Steward O (2014) A re-assessment of long distance growth and connectivity of neural stem cells after severe spinal cord injury. Exp Neurol 257: 186-204.
355. Silver J, Miller JH (2004) Regeneration beyond the glial scar. Nat Rev Neurosci 5: 146-156.

356. Sinha DB, Ledbetter NM, Barbour DL (2014) Spike-timing computation properties of a feed-forward neural network model. Front Comput Neurosci 8: 5.
357. Skiebe P (2001) Neuropeptides are ubiquitous chemical mediators: Using the stomatogastric nervous system as a model system. J Exp Biol 204: 2035-2048.
358. Smith E, Hargrave M, Yamada T, Begley CG, Little MH (2002) Coexpression of SCL and GATA3 in the V2 interneurons of the developing mouse spinal cord. Dev Dyn 224: 231-237.
359. Snider RK, Kabara JF, Roig BR, Bonds AB (1998) Burst firing and modulation of functional connectivity in cat striate cortex. J Neurophysiol 80: 730-744.
360. Song J, Ampatzis K, Bjornfors ER, El Manira A (2016) Motor neurons control locomotor circuit function retrogradely via gap junctions. Nature 529: 399-402.
361. Sporns O, Tononi G, Edelman GM (2000) Connectivity and complexity: the relationship between neuroanatomy and brain dynamics. Neural Netw 13: 909-922.
362. Sporns O, Chialvo DR, Kaiser M, Hilgetag CC (2004) Organization, development and function of complex brain networks. Trends Cogn Sci 8: 418-425.
363. Sporns O (2011) The non-random brain: efficiency, economy, and complex dynamics. Front Comput Neurosci 5: 5.
364. Stein PS, Daniels-McQueen S (2002) Modular organization of turtle spinal interneurons during normal and deletion fictive rostral scratching. J Neurosci 22: 6800-6809.
365. Stein PS (2005) Neuronal control of turtle hindlimb motor rhythms. J Comp Physiol A Neuroethol Sens Neural Behav Physiol 191: 213-229.
366. Sternfeld MJ, Hinckley CA, Moore NJ, Pankratz MT, Hilde KL, et al. (2017) Speed and segmentation control mechanisms characterized in rhythmically-active circuits created from spinal neurons produced from genetically-tagged embryonic stem cells. Elife 6.
367. Streit J, Tscherter A, Heuschkel MO, Renaud P (2001) The generation of rhythmic activity in dissociated cultures of rat spinal cord. Eur J Neurosci 14: 191-202.
368. Strubing C, Ahnert-Hilger G, Shan J, Wiedenmann B, Hescheler J, et al. (1995) Differentiation of pluripotent embryonic stem cells into the neuronal lineage in vitro gives rise to mature inhibitory and excitatory neurons. Mech Dev 53: 275-287.
369. Stutzki H, Leibig C, Andreadaki A, Fischer D, Zeck G (2014) Inflammatory stimulation preserves physiological properties of retinal ganglion cells after optic nerve injury. Front Cell Neurosci 8: 38.
370. Supekar K, Menon V, Rubin D, Musen M, Greicius MD (2008) Network analysis of intrinsic functional brain connectivity in Alzheimer's disease. PLoS Comput Biol 4: e1000100.
371. Taccola G, Margaryan G, Mladinic M, Nistri A (2008) Kainate and metabolic perturbation mimicking spinal injury differentially contribute to early damage of locomotor networks in the in vitro neonatal rat spinal cord. Neuroscience 155: 538-555.
372. Takahashi K, Yamanaka S (2006) Induction of pluripotent stem cells from mouse embryonic and adult fibroblast cultures by defined factors. Cell 126: 663-676.
373. Takeoka A, Vollenweider I, Courtine G, Arber S (2014) Muscle spindle feedback directs locomotor recovery and circuit reorganization after spinal cord injury. Cell 159: 1626-1639.
374. Talpalar AE, Bouvier J, Borgius L, Fortin G, Pierani A, et al. (2013) Dual-mode operation of neuronal networks involved in left-right alternation. Nature 500: 85-88.

375. Tarasenko YI, Gao J, Nie L, Johnson KM, Grady JJ, et al. (2007) Human fetal neural stem cells grafted into contusion-injured rat spinal cords improve behavior. J Neurosci Res 85: 47-57.
376. Tator CH, Koyanagi I (1997) Vascular mechanisms in the pathophysiology of human spinal cord injury. J Neurosurg 86: 483-492.
377. Taylor AM, Blurton-Jones M, Rhee SW, Cribbs DH, Cotman CW, et al. (2005) A microfluidic culture platform for CNS axonal injury, regeneration and transport. Nat Methods 2: 599-605.
378. Taylor AM, Rhee SW, Jeon NL (2006) Microfluidic chambers for cell migration and neuroscience research. Methods Mol Biol 321: 167-177.
379. Teng YD, Lavik EB, Qu X, Park KI, Ourednik J, et al. (2002) Functional recovery following traumatic spinal cord injury mediated by a unique polymer scaffold seeded with neural stem cells. Proc Natl Acad Sci U S A 99: 3024-3029.
380. Tetzlaff W, Okon EB, Karimi-Abdolrezaee S, Hill CE, Sparling JS, et al. (2011) A systematic review of cellular transplantation therapies for spinal cord injury. J Neurotrauma 28: 1611-1682.
381. Thallmair M, Metz GA, Z'Graggen WJ, Raineteau O, Kartje GL, et al. (1998) Neurite growth inhibitors restrict plasticity and functional recovery following corticospinal tract lesions. Nat Neurosci 1: 124-131.
382. Thomas CA, Jr., Springer PA, Loeb GE, Berwald-Netter Y, Okun LM (1972) A miniature microelectrode array to monitor the bioelectric activity of cultured cells. Exp Cell Res 74: 61-66.
383. Thuret S, Moon LD, Gage FH (2006) Therapeutic interventions after spinal cord injury. Nat Rev Neurosci 7: 628-643.
384. Tillakaratne NJ, de Leon RD, Hoang TX, Roy RR, Edgerton VR, et al. (2002) Use-dependent modulation of inhibitory capacity in the feline lumbar spinal cord. J Neurosci 22: 3130-3143.
385. Todorova S, Sadtler P, Batista A, Chase S, Ventura V (2014) To sort or not to sort: the impact of spike-sorting on neural decoding performance. J Neural Eng 11: 056005.
386. Totoiu MO, Nistor GI, Lane TE, Keirstead HS (2004) Remyelination, axonal sparing, and locomotor recovery following transplantation of glial-committed progenitor cells into the MHV model of multiple sclerosis. Exp Neurol 187: 254-265.
387. Tripodi M, Stepien AE, Arber S (2011) Motor antagonism exposed by spatial segregation and timing of neurogenesis. Nature 479: 61-66.
388. Trong PK, Rieke F (2008) Origin of correlated activity between parasol retinal ganglion cells. Nat Neurosci 11: 1343-1351.
389. Tsodyks M, Kenet T, Grinvald A, Arieli A (1999) Linking spontaneous activity of single cortical neurons and the underlying functional architecture. Science 286: 1943-1946.
390. Turker KS, Powers RK (2001) Effects of common excitatory and inhibitory inputs on motoneuron synchronization. J Neurophysiol 86: 2807-2822.
391. Turker KS, Powers RK (2002) The effects of common input characteristics and discharge rate on synchronization in rat hypoglossal motoneurones. J Physiol 541: 245-260.
392. van den Brand R, Heutschi J, Barraud Q, DiGiovanna J, Bartholdi K, et al. (2012) Restoring voluntary control of locomotion after paralyzing spinal cord injury. Science 336: 1182-1185.

393. van Pelt J, Wolters PS, Corner MA, Rutten WL, Ramakers GJ (2004) Long-term characterization of firing dynamics of spontaneous bursts in cultured neural networks. IEEE Trans Biomed Eng 51: 2051-2062.
394. van Wijk BC, Stam CJ, Daffertshofer A (2010) Comparing brain networks of different size and connectivity density using graph theory. PLoS One 5: e13701.
395. Veredas FJ, Vico FJ, Alonso JM (2005) Factors determining the precision of the correlated firing generated by a monosynaptic connection in the cat visual pathway. J Physiol 567: 1057-1078.
396. Victor JD, Purpura KP (1997) Metric-space analysis of spike trains: Theory, algorithms and application. Network-Computation in Neural Systems 8: 127-164.
397. Wada T, Honda M, Minami I, Tooi N, Amagai Y, et al. (2009) Highly efficient differentiation and enrichment of spinal motor neurons derived from human and monkey embryonic stem cells. PLoS One 4: e6722.
398. Wagenaar DA, Madhavan R, Pine J, Potter SM (2005) Controlling bursting in cortical cultures with closed-loop multi-electrode stimulation. J Neurosci 25: 680-688.
399. Wagenaar DA, Pine J, Potter SM (2006) An extremely rich repertoire of bursting patterns during the development of cortical cultures. BMC Neurosci 7: 11.
400. Wagenaar DA, Pine J, Potter SM (2006) Searching for plasticity in dissociated cortical cultures on multi-electrode arrays. J Negat Results Biomed 5: 16.
401. Waxman SG (1989) Demyelination in spinal cord injury. J Neurol Sci 91: 1-14.
402. Weimann JM, Marder E (1994) Switching neurons are integral members of multiple oscillatory networks. Curr Biol 4: 896-902.
403. Weiss S, Dunne C, Hewson J, Wohl C, Wheatley M, et al. (1996) Multipotent CNS stem cells are present in the adult mammalian spinal cord and ventricular neuroaxis. J Neurosci 16: 7599-7609.
404. Westbrook GL, Mayer ML (1984) Glutamate currents in mammalian spinal neurons: resolution of a paradox. Brain Res 301: 375-379.
405. White JG, Southgate E, Thomson JN, Brenner S (1986) The structure of the nervous system of the nematode Caenorhabditis elegans. Philos Trans R Soc Lond B Biol Sci 314: 1-340.
406. White TE, Lane MA, Sandhu MS, O'Steen BE, Fuller DD, et al. (2010) Neuronal progenitor transplantation and respiratory outcomes following upper cervical spinal cord injury in adult rats. Exp Neurol 225: 231-236.
407. Wilson DM, Wyman RJ (1965) Motor Output Patterns during Random and Rhythmic Stimulation of Locust Thoracic Ganglia. Biophys J 5: 121-143.
408. Wilson DM (1966) Central nervous mechanisms for the generation of rhythmic behaviour in arthropods. Symp Soc Exp Biol 20: 199-228.
409. Windhorst U (1996) On the role of recurrent inhibitory feedback in motor control. Prog Neurobiol 49: 517-587.
410. Wong RO, Meister M, Shatz CJ (1993) Transient period of correlated bursting activity during development of the mammalian retina. Neuron 11: 923-938.
411. Wood MR, Cohen MJ (1979) Synaptic regeneration in identified neurons of the lamprey spinal cords. Science 206: 344-347.
412. Woodward ND, Cascio CJ (2015) Resting-State Functional Connectivity in Psychiatric Disorders. JAMA Psychiatry 72: 743-744.
413. Wu CW, Kaas JH (1999) Reorganization in primary motor cortex of primates with long-standing therapeutic amputations. J Neurosci 19: 7679-7697.

414. Xiong Y, Rabchevsky AG, Hall ED (2007) Role of peroxynitrite in secondary oxidative damage after spinal cord injury. J Neurochem 100: 639-649.
415. Xu H, Iyer N, Huettner JE, Sakiyama-Elbert SE (2015) A puromycin selectable cell line for the enrichment of mouse embryonic stem cell-derived V3 interneurons. Stem Cell Res Ther 6: 220.
416. Xu H, Sakiyama-Elbert SE (2015) Directed Differentiation of V3 Interneurons from Mouse Embryonic Stem Cells. Stem Cells Dev 24: 2723-2732.
417. Zaaimi B, Edgley SA, Soteropoulos DS, Baker SN (2012) Changes in descending motor pathway connectivity after corticospinal tract lesion in macaque monkey. Brain 135: 2277-2289.
418. Zagoraiou L, Akay T, Martin JF, Brownstone RM, Jessell TM, et al. (2009) A cluster of cholinergic premotor interneurons modulates mouse locomotor activity. Neuron 64: 645-662.
419. Zhang HM, Li DP, Chen SR, Pan HL (2005) M2, M3, and M4 receptor subtypes contribute to muscarinic potentiation of GABAergic inputs to spinal dorsal horn neurons. J Pharmacol Exp Ther 313: 697-704.
420. Zhang J, Lanuza GM, Britz O, Wang Z, Siembab VC, et al. (2014) V1 and v2b interneurons secure the alternating flexor-extensor motor activity mice require for limbed locomotion. Neuron 82: 138-150.
421. Zhang SC, Lundberg C, Lipsitz D, O'Connor LT, Duncan ID (1998) Generation of oligodendroglial progenitors from neural stem cells. J Neurocytol 27: 475-489.
422. Zhang Y, Narayan S, Geiman E, Lanuza GM, Velasquez T, et al. (2008) V3 spinal neurons establish a robust and balanced locomotor rhythm during walking. Neuron 60: 84-96.
423. Zhang YW, Denham J, Thies RS (2006) Oligodendrocyte progenitor cells derived from human embryonic stem cells express neurotrophic factors. Stem Cells Dev 15: 943-952.
424. Zhong G, Droho S, Crone SA, Dietz S, Kwan AC, et al. (2010) Electrophysiological characterization of V2a interneurons and their locomotor-related activity in the neonatal mouse spinal cord. J Neurosci 30: 170-182.
425. Zhong G, Sharma K, Harris-Warrick RM (2011) Frequency-dependent recruitment of V2a interneurons during fictive locomotion in the mouse spinal cord. Nat Commun 2: 274.
426. Zhong G, Shevtsova NA, Rybak IA, Harris-Warrick RM (2012) Neuronal activity in the isolated mouse spinal cord during spontaneous deletions in fictive locomotion: insights into locomotor central pattern generator organization. J Physiol 590: 4735-4759.
427. Zhou Q, Poo MM (2004) Reversal and consolidation of activity-induced synaptic modifications. Trends Neurosci 27: 378-383.
428. Zhou Y, Yamamoto M, Engel JD (2000) GATA2 is required for the generation of V2 interneurons. Development 127: 3829-3838.

Vita

EDUCATION

Washington University in St Louis, Saint Louis, MO July 2011-March 2017
PhD Biomedical Engineering *March 2017*
MS Biomedical Engineering *May 2015*

Duke University, Durham, NC August 2007-May 2011
BS Biomedical Engineering, Minor: Neuroscience *May 2011*

RESEARCH EXPERIENCE

Washington University in St Louis, Biomedical Engineering 2011 – present
Doctoral Student, Mentor: Dennis Barbour
Thesis: *Developing an In Vitro Assay for Detection and Characterization of Functional Connectivity within Transplantation Candidate Embryonic Stem Cell-Derived V2a Interneuron Networks*

- Thesis work funded by University of Missouri System's Spinal Cord Injury Research Program and Washington University's Hope Center Pilot Award
- Spearheaded and manage a collaboration with the tissue engineering laboratory of Dr. Shelly Sakiyama-Elbert
- Combining multi-electrode arrays and transgenic stem cell lines to develop a novel high-throughput *in vitro* assay for the development of functional connectivity profiles of candidate transplant stem cell derived neuronal populations
- Secured approximately $300,000 of initial funding for the project by writing and submitting two grants to Washington University's Hope Center for Neurological Disease and the University of Missouri System's Spinal Cord Injury/Disease Research Program respectively

Duke University, Biomedical Engineering 2010-2011
Undergraduate Research Assistant, Mentor: Warren Grill

- Created a dynamic finite element computer model of vagal cuff stimulation utilizing MATLAB and COMSOL and imported simulated axonal voltage and coordinate data to NEURON in order to perform analysis of the recruitment of nerve fibers according to stimulus amplitude and pulse width

Washington University, Biomedical Engineering 2010
Summer Intern, Mentor: Dennis Barbour

- Analyzed spike trains previously recorded from the nonhuman primate auditory cortex for neural coding in the presence of noise by writing MATLAB code to incorporate various spike train comparison metrics and interface with the lab's previously existing code architecture

Duke University, Biomedical Engineering 2009-2010

Undergraduate Research Assistant, Mentor: Jennifer Groh

- Improve the organization, accessibility, and transparency of their lab data to the broader neuroscience community by creating an interactive reservoir of the lab's raw findings in the form of a website utilizing MATLAB & Adobe Flash

AWARDS

CCSN Fellowship, Washington University 2012-2014

Reginaldo Howard Memorial Scholarship, Duke University 2007-2011

PUBLICATIONS

1. Iyer N*, **Gamble JR***, Groneck L, Barbour D, Sakiyama-Elbert S. An *In Vitro* Aggregate Culture System Investigating the Response of Embryonic Stem Cell Derived V2a Interneurons to Neurotrophins and Co-Culture with Progenitor Motor Neurons. [In Preparation]
2. **Gamble JR***, Iyer N, Zhang E, Sakiyama-Elbert S, Barbour DL. *In Vitro* Assay for the Detection of Network Connectivity in Embryonic Stem Cell-Derived Cultures. *Journal of Neuroengineering* [In Submission]
3. Ni R*, Bender DA, Shaneshi AM, **Gamble JR**, Barbour DL. Contextual Effects of Noise on Vocalization Encoding in Primary Auditory Cortex. *Journal of Neurophysiology*. 117(2):713-727, 2016

CONFERENCE PRESENTATIONS AND PROCEEDINGS

4. **J.R. Gamble***, N. Iyer, S. Sakiyama-Elbert, D.L. Barbour. Novel *in vitro* characterization of embryonic stem cell-derived neural circuit connectivity. October 2015. Biomedical Engineering Society Annual Meeting. Tampa Bay, FL.
5. R. Ni*, D.A. Bender, **J.R. Gamble**, D.L. Barbour. Single and Population Neural Discrimination of Vocalizations in Noise. October 2015. Society for Neuroscience Annual Meeting. Chicago, IL.
6. **J.R. Gamble***, S. Sakiyama-Elbert, D. L. Barbour. Novel *in vitro* assessment of spinal circuit formation. June 2014. National Institute of Biomedical Imaging and Bioengineering Training Grantees Meeting. Bethesda, MD.
7. **J.R. Gamble***, J.A. Maurer, D.L. Barbour. Precise control neural network connectivity in neural cultures. November 2013. 6th Annual IEEE Engineering in Medicine and Biology Society Neural Engineering Conference. San Diego, CA.
8. **J.R. Gamble***, J.A. Maurer, D.L. Barbour. Precise control neural network connectivity in neural cultures. November 2013. Society for Neuroscience Annual Meeting. San Diego, CA.

*Presenting Author

PROFESSIONAL SOCIETIES

Biomedical Engineering Society 2015-present

Society for Neuroscience 2013-present

Institute of Electrical and Electronics Engineers 2013-present

TEACHING EXPERIENCE

Washington University in St. Louis

Teaching Assistant, Quantitative Physiology 2012

COMMUNITY OUTREACH

Network for Teaching Entrepreneurship, Volunteer 2017-present
InSITE Startup Consulting, Consultant 2015-present
Young Scientist Program Continuing Mentoring, Mentor 2012-2016
Cognitive, Computational and Systems Neuroscience Outreach, Volunteer 2012-2016
Reginaldo Howard Memorial Scholarship Program, Fellow 2007-2011

LEADERSHIP EXPERIENCE

Project Leader, Sling Health Startup Incubator 2015-2016
Cohort Liaison, Young Scientist Program Continuing Mentoring 2012-2016
Lead Facilitator, Cognitive, Computational and Systems Neuroscience Outreach 2013-2015
Co-President, Reginaldo Howard Scholarship Program 2010-2011